



Search for vector-boson resonances decaying to a top quark and bottom quark in the lepton plus jets final state in pp collisions at root s=13 TeV with the ATLAS detector

Aaboud, M.; Aad, G.; Abbott, B.; Abdinov, O.; Abeloos, B.; Abhayasinghe, DK; Abidi, S.H.; AbouZeid, Ossama Sherif Alexander; Abraham, NL; Abramowicz, H.; Abreu, H.; Abulaiti, Y.; Acharya, B.S.; Adachi, J.; Adamczyk, L.; Adelman, J.; Adersberger, M.; Adiguzel, A.; Adye, T.; Affolder, A. A.; Afik, Y. ; Agheorghiesei, C.; Aguilar-Saavedra, J. A.; Ahmadov, F.; Aielli, G.; Akatsuka, S.; Akesson, T. P. A.; Akilli, E.; Akimov, A. V.; Hansen, Jørgen Beck; Hansen, Peter Henrik; Alonso Diaz, Alejandro; Dam, Mogens; Besjes, Geert-Jan; Wiglesworth, Graig; Monk, James William; Bajic, Milena; Petersen, Troels Christian; Hansen, Jørn Dines; hqz214, hqz214; Stark, Simon Holm; Galster, Gorm Aske Gram Krohn; de Almeida Dias, Flavia; Xella, Stefania; ATLAS

Published in:
Physics Letters B

DOI:
[10.1016/j.physletb.2018.11.032](https://doi.org/10.1016/j.physletb.2018.11.032)

Publication date:
2019

Document version
Publisher's PDF, also known as Version of record

Document license:
[CC BY](#)

Citation for published version (APA):
Aaboud, M., Aad, G., Abbott, B., Abdinov, O., Abeloos, B., Abhayasinghe, DK., Abidi, S. H., AbouZeid, O. S. A., Abraham, NL., Abramowicz, H., Abreu, H., Abulaiti, Y., Acharya, B. S., Adachi, J., Adamczyk, L., Adelman, J., Adersberger, M., Adiguzel, A., Adye, T., ... ATLAS (2019). Search for vector-boson resonances decaying to a top quark and bottom quark in the lepton plus jets final state in pp collisions at root s=13 TeV with the ATLAS detector. *Physics Letters B*, 788, 347-370. <https://doi.org/10.1016/j.physletb.2018.11.032>



Search for vector-boson resonances decaying to a top quark and bottom quark in the lepton plus jets final state in pp collisions at $\sqrt{s} = 13$ TeV with the ATLAS detector

The ATLAS Collaboration^{*}

ARTICLE INFO

Article history:

Received 27 July 2018

Received in revised form 15 October 2018

Accepted 3 November 2018

Available online 22 November 2018

Editor: W.-D. Schlatter

ABSTRACT

A search for new charged massive gauge bosons, W' , is performed with the ATLAS detector at the LHC. Data were collected in proton–proton collisions at a center-of-mass energy of $\sqrt{s} = 13$ TeV and correspond to an integrated luminosity of 36.1 fb^{-1} . This analysis searches for W' bosons in the $W' \rightarrow t\bar{b}$ decay channel in final states with an electron or muon plus jets. The search covers resonance masses between 0.5 and 5.0 TeV and considers right-handed W' bosons. No significant deviation from the Standard Model (SM) expectation is observed and upper limits are set on the $W' \rightarrow t\bar{b}$ cross section times branching ratio and the W' boson effective couplings as a function of the W' boson mass. For right-handed W' bosons with coupling to the SM particles equal to the SM weak coupling constant, masses below 3.15 TeV are excluded at the 95% confidence level. This search is also combined with a previously published ATLAS result for $W' \rightarrow t\bar{b}$ in the fully hadronic final state. Using the combined searches, right-handed W' bosons with masses below 3.25 TeV are excluded at the 95% confidence level.

© 2018 The Author(s). Published by Elsevier B.V. This is an open access article under the CC BY license (<http://creativecommons.org/licenses/by/4.0/>). Funded by SCOAP³.

1. Introduction

Many approaches to theories beyond the Standard Model (SM) introduce new charged vector currents mediated by heavy gauge bosons, usually referred to as W' . For example, the W' boson can appear in theories with universal extra dimensions, such as Kaluza–Klein excitations of the SM W boson [1–3], or in models that extend fundamental symmetries of the SM and propose a massive right-handed counterpart to the W boson [4–6]. Little-Higgs [7] and composite-Higgs [8,9] theories also predict a W' boson. The search for a W' boson decaying into a top quark and a b -quark (illustrated in Fig. 1) explores models potentially inaccessible to searches for a W' boson decaying into leptons [10–15].

For instance, in the right-handed sector, the W' boson cannot decay into a charged lepton and a hypothetical right-handed neutrino if the latter has a mass greater than the W' boson mass (mixing between W' and SM W bosons is usually constrained to be small from experimental data [16]). Also, in several theories beyond the SM the W' boson is expected to couple more strongly to the third generation of quarks than to the first and second generations [17,18]. Searches for a W' boson decaying into the $t\bar{b}$ final

state¹ have been performed at the Tevatron [19,20] in the leptonic top-quark decay channel and at the Large Hadron Collider (LHC) in both the leptonic [21–25] and fully hadronic [26,27] final states, and the most recent results exclude right-handed W' bosons with masses up to about 3.6 TeV at the 95% confidence level. A previous ATLAS search in the leptonic channel [24] using proton–proton (pp) collisions at a center-of-mass energy of $\sqrt{s} = 8$ TeV yielded a lower limit of 1.92 TeV on the mass of W' boson with right-handed couplings. More recently, the CMS Collaboration reported results using a 13 TeV pp data set of 35.9 fb^{-1} [25], yielding a lower limit of 3.6 TeV on the mass of right-handed W' bosons. A search by the ATLAS Collaboration in the fully hadronic decay of the $t\bar{b}$ final state using 36.1 fb^{-1} of 13 TeV data yielded lower limits on the mass of right-handed W' bosons at 3.0 TeV [27]. In each of these analyses, the coupling strength of the W' boson to right-handed particles was assumed to be equal to the SM weak coupling constant.

This Letter presents a search for W' bosons using data collected during the period 2015–2016 by the ATLAS detector [28] at the LHC, corresponding to an integrated luminosity of 36.1 fb^{-1} from pp collisions at a center-of-mass energy of 13 TeV. The search is performed in the $W'_R \rightarrow t\bar{b} \rightarrow \ell\nu b\bar{b}$ decay channel, where the lep-

^{*} E-mail address: atlas.publications@cern.ch.

¹ The notation “ $t\bar{b}$ ” is used to describe both the $W'^+ \rightarrow t\bar{b}$ and $W'^- \rightarrow \bar{t}b$ processes.

Table 1

Event generators used for the simulation of the signal and background processes. The PS/Had column describes the program used for parton shower and hadronization.

Process	Generator	PS/Had	MC Tune	PDF
W'_R	MADGRAPH5_AMC@NLO	PYTHIA8	A14	NNPDF23LO
$t\bar{t}$	POWHEG-BOX	PYTHIA6	Perugia 2012	NLO CT10
Single-top t -channel	POWHEG-BOX	PYTHIA6	Perugia 2012	NLO CT10
Single-top $W + t$	POWHEG-BOX	PYTHIA6	Perugia 2012	NLO CT10
Single-top s -channel	POWHEG-BOX	PYTHIA6	Perugia 2012	NLO CT10
$W, Z + \text{jets}$	SHERPA 2.2.1	SHERPA 2.2.1	Default	NLO CT10
WW, WZ, ZZ	POWHEG-BOX	PYTHIA8	AZNLO	LO CTEQ6L1

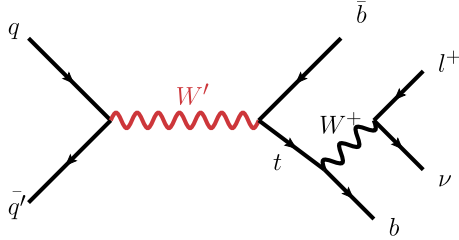


Fig. 1. Feynman diagram for W' boson production from quark-antiquark annihilation with the subsequent decay into $t\bar{b}$ and a leptonically decaying top quark.

ton, ℓ , is either an electron or a muon. Right-handed W' bosons, denoted W'_R , are searched for in the mass range of 0.5 to 5.0 TeV. A general Lorentz-invariant Lagrangian is used to describe the couplings of the W'_R boson to fermions as a function of its mass [29, 30]. The mass of the right-handed neutrino is supposed to be larger than the mass of the W'_R boson, thus non-hadronic decays of the W'_R boson have a negligible branching fraction. In this weakly coupled model, the resulting branching fraction of the W'_R to the $t\bar{b}$ final state increases as a function of mass from 29.9% at 0.5 TeV to 33.3% at 5 TeV.

2. ATLAS detector

The ATLAS detector at the LHC covers almost the entire solid angle around the collision point.² Charged particles in the pseudorapidity range $|\eta| < 2.5$ are reconstructed with the inner detector (ID), which consists of several layers of semiconductor detectors (pixel and strip) and a straw-tube transition-radiation tracker, the latter extending to $|\eta| = 2.0$. The high-granularity silicon pixel detector provides four measurements per track; the closest layer to the interaction point is known as the insertable B-layer [31, 32], which was added in 2014 and provides high-resolution hits at small radius to improve the tracking performance. The ID is immersed in a 2 T magnetic field provided by a superconducting solenoid. The solenoid is surrounded by electromagnetic and hadronic calorimeters, and a muon spectrometer incorporating three large superconducting air-core toroid magnet systems. The calorimeter system covers the pseudorapidity range $|\eta| < 4.9$. Electromagnetic calorimetry is provided by barrel and endcap high-granularity lead/liquid-argon (LAr) electromagnetic calorimeters, within the region $|\eta| < 3.2$. There is an additional thin LAr presampler covering $|\eta| < 1.8$ to correct for energy loss in material upstream of the calorimeters. For $|\eta| < 2.5$, the LAr calorimeters

are divided into three layers in depth. Hadronic calorimetry is provided by a steel/scintillator-tile calorimeter, segmented into three barrel structures within $|\eta| < 1.7$, and two copper/LAr hadronic endcap calorimeters, which cover the region $1.5 < |\eta| < 3.2$. The forward solid angle out to $|\eta| = 4.9$ is covered by copper/LAr and tungsten/LAr calorimeter modules, which are optimized for electromagnetic and hadronic measurements, respectively. The muon spectrometer comprises separate trigger and high-precision tracking chambers that measure the deflection of muons in a magnetic field generated by the three toroid magnet systems. The ATLAS detector selects events using a tiered trigger system [33]. The first level is implemented in custom electronics and reduces the event rate from the LHC crossing frequency of 40 MHz to a design value of 100 kHz. The second level is implemented in software running on a commodity PC farm which processes the events and reduces the rate of recorded events to 1.0 kHz.

3. Data and simulated samples

This analysis uses $36.1 \pm 0.8 \text{ fb}^{-1}$ of pp collisions data at $\sqrt{s} = 13 \text{ TeV}$ recorded using single-electron and single-muon triggers. Additional data-quality requirements are also imposed, and these are detailed in Section 4. During 2015 this corresponded to 3.2 fb^{-1} with an average of 13.4 interactions per bunch crossing. The 2016 data-taking period corresponds to 32.9 fb^{-1} with an average of 25.1 interactions per bunch crossing.

The W'_R boson search is performed in the semileptonic decay channel, where the W'_R decays into a top quark and a b -quark, the top quark decays into a W boson and a b -quark, and the W boson decays in turn into a lepton and a neutrino. The final-state signature therefore consists of two b -quarks, one charged lepton³ and a neutrino, which is undetected and results in missing transverse momentum, E_T^{miss} . The dominant background processes for this signature are therefore the production of $W/Z + \text{jets}$ (jets arising from light and heavy partons), electroweak single top quarks (t -channel, Wt and s -channel), $t\bar{t}$ pairs and dibosons (WW , WZ , and ZZ). An instrumental background due to multijet production, where a hadronic jet is misidentified as a lepton, is also present. Monte Carlo (MC) simulated events are used to model the W'_R signal and all the SM background processes, with the exception of the multijet background prediction, which is derived using data. The MC generator programs and configurations are summarized in Table 1, and described in greater detail in the text below.

Simulated signal events were generated at leading order (LO) by MADGRAPH5_AMC@NLO v2.2.3 [34–37] using a chiral W'_R boson model in which the couplings to the right-handed fermions are like those in the SM. MADGRAPH5_AMC@NLO is also used to model the decays of the top quark, taking spin correlations into account.

² ATLAS uses a right-handed coordinate system with its origin at the nominal interaction point in the center of the detector and the z -axis along the beam pipe. The x -axis points from the interaction point to the center of the LHC ring, and the y -axis points upward. Cylindrical coordinates (r, ϕ) are used in the transverse plane, ϕ being the azimuthal angle around the beam pipe. The pseudorapidity is defined in terms of the polar angle θ as $\eta = -\ln(\tan(\theta/2))$. Observables labeled “transverse” are projected into the x - y plane and angular distance is measured in units of $\Delta R = \sqrt{(\Delta\eta)^2 + (\Delta\phi)^2}$.

³ The analysis selects electrons or muons, while the simulation includes τ -leptons. Thus the event yield includes a small contribution due to leptonic decays of τ -leptons.

PYTHIA8 v8.186 [38] was used for parton showering and hadronization, wherein the NNPDF23LO [39] parton distribution functions (PDF) of the proton and a set of tuned parameters called the A14 PYTHIA tune [40] were used. All samples of simulated events were rescaled to next-to-leading-order (NLO) calculations using NLO/LO K -factors ranging from 1.1 to 1.4, decreasing as a function of the mass of the W'_R boson, calculated with ZTOP [30]. Signal samples were generated between 0.5 and 3 TeV in steps of 250 GeV, and between 3 and 5 TeV in steps of 500 GeV.

The benchmark signal model used for this work nominally assumes that the W'_R boson coupling strength to fermions, g' , is the same as for the W boson: $g' = g$, where g is the SM $SU(2)_L$ coupling. The coupling of left chiral fermions to the W'_R is assumed to be zero. The total width of the W'_R boson increases from 2 to 130 GeV for masses between 0.5 and 5 TeV [29] for $g' = g$ and scales as the square of the ratio g'/g . In order to explore the allowed range of the W'_R coupling g' , samples were also generated for values of g'/g up to 5.0, for several W'_R boson mass hypotheses, allowing the effect of increased W'_R width to also be included.

Simulated top-quark pair and single-top-quark processes (t -channel, s -channel and Wt) were produced using the NLO POWHEG-Box [41,42] generator with the CT10 PDF [43]. The parton shower and the underlying event were added using PYTHIA v6.42 [44] with the Perugia 2012 tune [45]. The top-quark pair production MC sample is normalized to an inclusive cross section of $\sigma_{t\bar{t}} = 832^{+46}_{-51}$ pb for a top-quark mass of 172.5 GeV as obtained from next-to-NLO (NNLO) plus next-to-next-to-leading-logarithm (NNLL) QCD calculations with the Top++2.0 program [46–52].

The background contributions from W and Z boson production in association with jets were simulated using the SHERPA v2.2.1 [53] generator. Matrix elements were calculated for up to two partons at NLO and four partons at LO and merged with the SHERPA parton shower using the ME+PS@NLO prescription [54–56]. The W/Z +jets samples are normalized to the inclusive NNLO cross sections calculated with FEWZ [57,58].

The production of vector-boson pairs (WW , WZ or ZZ) with at least one charged lepton in the final state was simulated by the POWHEG-Box generator in combination with PYTHIA8 and the leading-order CTEQ6L1 PDF [59]. The non-perturbative effects were modeled with the AZNLO set of tuned parameters [60].

For all MADGRAPH and POWHEG samples, the EVTGEN v1.2.0 program [61] was used for the bottom and charm hadron decays.

All simulated event samples include the effect of multiple pp interactions in the same and neighboring bunch crossings (pile-up) by overlaying, on each simulated signal or background event, simulated minimum-bias events generated using PYTHIA8, the A2 set of tuned parameters [62] and the MSTW2008LO PDF set [63].

Simulated samples were processed through the GEANT4-based ATLAS detector simulation or through a faster simulation making use of parameterized showers in the calorimeters [64,65]. Simulated events were then processed using the same reconstruction algorithms and analysis chain as used for data.

4. Event selection and background estimation

This search makes use of the reconstruction of multi-particle vertices, the identification and the kinematic properties of reconstructed electrons, muons, jets, and the determination of missing transverse momentum.

Collision vertices are reconstructed from at least two ID tracks with transverse momentum $p_T > 400$ MeV. The primary vertex is selected as the one with the highest $\sum p_T^2$, calculated considering all associated tracks.

Electrons are reconstructed from ID tracks that are matched to noise-suppressed topological clusters of energy depositions [66]

in the electromagnetic calorimeter. The clusters are reconstructed using the standard ATLAS sliding-window algorithm, which clusters calorimeter cells within fixed-size rectangles [67]. Electron candidates are required to satisfy criteria for the electromagnetic shower shape, track quality, and track-cluster matching; these criteria are applied using a likelihood-based approach. Electron candidates must meet the “Tight” working point requirements defined in Ref. [68] and are further required to have $p_T > 25$ GeV and a pseudorapidity of the calorimeter cluster position, $|\eta_{\text{cluster}}|$, smaller than 2.47. Events with electrons falling in the calorimeter barrel-endcap transition region, $1.37 < |\eta_{\text{cluster}}| < 1.52$, which has limited instrumentation, are rejected.

Muons are identified by matching tracks found in the ID to either full tracks or track segments reconstructed in the muon spectrometer (“combined muons”), or by stand-alone tracks in the muon spectrometer [69]. They are required to pass identification requirements based on quality criteria applied to the ID and muon spectrometer tracks. Muon candidates must meet the “Medium” identification working point requirements defined in Ref. [69], have a transverse momentum $p_T > 25$ GeV, and satisfy $|\eta| < 2.5$.

Electron and muon candidates must further satisfy additional isolation criteria that improve rejection of candidates arising from sources other than prompt W/Z boson decays (e.g. hadrons mimicking an electron signature, heavy-flavor hadron decays or photon conversions). Muons are required to be isolated using the requirement that the scalar sum of the p_T of the tracks in a variable-size cone around the muon direction (excluding the track identified as the muon) be less than 6% of the transverse momentum of the muon. The track isolation cone size is given by the minimum of $\Delta R = 10 \text{ GeV}/p_T^\mu$ and $\Delta R = 0.3$. Electrons are also required to be isolated using the same track-based variable as for muons, except that the maximum ΔR in this case is 0.2. For the purpose of multi-jet background estimation (see Section 5) electrons and muons satisfying a looser set of identification criteria, in particular without an isolation requirement, are also considered.

Jets are reconstructed from topological calorimeter clusters using the anti- k_t algorithm [70] with a radius parameter of $R = 0.4$, and must satisfy $p_T > 25$ GeV and $|\eta| < 2.5$. To suppress jets originating from in-time pile-up interactions, jets in the range $p_T < 60$ GeV and $|\eta| < 2.4$ are required to pass the jet vertex tagger [71] selection, which has an efficiency of about 90% for jets originating from the primary vertex. The closest jets overlapping with selected electron candidates within a cone of size ΔR equal to 0.2 are removed from events, as the jet and the electron very likely correspond to the same reconstructed object. If a remaining jet with $p_T > 25$ GeV is found close to an electron within a cone of size $\Delta R = 0.4$, then the electron candidate is discarded. Selected muon candidates near jets that satisfy $\Delta R(\text{muon, jet}) < 0.04 + 10 \text{ GeV}/p_T^\mu$ are rejected if the jet has at least three tracks originating from the primary vertex. Any jets with less than three tracks that overlap with a muon are rejected.

The identification of jets originating from the hadronization of b -quarks (“ b -tagging”) is based on properties specific to b -hadrons, such as long lifetime and large mass. Such jets are identified using the multivariate MV2c10 b -tagging algorithm [72,73], which makes use of information about the jet kinematic properties, the characteristics of tracks within jets, and the presence of displaced secondary vertices. The algorithm is used at the 77% efficiency working point and provides a rejection factor of 134 (6.21) for jets originating from light-quarks or gluons (charm quarks), as determined in simulated $t\bar{t}$ events. Jets satisfying these criteria are referred to as “ b -tagged” jets.

The presence of neutrinos can be inferred from an apparent momentum imbalance in the transverse plane. The missing transverse momentum (E_T^{miss}) is calculated as the modulus of the neg-

ative vectorial sum of the transverse momentum of all reconstructed objects (electrons, muons, jets) as well as specific “soft terms” considering tracks associated with the primary vertex that do not match the selected reconstructed objects [74].

Candidate events are required to have exactly one charged lepton, two to four jets with at least one of them b -tagged and a minimum E_T^{miss} threshold that depends on the lepton flavor. From these objects, W boson and top-quark candidates are reconstructed and final requirements on the event kinematic properties are applied to define several orthogonal regions with enriched signal content, as well as signal-depleted regions to validate data modeling. The jet, b -tag and lepton requirements define basic selections, which are labeled as X -jet Y -tag where $X = 2, 3, 4$ and $Y = 1, 2$, separated for electron and muon channel selections.

The W boson candidate is reconstructed from the lepton and E_T^{miss} , with the assumption that only one neutrino is present in the event. The z component of the neutrino momentum (p_z) is calculated from the invariant mass of the lepton– E_T^{miss} system with the constraint that $m_W = 80.4$ GeV. The constraint yields a quadratic equation and in the case of two real solutions, the smallest $|p_z|$ solution is chosen. If the transverse mass, m_T^W , of the reconstructed W boson is larger than the value m_W used in the constraint, the two solutions are imaginary. This case can be due to the resolution of the missing transverse momentum measurement. Here, the $E_{x,y}^{\text{miss}}$ components are adjusted to satisfy $m_T^W = m_W$, yielding a single real solution.

The four-momentum of the top-quark candidate is reconstructed by adding the four-momenta of the W -boson candidate and of the jet, among all selected jets in the event, that yields the invariant mass closest to the top-quark mass ($m_{\text{top}} = 172.5$ GeV). Thereafter, this jet is referred to as “ b_{top} ”, and may not be the jet actually b -tagged. Finally, the four-momentum of the candidate W' boson is reconstructed by adding the four-momentum of the reconstructed top-quark candidate and the four-momentum of the highest- p_T remaining jet (referred to as “ b_1 ”). The W' four-momentum is used to evaluate the invariant mass of the reconstructed $W' \rightarrow tb$ system (m_{tb}), which is the variable used for background discrimination for this search.

An event selection common to all signal and validation regions is defined as: lepton $p_T > 50$ GeV, $p_T(b_1) > 200$ GeV, $p_T(\text{top}) > 200$ GeV, and $E_T^{\text{miss}} > 30$ GeV. In order to keep the multijet background at a low level an additional selection is imposed, in the muon channel, on the sum of m_T^W and E_T^{miss} : $m_T^W + E_T^{\text{miss}} > 100$ GeV. In the electron channel the same requirement is applied to keep the selection in both channels as similar as possible, and, in addition the E_T^{miss} threshold is raised to 80 GeV to further suppress the multijet background. This phase space is then subdivided into a signal region (SR), a validation region enriched with the W +jets background (VR_{pretag}), a validation region enriched with the $t\bar{t}$ background (VR_{t \bar{t}}), and a validation region enriched with the W +heavy-flavor jets background (VR_{HF}). All regions consist of events with two or three jets, except for the VR_{t \bar{t}} where events with exactly four jets are selected. The SR and VR_{t \bar{t}} require that one or two jets are b -tagged, while only one b -tagged jet is required in the VR_{HF}. No b -tagging requirement is applied in the VR_{pretag}. Specific selections are then applied in the two following cases. The SR is defined by requiring that the angular separation of the lepton and b_{top} be small: $\Delta R(\ell, b_{\text{top}}) < 1.0$. An additional criterion $m_{tb} > 500$ GeV is applied to remove a small number of low-mass W +jets and $t\bar{t}$ events. The VR_{HF} consists of events where the lepton–jet and jet–jet separations are large: $\Delta R(\ell, b_{\text{top}}) > 2.0$ and $\Delta R(b_1, b_{\text{top}}) > 1.5$. The application of these two selections reduces the $t\bar{t}$ background in the VR_{HF} region by 90%. The expected signal contamination in the validation regions is at most 5% for low

Table 2

Summary of the event selection criteria used to define signal and validation regions. The E_T^{miss} selection cut is harder for events with electrons than with muons.

Common selection			
$p_T(\ell) > 50$ GeV, $p_T(b_1) > 200$ GeV, $p_T(\text{top}) > 200$ GeV $E_T^{\text{miss}} > 30$ (80) GeV, $m_T^W + E_T^{\text{miss}} > 100$ GeV			
Signal region	VR _{pretag}	VR _{t\bar{t}}	VR _{HF}
2 or 3 jets	2 or 3 jets	4 jets	2 or 3 jets
1 or 2 b -jets	pretag	1 or 2 b -jets	1 b -jet
$\Delta R(\ell, b_{\text{top}}) < 1.0$			$\Delta R(\ell, b_{\text{top}}) > 2.0$
$m_{tb} > 500$ GeV			$\Delta R(b_1, b_{\text{top}}) > 1.5$

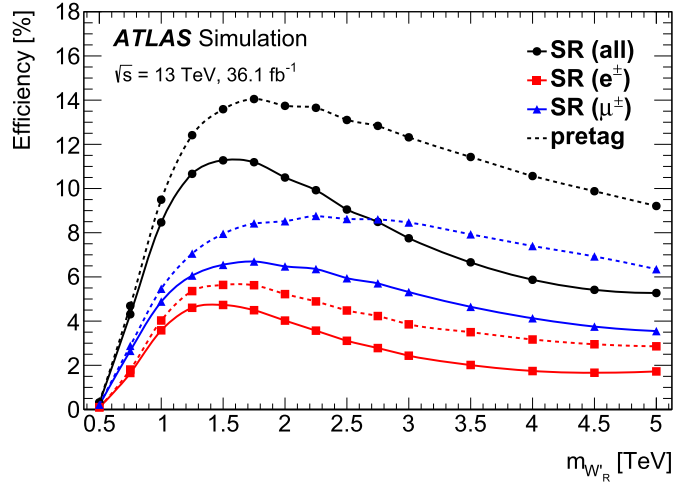


Fig. 2. Signal selection efficiency (efficiency is defined as the number of events passing all selections divided by the total number of simulated $W' \rightarrow t\bar{b} \rightarrow \ell\nu b\bar{b}$ events) in the signal region as a function of the simulated W'_R mass. Efficiencies are shown for: all channels combined (full circle), electron channels only (full square) and muon channels only (full triangle). For reference, signal efficiency curves are also shown without the requirement on b -tagging (pretag selection: dotted lines).

W' masses, and falls below 10^{-4} for W' masses above 3 TeV. The event selection criteria for each region are summarized in Table 2.

The signal selection efficiency (defined as the number of events passing all selection requirements divided by the total number of simulated $W' \rightarrow t\bar{b} \rightarrow \ell\nu b\bar{b}$ events) in the signal region is shown, as a function of the simulated W'_R mass, in Fig. 2. Selection efficiency curves are shown for the electron and muon channels separately, as well as for the pretag selection. Due to the jet p_T and $\Delta R(\ell, b_{\text{top}})$ requirements, the signal has vanishing efficiency for a W'_R mass of 500 GeV, but the efficiency rises as the decay products become more boosted. The maximum SR signal efficiency, 11.3%, is obtained for a mass of 1.5 TeV, then the efficiency decreases for higher masses to 5.3% at 5 TeV. The application of the b -tagging requirement has a larger impact on the signal efficiency at high W'_R boson mass values. In the electron channel the electron–jet overlap criterion does not allow the electron to be close ($\Delta R(\ell, \text{jet}) < 0.4$) to the jet. In the muon channel, this criterion is relaxed by using a variable ΔR cone size, resulting in an improved signal acceptance.

5. Background estimation

The $t\bar{t}$, single-top-quark, diboson and W/Z +jets backgrounds are modeled using the simulated MC samples and are normalized to the theory predictions of the inclusive cross sections, while the multijet background is estimated using the data as described below in this section. Each of these background samples gives rise to individual differential m_{tb} templates predicting their unique kinematic properties. These initial background normalizations are taken as

starting values, and the final normalization is determined through a maximum-likelihood fit of the background templates to the data in which the background normalizations are parameters of the fit (described in Section 7). Because the signal regions are dominated by $t\bar{t}$ and W +jets production, the normalization of these backgrounds is allowed to float freely in the maximum-likelihood fit with no prior.

The background arising from multijet production consists of events with a jet that is misreconstructed as a lepton or with a non-prompt lepton that satisfies the lepton identification criteria. The simulation of this background source is challenging as it suffers from large systematic uncertainties and does not reliably reproduce the observed data in regions enriched with multijet events. Therefore the multijet background is estimated from data with the so-called *matrix method*, which is used to disentangle the mixture of non-prompt leptons found in the multijet background and prompt leptons originating from W/Z bosons [75]. This method uses a data sample, with loosened identification criteria, dominated by multijet production and with a small contamination of electroweak (EW) W/Z -jets production. The probability that a jet from multijet production which passes the loose selection also satisfies the tight selection criteria is estimated in this control region. The multijet purity in this sample is improved by subtracting, using MC simulation, the EW contamination to remove bias due to prompt-lepton sources. The efficiency for prompt leptons passing the loose selection to also pass the tight selection is determined using $t\bar{t}$ MC samples, corrected using comparisons of MC and data $Z \rightarrow \ell\ell$ events. The number of multijet background events satisfying the selection criteria is estimated from these efficiencies using data events that satisfy all criteria, except that loose lepton identification criteria are used. While this data-driven method is a significant improvement on the use of MC simulation, the low number of events and inherent systematic variations of the EW contribution lead to a significant systematic uncertainty. Systematic uncertainties on the multijet background are evaluated [76] using various definitions of multijet control regions and by considering systematic uncertainties associated with object reconstruction and MC simulation. The uncertainty on this background is taken as 50% of the total rate and treated as uncorrelated between selected regions.

Fig. 3 shows the distributions of the reconstructed invariant mass of the W' boson candidate for data and for background predictions in the 2-jet 1-tag VR_{HF} and 4-jet 2-tag $VR_{t\bar{t}}$ validation regions. Background templates are fit to data in each VR using the same statistical method as for the signal region except that the normalizations of $t\bar{t}$ and W +jets backgrounds are constrained to the post-fit rates obtained in the signal region (see Section 7).

6. Systematic uncertainties

Two primary sources of systematic uncertainty, experimental and modeling, affect the reconstruction of the m_{tb} distributions. Experimental uncertainties arise due to the trigger selection, the object reconstruction and identification, as well as the object energy, momentum and mass calibrations and their resolutions. Modeling uncertainties result in shape and normalization uncertainties of the different MC samples used to model the signal and backgrounds. These stem from uncertainties in the generator matrix-element calculation, the choice of parton shower and hadronization models and their parameter values, the PDF set and the choice of renormalization and factorization scales. The impact on the signal and background event yields of the main systematic uncertainties is summarized in Table 3, wherein the uncertainty on the overall yield is presented for each background source. All values are given as a percentage change in overall yield and represent the

prior values assigned before fitting. The source of each uncertainty is described in this section, and uncertainties are considered fully correlated across all eight signal regions and among processes, unless specifically noted.

The selection of jets and E_T^{miss} has an associated uncertainty related to the calorimeter calibration of the energy scale and the calorimeter resolution, as well as to the identification/reconstruction efficiencies of objects reconstructed using the calorimeter, sample flavor composition and corrections for pile-up and neutrinos produced in hadron decays. The uncertainty contributed by each source is typically 1–5% of the expected event rates and can impact the shape of differential distributions. In addition, the E_T^{miss} calculation leads to a typical uncertainty in the event yield of less than 1%.

The process of b -tagging jets has an uncertainty in the scale factors required to match the tagging efficiency between data and simulation. These uncertainties are evaluated independently for jets arising from b -quarks, c -quarks and light-quarks or gluons. The uncertainty in the selection efficiency for tagging b -quarks is typically small (1–5% per jet) except for very high p_T jets where it can increase to 6% per jet, and the mis-tagging of c -light-quarks and gluons can be as large as 10%. These sources of uncertainty can additionally induce non-uniform variations in differential distributions of up to 10%.

The uncertainty in the reconstruction efficiency and acceptance of leptons due to trigger, reconstruction and selection efficiencies in simulated samples is roughly 1% of the total event yield. The energy/momentum scale and resolution for leptons is corrected in simulation to match data measurements, and the resulting uncertainty in the efficiency arising from these corrections is less than 1–2%.

The normalization of simulated samples has an associated uncertainty that varies by production process. The uncertainty in the cross section times branching fraction for single-top and diboson production is taken as 6% [77–79] and 11% [80], respectively. An uncertainty of 20% is assumed for Z +jets rate, which represents a very small background, in line with the modeling uncertainty assigned for W +jets (see below in this section). The cross sections for the $t\bar{t}$ and W +jets samples are normalized using freely floating parameters whose values are determined by fitting to data. All simulated samples that are normalized to the ATLAS luminosity measurement are assigned a luminosity uncertainty of 2.1%. This uncertainty is derived, following a methodology similar to that detailed in Ref. [81], from a calibration of the luminosity scale using x - y beam-separation scans performed in August 2015 and May 2016.

Differences due to the choice of MC generator, fragmentation/hadronization model, and initial/final-state radiation model are treated as a source of uncertainty for the $t\bar{t}$ and t -channel single-top-quark simulations. The uncertainty due to the choice of MC generator is evaluated as the difference in yield between the nominal choice of POWHEG-Box and the alternative MADGRAPH5_AMC@NLO [82] generator, using Herwig++ [83,84] for showering in both instances. The uncertainty due to the fragmentation/hadronization model is evaluated by comparing PYTHIA6 and Herwig++ simulated samples. Variations of the amount of additional radiation are studied by changing the scale of the hard-scatter process and the scales in parton-shower simulation simultaneously using the POWHEG-Box+PYTHIA6 set-up. In these samples, a variation of the factorization and renormalization scales by a factor of two is combined with the Perugia2012radLo tune and a variation of both scales by a factor of 0.5 is combined with the Perugia2012radHi tune [45]. In the case of $t\bar{t}$ production the POWHEG-Box h_{damp} parameter, which controls the transverse momentum of the first additional emission beyond the Born con-

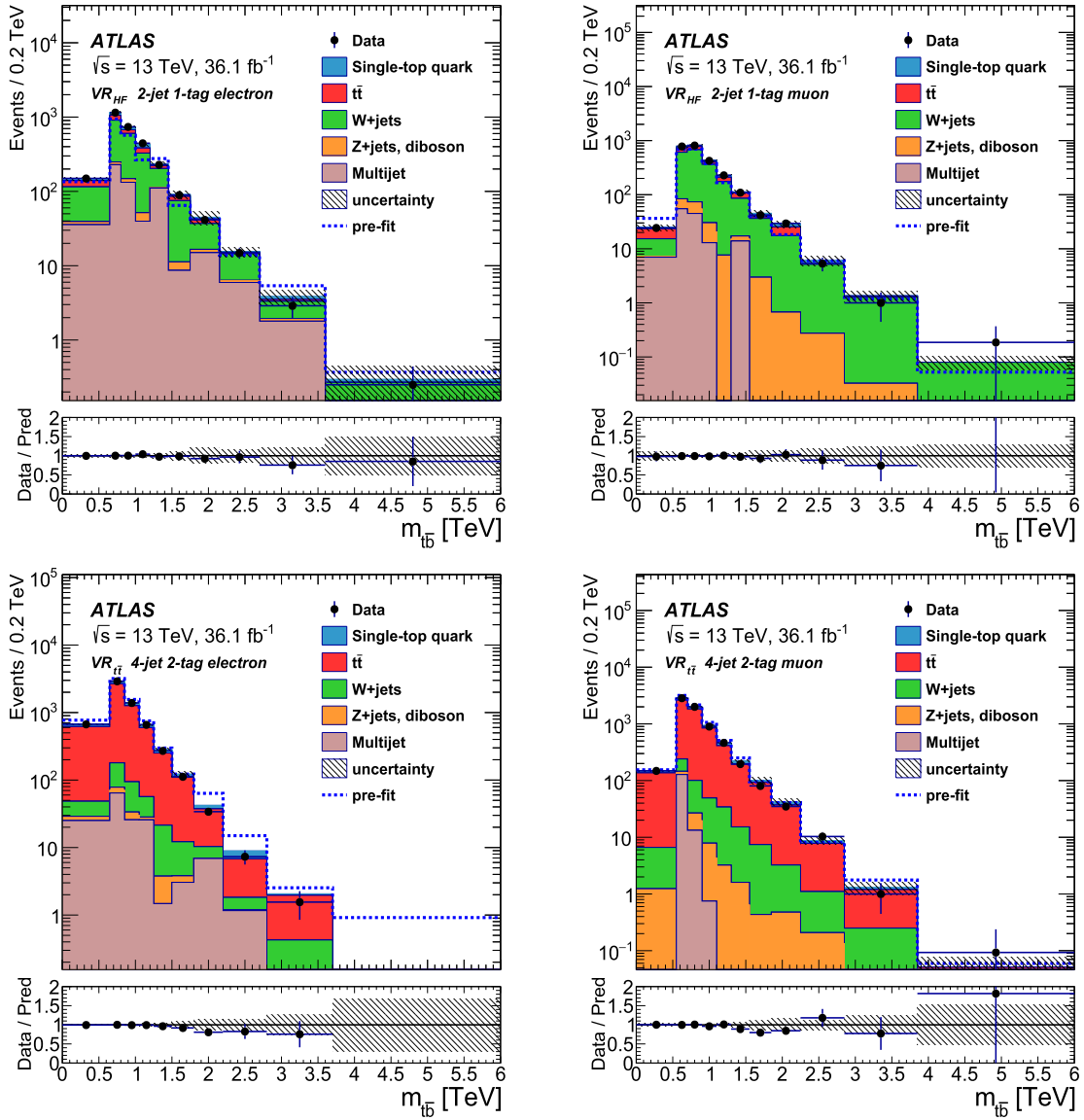


Fig. 3. Distributions of the reconstructed invariant mass of the W' boson candidate in the (top) 2-jet 1-tag VR_{HF} and (bottom) 4-jet 2-tag VR_{tt} validation regions. Background templates are fit to data in each VR using the same statistical method as for the signal region except that the normalizations of $t\bar{t}$ and W +jets backgrounds are constrained to the post-fit rates obtained in the signal region (see Section 7). The pre-fit line presents the background prediction before the fit is performed. Uncertainty bands include all the systematic and statistical uncertainties. The residual difference between the data and MC yields is shown as a ratio in the bottom portion of each figure, wherein the error bars on the data points correspond to the data Poisson uncertainty.

figuration, is also changed simultaneously, using values of m_{top} and $2 \times m_{top}$, respectively. An uncertainty associated with the NLO calculation of Wt production [85] is evaluated by comparing the baseline sample generated with the diagram removal scheme to a Wt sample generated with the diagram subtraction scheme.

These differences yield relative variations in shape and normalization of 1–3% on average, although the variation can be larger than 10% in the highest m_{tb} regions probed. The normalization component of these modeling uncertainties is removed for the $t\bar{t}$ samples because the overall normalization is determined via the data in this case.

Differences between the predictions for the ratio of 2-jet to 3-jet yields from different showering simulations were studied for the $t\bar{t}$ and W +jets simulation. These differences are estimated by simultaneously varying the renormalization and factorization scales, and by using different MC generators. While only small differences were observed for $t\bar{t}$ simulation, the ratio of the yields of

2-jet to 3-jet selections in W +jets simulation varied by up to 20%. Thus, an additional uncertainty of 20% is assigned to the W +jets yield in the 3-jet selection.⁴

Uncertainties in W +jets modeling are determined by comparing the nominal SHERPA simulation with an alternative sample produced with the MADGRAPH5_AMC@NLO generator interfaced to PYTHIA8 for parton showering and hadronization. The uncertainty in our knowledge of the flavor fraction in the W +jets sample is tested by splitting the W +jets sample into light-quark/gluon and heavy-flavor components and by decorrelating the W +jets shape uncertainty between 2-jet and 3-jet events. In each case, no significant effect on the extracted results is observed.

⁴ For the Z +jets background a similar variation could be expected, but since this background is minor, a 20% constant rate uncertainty is simply assumed.

Table 3

Impact of the main sources of uncertainty on the signal and background event yields. All values are given as a percentage change in the overall yield and represent the prior values assigned before fitting. Uncertainties for the signal are given for a W'_R mass hypothesis of 2 TeV. Uncertainties in the background are the same for all signal masses. Systematic uncertainties in the normalization, 2-jet vs 3-jet region cross-extrapolation, and reconstructed m_{tb} shape of the signal and background processes are described in the text. Sources of uncertainty may affect both the total event yield and the shape of the m_{tb} distribution. An “S” indicates that a shape variation has been included, in addition to the rate variation, due to the sources listed. “U” refers to regions that are not correlated with one another and “F” refers to a normalization that floats freely. In certain instances of freely floating normalizations, the rate variation of systematic effects is removed, thus leaving only a shape variation. Such cases are indicated with a “*” symbol. The “Jets” column includes uncertainties related to E_T^{miss} . A range of values correspond to the lowest and the highest values determined across different channels in the SR. The final column describes the uncertainty in extrapolating event yields between the 2-jet and 3-jet selections.

Process	Norm.	Lumi.	b -Tagging [S]	Jets [S]	Leptons	Modeling [S]	2j/3j Extrap.
W'_R	–	2.1	8–12	1–4	1–2	–	–
$t\bar{t}$	F	–	2–6	4–8	1–2	0 [*]	–
W +jets	F	–	6–15	2–12	1–3	0 [*]	20
Z +jets	20	2.1	6–12	2–9	1–3	–	–
Diboson	11	2.1	3–10	2–8	1–2	–	–
Single top quark	6	2.1	2–7	1–4	1–2	6–22	–
Multijet	50 [U]	–	–	–	–	–	–

Table 4

The numbers of signal and background events and the numbers of observed data events are shown in the 2-jet 1-tag and 3-jet 1-tag signal regions. For signal, the values correspond to expected event yields and quoted uncertainties account for the statistical uncertainty of the number of events in the simulated samples. The number of background events is obtained following a ML fit to the data and uncertainties contain statistical and systematic uncertainties.

	2-jet 1-tag (e^\pm)			2-jet 1-tag (μ^\pm)			3-jet 1-tag (e^\pm)			3-jet 1-tag (μ^\pm)		
W'_R (1.0 TeV)	1517	±	32	2030	±	40	1159	±	31	1665	±	35
W'_R (2.0 TeV)	83.4	±	1.7	132.9	±	2.1	105.0	±	1.9	167.4	±	2.2
W'_R (3.0 TeV)	4.7	±	0.1	10.4	±	0.2	7.0	±	0.2	15.7	±	0.2
W'_R (4.0 TeV)	0.43	±	0.01	1.01	±	0.02	0.64	±	0.02	1.62	±	0.03
W'_R (5.0 TeV)	0.076	±	0.002	0.153	±	0.003	0.096	±	0.003	0.232	±	0.004
$t\bar{t}$	1112	±	23	1505	±	28	3220	±	50	4090	±	70
Single-top	472	±	20	657	±	25	482	±	21	624	±	24
W +jets	520	±	50	1280	±	120	550	±	40	1130	±	90
Multijets	358	±	35	630	±	100	196	±	20	390	±	60
Z +jets, diboson	129	±	14	211	±	19	128	±	12	242	±	20
Total background	2590	±	60	4290	±	160	4580	±	70	6470	±	130
Data	2622			4260			4555			6433		

The uncertainty in the yield of simulated $t\bar{t}$ background events due to the choice of PDF is evaluated using the PDF4LHC recommendations [86]. The statistical uncertainty of the limited MC samples is included in each histogram bin of the m_{tb} distribution.

7. Results

In order to test for the presence of a massive resonance, the m_{tb} templates obtained from the signal and background simulated event samples are fit to data using a binned maximum-likelihood (ML) approach based on the RooStats framework [87–89]. Each signal region selection is considered simultaneously as an independent search channel, for a total of eight regions corresponding to mutually exclusive categories of electron and muon, 2-jet and 3-jet, and 1- b -tag and 2- b -tags.

The normalizations of the $t\bar{t}$ and W +jets backgrounds are free parameters in the fit, while other background normalizations are assigned Gaussian priors based on their respective normalization uncertainties. The systematic uncertainties described in Section 6 are incorporated in the fit as nuisance parameters with correlations across regions and processes taken into account. The signal normalization is a free parameter in the fit.

The expected and observed event yields after the ML fit are shown in Tables 4 and 5 and correspond to an integrated luminosity of 36.1 fb^{-1} . The fitted $t\bar{t}$ and W +jets rates relative to their nominal predictions are found to be 0.98 ± 0.04 and 0.78 ± 0.19 , respectively. For these two backgrounds the total uncertainty reported in the event yield tables is smaller than the uncertainty in

the fitted normalization factor because there are anticorrelations between nuisance parameters in the likelihood fit.

The m_{tb} distributions for the SR after the ML fit are shown in Figs. 4 and 5. An expected signal contribution corresponding to a W'_R boson with a mass of 2.0 TeV is shown as a dashed histogram overlay. The binning of the m_{tb} distribution is chosen to optimize the search sensitivity while minimizing statistical fluctuations. Requirements are imposed on the expected number of background events per bin, and the bin width is adapted to a resolution function that represents the width of the reconstructed mass peak for each studied W'_R boson signal sample.

For a W'_R boson with a mass of 2 TeV and nominal $g'/g = 1$ coupling the total expected uncertainty in estimating the signal strength⁵ is 12%. The total systematic uncertainty is 9%, and the largest uncertainties are due to the $t\bar{t}$ generator (4.0%), jet energy scale (JES) (2.8%), $t\bar{t}$ showering (2.5%), $t\bar{t}$ normalization (2.0%) and JES η intercalibration modeling (1.3%). For resonances with a mass of 2.5 TeV or above, the data Poisson uncertainty becomes the largest uncertainty in estimating the signal rate, while the total systematic uncertainty is dominated by the uncertainty on the b -tagging efficiency.

As no significant excess over the background prediction is observed, upper limits at the 95% confidence level (CL) are set on the production cross section times the branching fraction for

⁵ The signal strength is defined as the ratio of the signal cross section estimated using the data to the predicted signal cross section.

Table 5

The numbers of signal and background events and the numbers of observed data events are shown in the 2-jet 2-tag and 3-jet 2-tag signal regions. For signal, the values correspond to expected event yields and quoted uncertainties account for the statistical uncertainty of the number of events in the simulated samples. The number of background events is obtained following a ML fit to the data and uncertainties contain statistical and systematic uncertainties.

	2-jet 2-tag (e^\pm)			2-jet 2-tag (μ^\pm)			3-jet 2-tag (e^\pm)			3-jet 2-tag (μ^\pm)		
W'_R (1.0 TeV)	1584	\pm	35	2060	\pm	40	1241	\pm	30	1749	\pm	34
W'_R (2.0 TeV)	33.5	\pm	1.0	55.5	\pm	1.2	51.6	\pm	1.2	84.3	\pm	1.5
W'_R (3.0 TeV)	1.4	\pm	0.1	2.6	\pm	0.1	2.5	\pm	0.1	5.1	\pm	0.1
W'_R (4.0 TeV)	0.131	\pm	0.007	0.25	\pm	0.01	0.21	\pm	0.01	0.46	\pm	0.01
W'_R (5.0 TeV)	0.035	\pm	0.002	0.053	\pm	0.002	0.044	\pm	0.002	0.080	\pm	0.002
$t\bar{t}$	536	\pm	14	789	\pm	16	2459	\pm	31	3200	\pm	40
Single-top	121	\pm	6	176	\pm	10	235	\pm	12	347	\pm	17
W +jets	28	\pm	6	42	\pm	4.0	50	\pm	5	97	\pm	9
Multijets	36	\pm	6	71	\pm	13	95	\pm	11	135	\pm	22
Z +jets, diboson	2.5	\pm	0.4	11.5	\pm	1.3	21.2	\pm	2.1	26.9	\pm	2.3
Total background	723	\pm	16	1088	\pm	21	2859	\pm	33	3810	\pm	50
Data	683			1091			2869			3797		

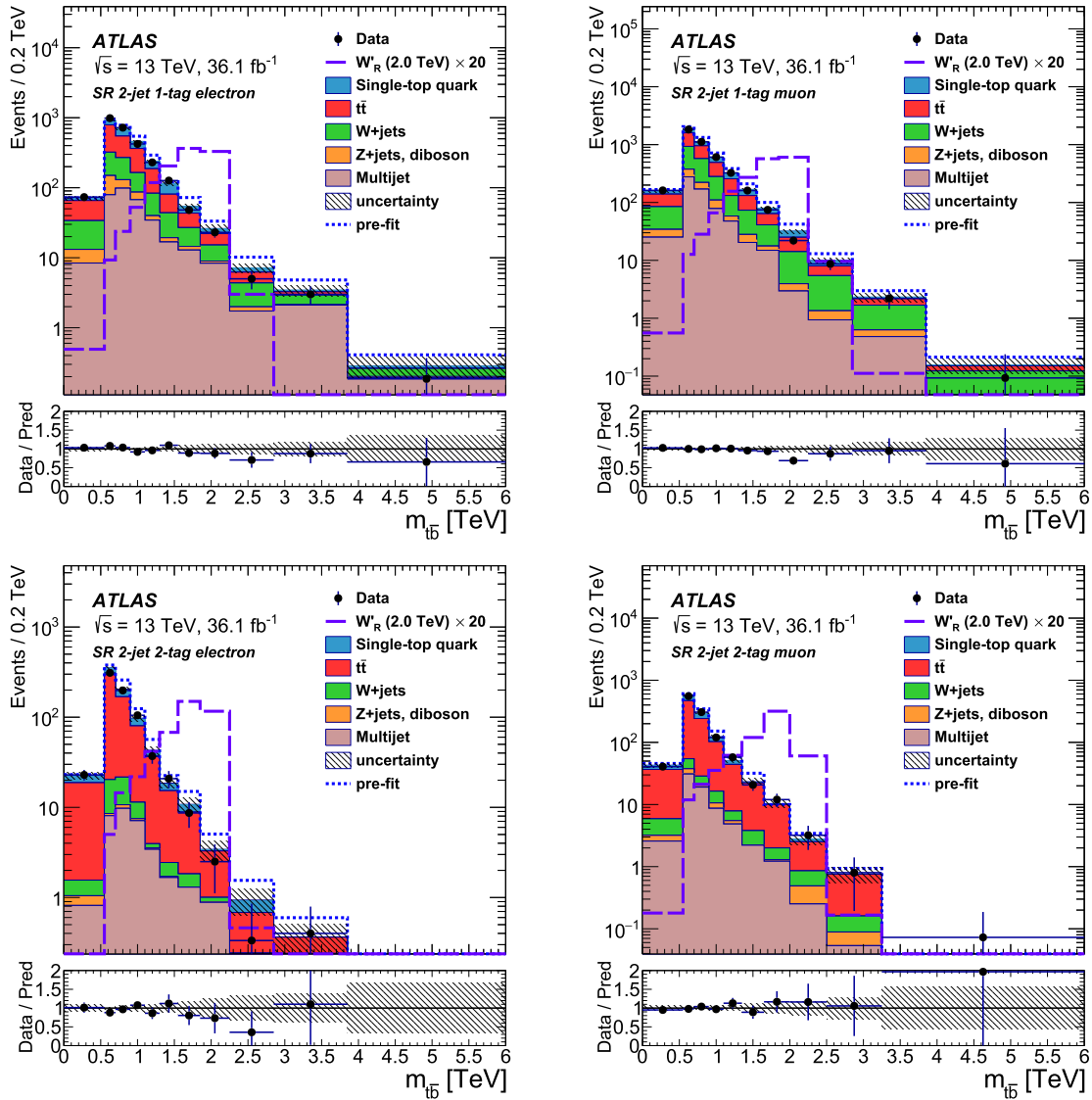


Fig. 4. Post-fit distributions of the reconstructed mass of the W'_R boson candidate in the (top) 2-jet 1-tag and (bottom) 2-jet 2-tag signal regions, for (left) electron and (right) muon channels. An expected signal contribution corresponding to a W'_R boson mass of 2.0 TeV enhanced 20 times is shown. The pre-fit line presents the background prediction before the fit is performed. Uncertainty bands include all the systematic and statistical uncertainties. The residual difference between the data and MC yields is shown as a ratio in the bottom portion of each figure, wherein the error bars on the data points correspond to the data Poisson uncertainty.

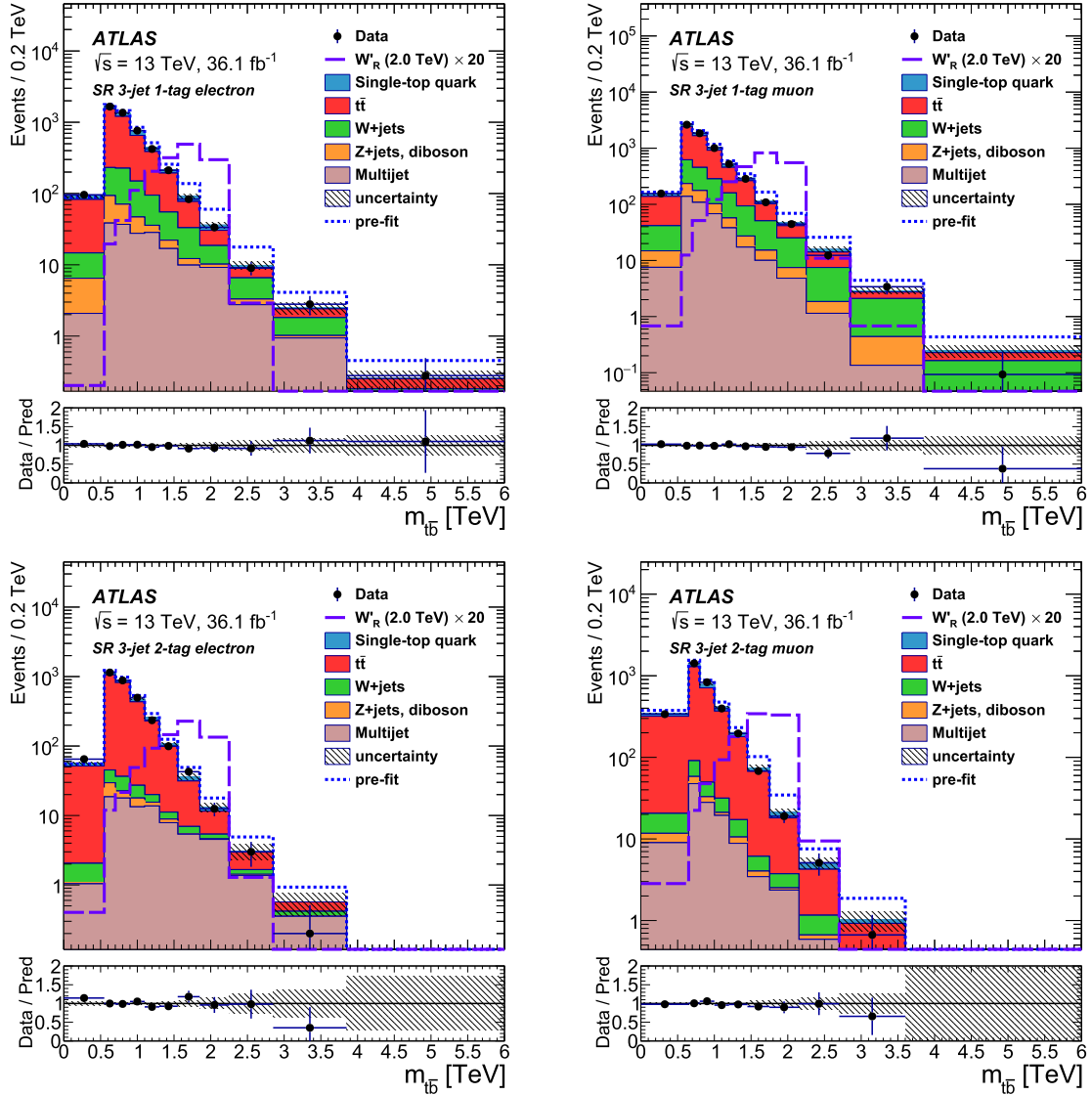


Fig. 5. Post-fit distributions of the reconstructed mass of the W'_R boson candidate in the (top) 3-jet 1-tag and (bottom) 3-jet 2-tag signal regions, for (left) electron and (right) muon channels. An expected signal contribution corresponding to a W'_R boson mass of 2.0 TeV enhanced 20 times is shown. The pre-fit line presents the background prediction before the fit is performed. Uncertainty bands include all the systematic and statistical uncertainties. The residual difference between the data and MC yields is shown as a ratio in the bottom portion of each figure, wherein the error bars on the data points correspond to the data Poisson uncertainty.

each model. The limits are evaluated using a modified frequentist method known as CL_s [90] with a profile-likelihood-ratio test statistic [91] using the asymptotic approximation.

The 95% CL upper limits on the production cross section multiplied by the branching fraction for $W'_R \rightarrow t\bar{b}$ are shown in Fig. 6 as a function of the resonance mass. The observed and expected limits are derived using a linear interpolation between simulated signal mass hypotheses. The exclusion limits range between 4.9 pb and 2.9×10^{-2} pb for W'_R boson masses from 0.5 TeV to 5 TeV. The lower observed limits for W'_R masses around 2.5 TeV are due to a deficit of data events in the 2–2.5 TeV $m_{t\bar{b}}$ range in the 2-jet 1-tag and 3-jet 1 tag (muon) signal regions. The existence of W'_R bosons with masses $m_{W'_R} < 3.15$ TeV is excluded for the ZTOP benchmark model for W'_R , assuming that the W'_R coupling g' is equal to the SM weak coupling constant g .

Limits on the ratio of couplings g'/g as a function of the W'_R boson mass can be derived from the limits on the W'_R boson cross section. Limits can also be set for $g'/g > 1$, as models remain perturbative up to a ratio of about five [30]. The W'_R boson cross sec-

tion has a dependence on the coupling g' , coming from the variation of the resonance width. The scaling of the W'_R boson cross section as a function of g'/g and $m_{W'_R}$ is estimated at NLO using the ZTOP generator. In addition, specific signal samples are used in order to take into account the effect on the acceptance and on kinematical distributions of the increased signal width (compared with the nominal samples) for values of $g'/g > 1$. Fig. 7 shows the excluded parameter space as a function of the W'_R resonance mass, wherein the effect of increasing W'_R width for coupling values of $g'/g > 1$ is included for signal acceptance and differential distributions. The lowest observed (expected) limit on g'/g , obtained for a W'_R boson mass of 0.75 TeV, is 0.13 (0.13).

The ATLAS experiment has recently searched for $W'_R \rightarrow t\bar{b}$ in the fully hadronic final state [27] using 36.1 fb^{-1} , corresponding to the same data collection period as the analysis presented here. As these two searches are complementary and use mutually orthogonal event selections, a more general and powerful search for $W'_R \rightarrow t\bar{b}$ production can be obtained via their statistical combination. The signal simulation was produced in the same manner for

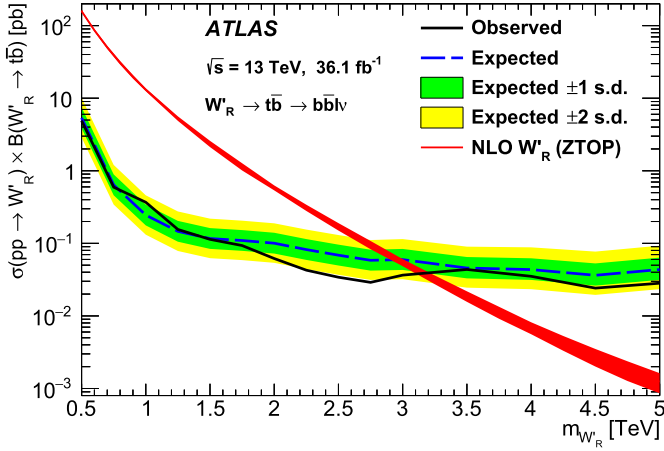


Fig. 6. Upper limits at the 95% CL on the W'_R production cross section times the $W'_R \rightarrow t\bar{b}$ branching fraction as a function of resonance mass, assuming $g'/g = 1$. The solid curve corresponds to the observed limit, while the dashed curve and shaded bands correspond to the limit expected in the absence of signal and the regions enclosing one/two standard deviation (s.d.) fluctuations of the expected limit. The prediction made by the benchmark model generator ZTOP [30], and its width that correspond to variations due to scale and PDF uncertainty, are also shown.

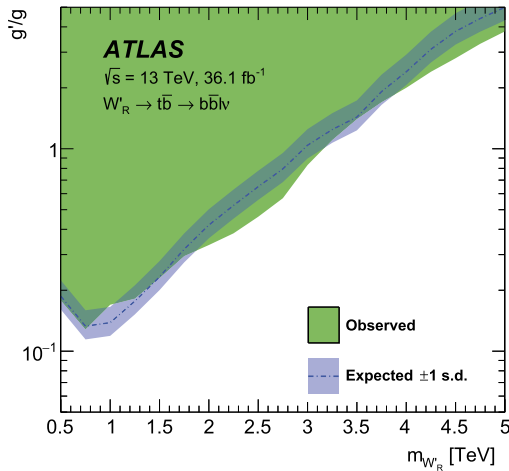


Fig. 7. Observed and expected 95% CL limit on the ratio g'/g , as a function of resonance mass, for right-handed W' coupling. The filled area correspond to the observed limit while the dashed line and the one standard deviation (s.d.) band correspond the expected limit. The impact of the increased W'_R width for coupling values of $g'/g > 1$ on the acceptance and on kinematical distributions is taken into account.

both searches, and the simulation of shared background sources is obtained with identical or similar tools. The fully hadronic search has a background dominated by QCD multijet production, which is estimated via data-driven methods. The smaller contribution from $t\bar{t}$ and singly produced top quarks is common to the two analyses, and thus all systematic uncertainties related to shared reconstruction or selection methods are treated as fully correlated.

The result of the combination of the cross section times branching fraction limits of the leptonic and fully hadronic analyses is shown in Fig. 8. The individual limits and their combination are shown in Fig. 9. The expected limits produced by the two searches are similar above a resonance mass of 2 TeV, below which the fully hadronic search suffers due to inefficiency from dijet trigger thresholds causing it not to contribute for resonance masses below 1 TeV. Thus, the expected limits on the production cross section multiplied by the branching fraction improve by approximately 35% above 1 TeV and the combined result raises the lower limit on

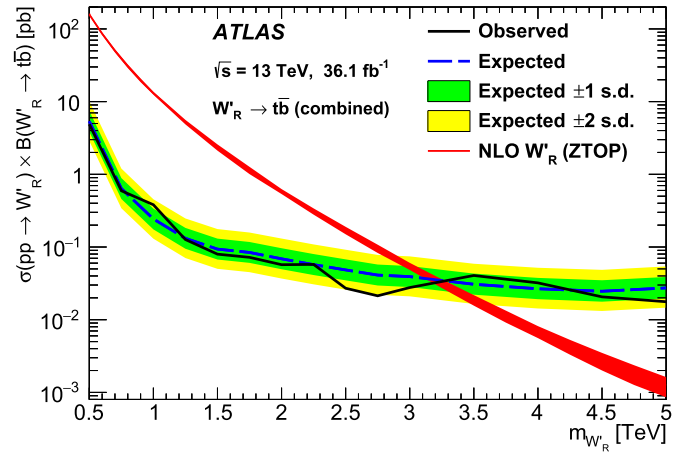


Fig. 8. Observed and expected 95% CL upper limit on the W'_R production cross section times the $W'_R \rightarrow t\bar{b}$ branching fraction as a function of resonance mass for the combination of semileptonic and hadronic [27] $W' \rightarrow t\bar{b}$ searches, assuming $g'/g = 1$. The hadronic search covers a mass range between 1.0 and 5.0 TeV. The solid black curve corresponds to the observed limit, while the dashed curve and shaded bands correspond to the limit expected in the absence of signal and the regions enclosing one/two standard deviation (s.d.) fluctuations of the expected limit. The prediction made by the benchmark model generator ZTOP [30], and its width that correspond to variations due to scale and PDF uncertainty, are also shown.

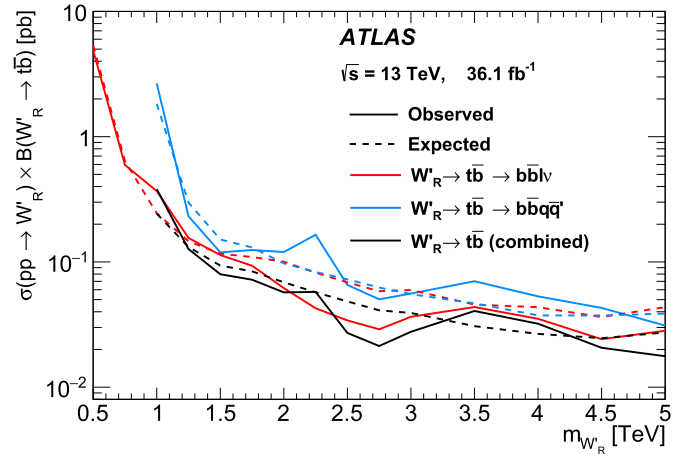


Fig. 9. Observed and expected 95% CL upper limit on the W'_R production cross section times the $W'_R \rightarrow t\bar{b}$ branching fraction as a function of resonance mass, for the semileptonic and hadronic [27] $W' \rightarrow t\bar{b}$ searches, as well as their combination. The solid curves correspond to the observed upper limits, while the dashed lines are the expected limits.

the W'_R mass to 3.25 TeV. On the other hand, the gain from combining the observed cross section times branching fraction limits is rather modest, compared with the result of the leptonic analysis only, because of upward fluctuations observed in the fully hadronic analysis data.

8. Conclusion

A search for $W'_R \rightarrow t\bar{b}$ in the lepton plus jets final state is performed using 36.1 fb⁻¹ of 13 TeV pp collision data collected with the ATLAS detector at the LHC. No significant excess of events is observed above the SM predictions. Upper limits are placed at the 95% CL on the cross section times branching fraction, $\sigma(pp \rightarrow W'_R \rightarrow t\bar{b})$, ranging between 4.9 pb and 2.9×10^{-2} pb in the mass range of 0.5 TeV to 5 TeV for a right-handed W' boson. Exclusion limits are also calculated for the ratio of the couplings g'/g

and the lowest observed limit, obtained for a W'_R boson mass of 0.75 TeV, is 0.13. A statistical combination of the cross-section limits is performed with the results obtained when the fully hadronic decays of $W'_R \rightarrow t\bar{b}$ are considered. The upper limits on the cross section times branching fraction improve by approximately 35% above 1 TeV. Masses below 3.15 (3.25) TeV are excluded for W'_R bosons in the benchmark ZTOP model for the semileptonic (combined semileptonic and hadronic) scenarios.

Acknowledgements

We thank CERN for the very successful operation of the LHC, as well as the support staff from our institutions without whom ATLAS could not be operated efficiently.

We acknowledge the support of ANPCyT, Argentina; YerPhI, Armenia; ARC, Australia; BMWFW and FWF, Austria; ANAS, Azerbaijan; SSTC, Belarus; CNPq and FAPESP, Brazil; NSERC, NRC and CFI, Canada; CERN; CONICYT, Chile; CAS, MOST and NSFC, China; COLCIENCIAS, Colombia; MSMT CR, MPO CR and VSC CR, Czech Republic; DNRF and DNSRC, Denmark; IN2P3-CNRS, CEA-DRF/IRFU, France; SRNSFG, Georgia; BMBF, HGF, and MPG, Germany; GSRT, Greece; RGC, Hong Kong SAR, China; ISF and Benoziyo Center, Israel; INFN, Italy; MEXT and JSPS, Japan; CNRST, Morocco; NWO, Netherlands; RCN, Norway; MNiSW and NCN, Poland; FCT, Portugal; MNE/IFA, Romania; MES of Russia and NRC KI, Russian Federation; JINR; MESTD, Serbia; MSSR, Slovakia; ARRS and MIZŠ, Slovenia; DST/NRF, South Africa; MINECO, Spain; SRC and Wallenberg Foundation, Sweden; SERI, SNSF and Cantons of Bern and Geneva, Switzerland; MOST, Taiwan; TAEK, Turkey; STFC, United Kingdom; DOE and NSF, United States of America. In addition, individual groups and members have received support from BCKDF, the Canada Council, Canarie, CRC, Compute Canada, FQRNT, and the Ontario Innovation Trust, Canada; EPLANET, ERC, ERDF, FP7, Horizon 2020 and Marie Skłodowska-Curie Actions, European Union; Investissements d'Avenir Labex and Idex, ANR, Région Auvergne and Fondation Partager le Savoir, France; DFG and AvH Foundation, Germany; Herakleitos, Thales and Aristeia programmes co-financed by EU-ESF and the Greek NSRF; BSF, GIF and Minerva, Israel; BRF, Norway; CERCA Programme Generalitat de Catalunya, Generalitat Valenciana, Spain; the Royal Society and Leverhulme Trust, United Kingdom.

The crucial computing support from all WLCG partners is acknowledged gratefully, in particular from CERN, the ATLAS Tier-1 facilities at TRIUMF (Canada), NDGF (Denmark, Norway, Sweden), CC-IN2P3 (France), KIT/GridKA (Germany), INFN-CNAF (Italy), NL-T1 (Netherlands), PIC (Spain), ASGC (Taiwan), RAL (UK) and BNL (USA), the Tier-2 facilities worldwide and large non-WLCG resource providers. Major contributors of computing resources are listed in Ref. [92].

References

- [1] G. Burdman, B.A. Dobrescu, E. Ponton, Resonances from two universal extra dimensions, *Phys. Rev. D* 74 (2006) 075008, arXiv:hep-ph/0601186.
- [2] H.-C. Cheng, C.T. Hill, S. Pokorski, J. Wang, Standard model in the latticized bulk, *Phys. Rev. D* 64 (2001) 065007, arXiv:hep-th/0104179.
- [3] T. Appelquist, H.-C. Cheng, B.A. Dobrescu, Bounds on universal extra dimensions, *Phys. Rev. D* 64 (2001) 035002, arXiv:hep-ph/0012100.
- [4] J.C. Pati, A. Salam, Lepton number as the fourth "color", *Phys. Rev. D* 10 (1974) 275–289.
- [5] R.N. Mohapatra, J.C. Pati, Left-right gauge symmetry and an "isoconjugate" model of CP violation, *Phys. Rev. D* 11 (1975) 566–571.
- [6] G. Senjanovic, R.N. Mohapatra, Exact left-right symmetry and spontaneous violation of parity, *Phys. Rev. D* 12 (1975) 1502–1505.
- [7] M. Perelstein, Little Higgs models and their phenomenology, *Prog. Part. Nucl. Phys.* 58 (2007) 247–291, arXiv:hep-ph/0512128.
- [8] M.J. Dugan, H. Georgi, D.B. Kaplan, Anatomy of a composite Higgs model, *Nucl. Phys. B* 254 (1985) 299.
- [9] K. Agashe, R. Contino, A. Pomarol, The minimal composite Higgs model, *Nucl. Phys. B* 719 (2005) 165–187, arXiv:hep-ph/0412089.
- [10] D0 Collaboration, Search for W' bosons decaying to an electron and a neutrino with the D0 detector, *Phys. Rev. Lett.* 100 (2008) 031804, eprint, arXiv:0710.2966.
- [11] CDF Collaboration, Search for a new heavy gauge boson W' with event signature electron + missing transverse energy in $p\bar{p}$ collisions at $\sqrt{s} = 1.96$ TeV, *Phys. Rev. D* 83 (2011) 031102, arXiv:1012.5145.
- [12] CMS Collaboration, Search for physics beyond the standard model in final states with a lepton and missing transverse energy in proton–proton collisions at $\sqrt{s} = 8$ TeV, *Phys. Rev. D* 91 (2015) 092005, arXiv:1408.2745 [hep-ex].
- [13] ATLAS Collaboration, Search for new particles in events with one lepton and missing transverse momentum in pp collisions at $\sqrt{s} = 8$ TeV with the ATLAS detector, *J. High Energy Phys.* 09 (2014) 037, arXiv:1407.7494 [hep-ex].
- [14] ATLAS Collaboration, Search for new resonances in events with one lepton and missing transverse momentum in pp collisions at $\sqrt{s} = 13$ TeV with the ATLAS detector, *Phys. Lett. B* 762 (2016) 334, arXiv:1606.03977 [hep-ex].
- [15] CMS Collaboration, Search for heavy gauge W' boson in events with an energetic lepton and large missing transverse momentum at $\sqrt{s} = 13$ TeV, *Phys. Lett. B* 770 (2017) 278, arXiv:1612.09274 [hep-ex].
- [16] C. Patrignani, et al., *Rev. Particle Phys.*, *Chin. Phys. C* 40 (2016) 100001.
- [17] D.J. Muller, S. Nandi, Topflavor: a separate SU(2) for the third family, *Phys. Lett. B* (ISSN 0370-2693) 383 (1996) 345–350.
- [18] E. Malkawi, T.M. Tait, C. Yuan, A model of strong flavor dynamics for the top quark, *Phys. Lett. B* 385 (1996) 304–310, arXiv:hep-ph/9603349.
- [19] D0 Collaboration, Search for $W' \rightarrow t\bar{b}$ resonances with left- and right-handed couplings to fermions, *Phys. Lett. B* 699 (2011) 145–150, arXiv:1101.0806.
- [20] CDF Collaboration, Search for the production of narrow t anti- b resonances in 1.9 fb^{-1} of $p\bar{p}$ collisions at $\sqrt{s} = 1.96$ TeV, *Phys. Rev. Lett.* 103 (2009) 041801, arXiv:0902.3276.
- [21] ATLAS Collaboration, Search for $t\bar{b}$ resonances in proton–proton collisions at $\sqrt{s} = 7$ TeV with the ATLAS detector, *Phys. Rev. Lett.* 109 (2012) 081801, arXiv:1205.1016.
- [22] CMS Collaboration, Search for a W' boson decaying to a bottom quark and a top quark in pp collisions at $\sqrt{s} = 7$ TeV, *Phys. Lett. B* 718 (2013) 1229–1251, arXiv:1208.0956.
- [23] CMS Collaboration, Search for $W' \rightarrow t\bar{b}$ decays in the lepton + jets final state in pp collisions at $\sqrt{s} = 8$ TeV, *J. High Energy Phys.* 05 (2014) 108, arXiv:1402.2176.
- [24] ATLAS Collaboration, Search for $W' \rightarrow t\bar{b}$ in the lepton plus jets final state in proton–proton collisions at a centre-of-mass energy of $\sqrt{s} = 8$ TeV with the ATLAS detector, *Phys. Lett. B* 743 (2015) 235–255, arXiv:1410.4103 [hep-ex].
- [25] CMS Collaboration, Search for heavy resonances decaying to a top quark and a bottom quark in the lepton + jets final state in proton–proton collisions at 13 TeV, *Phys. Lett. B* 777 (2018) 39–63, arXiv:1708.08539 [hep-ex].
- [26] ATLAS Collaboration, Search for $W' \rightarrow t\bar{b} \rightarrow q\bar{q}b\bar{b}$ decays in pp collisions at $\sqrt{s} = 8$ TeV with the ATLAS detector, *Eur. Phys. J. C* 75 (2015) 165, arXiv:1408.0886 [hep-ex].
- [27] ATLAS Collaboration, Search for $W' \rightarrow t\bar{b}$ decays in the hadronic final state using pp collisions at $\sqrt{s} = 13$ TeV with the ATLAS detector, *Phys. Lett. B* 781 (2018) 327–348, arXiv:1801.07893 [hep-ex].
- [28] ATLAS Collaboration, The ATLAS experiment at the CERN large hadron collider, *J. Instrum.* 3 (2008) S08003.
- [29] Z. Sullivan, Fully differential W' production and decay at next-to-leading order in QCD, *Phys. Rev. D* 66 (2002) 075011, arXiv:hep-ph/0207290.
- [30] D. Duffy, Z. Sullivan, Model independent reach for W' -prime bosons at the LHC, *Phys. Rev. D* 86 (2012) 075018, arXiv:1208.4858.
- [31] ATLAS Collaboration, ATLAS Insertable B-Layer Technical Design Report, CERN-LHCC-2010-013, ATLAS-TDR-19, <https://cds.cern.ch/record/1291633>, 2010.
- [32] ATLAS Collaboration, ATLAS Insertable B-Layer Technical Design Report Addendum, Addendum to CERN-LHCC-2010-013, ATLAS-TDR-019, <https://cds.cern.ch/record/1451888>, 2012.
- [33] ATLAS Collaboration, Performance of the ATLAS trigger system in 2015, *Eur. Phys. J. C* 77 (2017) 317, <https://doi.org/10.1140/epjc/s10052-017-4852-3>.
- [34] J. Alwall, M. Herquet, F. Maltoni, O. Mattelaer, T. Stelzer, MadGraph 5: going beyond, *J. High Energy Phys.* 06 (2011) 128, arXiv:1106.0522.
- [35] J. Alwall, et al., The automated computation of tree-level and next-to-leading order differential cross sections, and their matching to parton shower simulations, *J. High Energy Phys.* 07 (2014) 079, arXiv:1405.0301 [hep-ph].
- [36] C. Degrande, et al., UFO – The Universal FeynRules Output, *Comput. Phys. Commun.* 183 (2012) 1201–1214, arXiv:1108.2040.
- [37] A. Alloul, N.D. Christensen, C. Degrande, C. Duhr, B. Fuks, FeynRules 2.0 – a complete toolbox for tree-level phenomenology, *Comput. Phys. Commun.* 185 (2014) 2250–2300, arXiv:1310.1921.
- [38] T. Sjöstrand, S. Mrenna, P.Z. Skands, A brief introduction to PYTHIA 8.1, *Comput. Phys. Commun.* 178 (2008) 852–867, arXiv:0710.3820.
- [39] R.D. Ball, L. Del Debbio, S. Forte, A. Guffanti, J.I. Latorre, et al., A first unbiased global NLO determination of parton distributions and their uncertainties, *Nucl. Phys. B* 838 (2010) 136–206, arXiv:1002.4407 [hep-ph].

- [40] ATLAS Collaboration, ATLAS Pythia 8 tunes to 7 TeV data, ATL-PHYS-PUB-2014-021, <https://cds.cern.ch/record/1966419>, 2014.
- [41] S. Alioli, P. Nason, C. Oleari, E. Re, A general framework for implementing NLO calculations in shower Monte Carlo programs: the POWHEG BOX, *J. High Energy Phys.* 06 (2010) 043, arXiv:1002.2581.
- [42] S. Frixione, P. Nason, G. Ridolfi, A positive-weight next-to-leading-order Monte Carlo for heavy flavour hadroproduction, *J. High Energy Phys.* 09 (2007) 126, arXiv:0707.3088.
- [43] H.-L. Lai, et al., New parton distributions for collider physics, *Phys. Rev. D* 82 (2010) 074024, arXiv:1007.2241 [hep-ph].
- [44] T. Sjöstrand, et al., High-energy physics event generation with PYTHIA 6.1, *Comput. Phys. Commun.* 135 (2001) 238–259, arXiv:hep-ph/0010017.
- [45] P.Z. Skands, Tuning Monte Carlo generators: The Perugia Tunes, *Phys. Rev. D* 82 (2010) 074018, arXiv:1005.3457 [hep-ph].
- [46] M. Cacciari, M. Czakon, M. Mangano, A. Mitov, P. Nason, Top-pair production at hadron colliders with next-to-next-to-leading logarithmic soft-gluon resummation, *Phys. Lett. B* 710 (2012) 612–622, arXiv:1111.5869.
- [47] M. Beneke, P. Falgari, S. Klein, C. Schwinn, Hadronic top-quark pair production with NNLL threshold resummation, *Nucl. Phys. B* 855 (2012) 695–741, arXiv:1109.1536.
- [48] P. Baernreuther, M. Czakon, A. Mitov, Percent-level-precision physics at the Tevatron: next-to-next-to-leading order QCD corrections to $q\bar{q} \rightarrow t\bar{t} + X$, *Phys. Rev. Lett.* 109 (2012) 132001, arXiv:1204.5201.
- [49] M. Czakon, P. Fiedler, A. Mitov, Total top-quark pair-production cross section at hadron colliders through $\mathcal{O}(\alpha_s^4)$, *Phys. Rev. Lett.* 110 (25) (2013) 252004, arXiv:1303.6254.
- [50] M. Czakon, A. Mitov, NNLO corrections to top pair production at hadron colliders: the quark–gluon reaction, *J. High Energy Phys.* 01 (2013) 080, arXiv:1210.6832.
- [51] M. Czakon, A. Mitov, NNLO corrections to top-pair production at hadron colliders: the all-fermionic scattering channels, *J. High Energy Phys.* 12 (2012) 054, arXiv:1207.0236.
- [52] M. Czakon, A. Mitov, Top++: a program for the calculation of the top-pair cross-section at hadron colliders, *Comput. Phys. Commun.* (ISSN 0010-4655) 185 (2014) 2930–2938.
- [53] T. Gleisberg, et al., Event generation with SHERPA 1.1, *J. High Energy Phys.* 02 (2009) 007, arXiv:0811.4622 [hep-ph].
- [54] S. Höche, F. Krauss, S. Schumann, F. Siegert, QCD matrix elements and truncated showers, *J. High Energy Phys.* 05 (2009) 053, arXiv:0903.1219 [hep-ph].
- [55] T. Gleisberg, S. Höche, Comix, a new matrix element generator, *J. High Energy Phys.* 12 (2008) 039, arXiv:0808.3674 [hep-ph].
- [56] S. Schumann, F. Krauss, A Parton shower algorithm based on Catani–Seymour dipole factorisation, *J. High Energy Phys.* 03 (2008) 038, arXiv:0709.1027 [hep-ph].
- [57] R. Hamberg, W. Van Neerven, T. Matsuura, A complete calculation of the order α_s^2 correction to the Drell–Yan K factor, *Nucl. Phys. B* 359 (1991) 343–405; R. Hamberg, W. Van Neerven, T. Matsuura, *Nucl. Phys. B* 644 (2002) 403 (Erratum).
- [58] C. Anastasiou, L.J. Dixon, K. Melnikov, F. Petriello, High precision QCD at hadron colliders: electroweak gauge boson rapidity distributions at NNLO, *Phys. Rev. D* 69 (2004) 094008, arXiv:hep-ph/0312266.
- [59] J. Pumplin, et al., New generation of parton distributions with uncertainties from global QCD analysis, *J. High Energy Phys.* 07 (2002) 012, arXiv:hep-ph/0201195 [hep-ph].
- [60] ATLAS Collaboration, Measurement of the Z/γ^* boson transverse momentum distribution in pp collisions at $\sqrt{s} = 7$ TeV with the ATLAS detector, *J. High Energy Phys.* 09 (2014) 55.
- [61] D.J. Lange, The EvtGen particle decay simulation package, *Nucl. Instrum. Methods A* 462 (2001) 152–155.
- [62] ATLAS Collaboration, Summary of ATLAS Pythia 8 tunes, ATL-PHYS-PUB-2012-003, <https://cds.cern.ch/record/1474107>, 2012.
- [63] A.D. Martin, W.J. Stirling, R.S. Thorne, G. Watt, Parton distributions for the LHC, *Eur. Phys. J. C* 63 (2009) 189–285, arXiv:0901.0002 [hep-ph].
- [64] ATLAS Collaboration, The ATLAS simulation infrastructure, *Eur. Phys. J. C* 70 (2010) 823–874, arXiv:1005.4568.
- [65] S. Agostinelli, et al., GEANT4 – a simulation toolkit, *Nucl. Instrum. Methods A* 506 (2003) 250–303.
- [66] W. Lampl, et al., Calorimeter clustering algorithms: description and performance, ATL-LARG-PUB-2008-002, <https://cds.cern.ch/record/1099735>, 2008.
- [67] ATLAS Collaboration, Electron and photon energy calibration with the ATLAS detector using LHC Run 1 data, *Eur. Phys. J. C* 74 (2014) 3071, arXiv:1407.5063 [hep-ex].
- [68] ATLAS Collaboration, Electron reconstruction and identification efficiency measurements with the ATLAS detector using the 2011 LHC proton–proton collision data, *Eur. Phys. J. C* 74 (2014) 2941, arXiv:1404.2240 [hep-ex].
- [69] ATLAS Collaboration, Muon reconstruction performance of the ATLAS detector in proton–proton collision data at $\sqrt{s} = 13$ TeV, *Eur. Phys. J. C* 76 (2016) 292, arXiv:1603.05598 [hep-ex].
- [70] M. Cacciari, G.P. Salam, G. Soyez, The anti- k_t jet clustering algorithm, *J. High Energy Phys.* 04 (2008) 063, arXiv:0802.1189.
- [71] ATLAS Collaboration, Performance of pile-up mitigation techniques for jets in pp collisions at $\sqrt{s} = 8$ TeV using the ATLAS detector, *Eur. Phys. J. C* 76 (2016) 581, arXiv:1510.03823 [hep-ex].
- [72] ATLAS Collaboration, Performance of b -jet identification in the ATLAS Experiment, *J. Instrum.* 11 (2016) P04008, arXiv:1512.01094 [hep-ex].
- [73] ATLAS Collaboration, Optimisation of the ATLAS b -tagging performance for the 2016 LHC Run, ATL-PHYS-PUB-2016-012, <https://cds.cern.ch/record/2160731>, 2016.
- [74] M. Aaboud, et al., Performance of missing transverse momentum reconstruction with the ATLAS detector using proton–proton collisions at $\sqrt{s} = 13$ TeV, arXiv:1802.08168 [hep-ex], 2018.
- [75] ATLAS Collaboration, Measurement of the top quark pair production cross-section with ATLAS in the single lepton channel, *Phys. Lett. B* 711 (2012) 244, arXiv:1201.1889 [hep-ex].
- [76] ATLAS Collaboration, Search for heavy particles decaying into top-quark pairs using lepton-plus-jets events in proton–proton collisions at $\sqrt{s} = 13$ TeV with the ATLAS detector, *Eur. Phys. J. C* 78 (2018) 565, arXiv:1804.10823 [hep-ex].
- [77] N. Kidonakis, Next-to-next-to-leading-order collinear and soft gluon corrections for t -channel single top quark production, *Phys. Rev. D* 83 (2011) 091503, arXiv:1103.2792 [hep-ph].
- [78] N. Kidonakis, NNLL resummation for s -channel single top quark production, *Phys. Rev. D* 81 (2010) 054028, arXiv:1001.5034.
- [79] N. Kidonakis, Two-loop soft anomalous dimensions for single top quark associated production with a W^- or H^- , *Phys. Rev. D* 82 (2010) 054018, arXiv:1005.4451.
- [80] J.M. Campbell, R. Ellis, MCFM for the Tevatron and the LHC, *Nucl. Phys. B, Proc. Suppl.* 205–206 (2010), arXiv:1007.3492 [hep-ph].
- [81] ATLAS Collaboration, Luminosity determination in pp collisions at $\sqrt{s} = 8$ TeV using the ATLAS detector at the LHC, *Eur. Phys. J. C* 76 (2016) 653, arXiv:1608.03953 [hep-ex].
- [82] J. Alwall, R. Frederix, S. Frixione, V. Hirschi, F. Maltoni, et al., The automated computation of tree-level and next-to-leading order differential cross sections, and their matching to parton shower simulations, arXiv:1405.0301 [hep-ph], 2014.
- [83] M. Bahr, et al., Herwig++ physics and manual, *Eur. Phys. J. C* 58 (2008) 639–707, arXiv:0803.0883 [hep-ph].
- [84] J. Bellm, et al., Herwig 7.0/Herwig++ 3.0 release note, *Eur. Phys. J. C* 76 (2016) 196, arXiv:1512.01178 [hep-ph].
- [85] S. Frixione, et al., Single-top hadroproduction in association with a W boson, *J. High Energy Phys.* 07 (2008) 029, arXiv:0805.3067.
- [86] J. Butterworth, et al., PDF4LHC recommendations for LHC Run II, *J. Phys. G* 43 (2016) 023001, arXiv:1510.03865 [hep-ph].
- [87] L. Moneta, K. Cranmer, G. Schott, W. Verkerke, The RooStats project, 57, arXiv:1009.1003 [physics.data-an], 2010.
- [88] W. Verkerke, D.P. Kirkby, The RooFit toolkit for data modeling, eConf C 0303241 (2003), MOLT007, 186, arXiv:physics/0306116 [physics], 2003.
- [89] M. Baak, et al., HistFitter software framework for statistical data analysis, *Eur. Phys. J. C* 75 (2015) 153, arXiv:1410.1280 [hep-ex].
- [90] A.L. Read, Presentation of search results: the CLs technique, *J. Phys. G* 28 (2002) 2693–2704, 11(2002).
- [91] G. Cowan, K. Cranmer, E. Gross, O. Vitells, Asymptotic formulae for likelihood-based tests of new physics, *Eur. Phys. J. C* 71 (2011) 1554; Erratum, *Eur. Phys. J. C* 73 (2013) 2501, arXiv:1007.1727 [physics.data-an].
- [92] ATLAS Collaboration, ATLAS computing acknowledgements, ATL-GEN-PUB-2016-002 <https://cds.cern.ch/record/2202407>.

The ATLAS Collaboration

M. Aaboud^{34d}, G. Aad⁹⁹, B. Abbott¹²⁴, O. Abidinov^{13,*}, B. Abeloos¹²⁸, D.K. Abhayasinghe⁹¹, S.H. Abidi¹⁶⁴, O.S. AbouZeid³⁹, N.L. Abraham¹⁵³, H. Abramowicz¹⁵⁸, H. Abreu¹⁵⁷, Y. Abulaiti⁶, B.S. Acharya^{64a,64b,n}, S. Adachi¹⁶⁰, L. Adamczyk^{81a}, J. Adelman¹¹⁹, M. Adersberger¹¹², A. Adiguzel^{12c,af},

T. Adye¹⁴¹, A.A. Affolder¹⁴³, Y. Afik¹⁵⁷, C. Agheorghiesei^{27c}, J.A. Aguilar-Saavedra^{136f,136a}, F. Ahmadov^{77,ad}, G. Aielli^{71a,71b}, S. Akatsuka⁸³, T.P.A. Åkesson⁹⁴, E. Akilli⁵², A.V. Akimov¹⁰⁸, G.L. Alberghi^{23b,23a}, J. Albert¹⁷³, P. Albicocco⁴⁹, M.J. Alconada Verzini⁸⁶, S. Alderweireldt¹¹⁷, M. Aleksa³⁵, I.N. Aleksandrov⁷⁷, C. Alexa^{27b}, T. Alexopoulos¹⁰, M. Alhroob¹²⁴, B. Ali¹³⁸, G. Alimonti^{66a}, J. Alison³⁶, S.P. Alkire¹⁴⁵, C. Allaire¹²⁸, B.M.M. Allbrooke¹⁵³, B.W. Allen¹²⁷, P.P. Allport²¹, A. Aloisio^{67a,67b}, A. Alonso³⁹, F. Alonso⁸⁶, C. Alpigiani¹⁴⁵, A.A. Alshehri⁵⁵, M.I. Alstady⁹⁹, B. Alvarez Gonzalez³⁵, D. Álvarez Piqueras¹⁷¹, M.G. Alviggi^{67a,67b}, B.T. Amadio¹⁸, Y. Amaral Coutinho^{78b}, L. Ambroz¹³¹, C. Amelung²⁶, D. Amidei¹⁰³, S.P. Amor Dos Santos^{136a,136c}, S. Amoroso⁴⁴, C.S. Amrouche⁵², C. Anastopoulos¹⁴⁶, L.S. Ancu⁵², N. Andari¹⁴², T. Andeen¹¹, C.F. Anders^{59b}, J.K. Anders²⁰, K.J. Anderson³⁶, A. Andreazza^{66a,66b}, V. Andrei^{59a}, C.R. Anelli¹⁷³, S. Angelidakis³⁷, I. Angelozzi¹¹⁸, A. Angerami³⁸, A.V. Anisenkov^{120b,120a}, A. Annovi^{69a}, C. Antel^{59a}, M.T. Anthony¹⁴⁶, M. Antonelli⁴⁹, D.J.A. Antrim¹⁶⁸, F. Anulli^{70a}, M. Aoki⁷⁹, J.A. Aparisi Pozo¹⁷¹, L. Aperio Bella³⁵, G. Arabidze¹⁰⁴, J.P. Araque^{136a}, V. Araujo Ferraz^{78b}, R. Araujo Pereira^{78b}, A.T.H. Arce⁴⁷, R.E. Ardell⁹¹, F.A. Arduh⁸⁶, J-F. Arguin¹⁰⁷, S. Argyropoulos⁷⁵, A.J. Armbruster³⁵, L.J. Armitage⁹⁰, A. Armstrong¹⁶⁸, O. Arnaez¹⁶⁴, H. Arnold¹¹⁸, M. Arratia³¹, O. Arslan²⁴, A. Artamonov^{109,*}, G. Artoni¹³¹, S. Artz⁹⁷, S. Asai¹⁶⁰, N. Asbah⁵⁷, A. Ashkenazi¹⁵⁸, E.M. Asimakopoulou¹⁶⁹, L. Asquith¹⁵³, K. Assamagan²⁹, R. Astalos^{28a}, R.J. Atkin^{32a}, M. Atkinson¹⁷⁰, N.B. Atlay¹⁴⁸, K. Augsten¹³⁸, G. Avolio³⁵, R. Avramidou^{58a}, M.K. Ayoub^{15a}, G. Azuelos^{107,aq}, A.E. Baas^{59a}, M.J. Baca²¹, H. Bachacou¹⁴², K. Bachas^{65a,65b}, M. Backes¹³¹, P. Bagnaia^{70a,70b}, M. Bahmani⁸², H. Bahrasemani¹⁴⁹, A.J. Bailey¹⁷¹, J.T. Baines¹⁴¹, M. Bajic³⁹, C. Bakalis¹⁰, O.K. Baker¹⁸⁰, P.J. Bakker¹¹⁸, D. Bakshi Gupta⁹³, E.M. Baldin^{120b,120a}, P. Balek¹⁷⁷, F. Balli¹⁴², W.K. Balunas¹³³, J. Balz⁹⁷, E. Banas⁸², A. Bandyopadhyay²⁴, S. Banerjee^{178,j}, A.A.E. Bannoura¹⁷⁹, L. Barak¹⁵⁸, W.M. Barbe³⁷, E.L. Barberio¹⁰², D. Barberis^{53b,53a}, M. Barbero⁹⁹, T. Barillari¹¹³, M-S. Barisits³⁵, J. Barkeloo¹²⁷, T. Barklow¹⁵⁰, N. Barlow³¹, R. Barnea¹⁵⁷, S.L. Barnes^{58c}, B.M. Barnett¹⁴¹, R.M. Barnett¹⁸, Z. Barnovska-Blenessy^{58a}, A. Baroncelli^{72a}, G. Barone²⁶, A.J. Barr¹³¹, L. Barranco Navarro¹⁷¹, F. Barreiro⁹⁶, J. Barreiro Guimarães da Costa^{15a}, R. Bartoldus¹⁵⁰, A.E. Barton⁸⁷, P. Bartos^{28a}, A. Basalae¹³⁴, A. Bassalat¹²⁸, R.L. Bates⁵⁵, S.J. Batista¹⁶⁴, S. Batlamous^{34e}, J.R. Batley³¹, M. Battaglia¹⁴³, M. Bause^{70a,70b}, F. Bauer¹⁴², K.T. Bauer¹⁶⁸, H.S. Bawa^{150,l}, J.B. Beacham¹²², T. Beau¹³², P.H. Beauchemin¹⁶⁷, P. Bechtel²⁴, H.C. Beck⁵¹, H.P. Beck^{20,p}, K. Becker⁵⁰, M. Becker⁹⁷, C. Becot⁴⁴, A. Beddall^{12d}, A.J. Beddall^{12a}, V.A. Bednyakov⁷⁷, M. Bedognetti¹¹⁸, C.P. Bee¹⁵², T.A. Beermann³⁵, M. Begalli^{78b}, M. Begel²⁹, A. Behera¹⁵², J.K. Behr⁴⁴, A.S. Bell⁹², G. Bella¹⁵⁸, L. Bellagamba^{23b}, A. Bellerive³³, M. Bellomo¹⁵⁷, P. Bellos⁹, K. Belotskiy¹¹⁰, N.L. Belyaev¹¹⁰, O. Benary^{158,*}, D. Benchechroun^{34a}, M. Bender¹¹², N. Benekos¹⁰, Y. Benhammou¹⁵⁸, E. Benhar Noccioli¹⁸⁰, J. Benitez⁷⁵, D.P. Benjamin⁴⁷, M. Benoit⁵², J.R. Bensinger²⁶, S. Bentvelsen¹¹⁸, L. Beresford¹³¹, M. Beretta⁴⁹, D. Berge⁴⁴, E. Bergeaas Kuutmann¹⁶⁹, N. Berger⁵, L.J. Bergsten²⁶, J. Beringer¹⁸, S. Berlendis⁷, N.R. Bernard¹⁰⁰, G. Bernardi¹³², C. Bernius¹⁵⁰, F.U. Bernlochner²⁴, T. Berry⁹¹, P. Berta⁹⁷, C. Bertella^{15a}, G. Bertoli^{43a,43b}, I.A. Bertram⁸⁷, G.J. Besjes³⁹, O. Bessidskaia Bylund¹⁷⁹, M. Bessner⁴⁴, N. Besson¹⁴², A. Bethani⁹⁸, S. Bethke¹¹³, A. Betti²⁴, A.J. Bevan⁹⁰, J. Beyer¹¹³, R.M.B. Bianchi¹³⁵, O. Biebel¹¹², D. Biedermann¹⁹, R. Bielski³⁵, K. Bierwagen⁹⁷, N.V. Biesuz^{69a,69b}, M. Biglietti^{72a}, T.R.V. Billoud¹⁰⁷, M. Bindi⁵¹, A. Bingul^{12d}, C. Bini^{70a,70b}, S. Biondi^{23b,23a}, M. Birman¹⁷⁷, T. Bisanz⁵¹, J.P. Biswal¹⁵⁸, C. Bittrich⁴⁶, D.M. Bjergaard⁴⁷, J.E. Black¹⁵⁰, K.M. Black²⁵, T. Blazek^{28a}, I. Bloch⁴⁴, C. Blocker²⁶, A. Blue⁵⁵, U. Blumenschein⁹⁰, Dr. Blunier^{144a}, G.J. Bobbink¹¹⁸, V.S. Bobrovnikov^{120b,120a}, S.S. Bocchetta⁹⁴, A. Bocci⁴⁷, D. Boerner¹⁷⁹, D. Bogavac¹¹², A.G. Bogdanchikov^{120b,120a}, C. Böhm^{43a}, V. Boisvert⁹¹, P. Bokan^{169,w}, T. Bold^{81a}, A.S. Boldyrev¹¹¹, A.E. Bolz^{59b}, M. Bomben¹³², M. Bona⁹⁰, J.S. Bonilla¹²⁷, M. Boonekamp¹⁴², A. Borisov¹⁴⁰, G. Borissov⁸⁷, J. Bortfeldt³⁵, D. Bortoletto¹³¹, V. Bortolotto^{71a,71b}, D. Boscherini^{23b}, M. Bosman¹⁴, J.D. Bossio Sola³⁰, K. Bouaouda^{34a}, J. Boudreau¹³⁵, E.V. Bouhova-Thacker⁸⁷, D. Boumediene³⁷, C. Bourdarios¹²⁸, S.K. Boutle⁵⁵, A. Boveia¹²², J. Boyd³⁵, D. Boye^{32b}, I.R. Boyko⁷⁷, A.J. Bozson⁹¹, J. Bracinik²¹, N. Brahimi⁹⁹, A. Brandt⁸, G. Brandt¹⁷⁹, O. Brandt^{59a}, F. Braren⁴⁴, U. Bratzler¹⁶¹, B. Brau¹⁰⁰, J.E. Brau¹²⁷, W.D. Breaden Madden⁵⁵, K. Brendlinger⁴⁴, A.J. Brennan¹⁰², L. Brenner⁴⁴, R. Brenner¹⁶⁹, S. Bressler¹⁷⁷, B. Brickwedde⁹⁷, D.L. Briglin²¹, D. Britton⁵⁵, D. Britzger^{59b}, I. Brock²⁴, R. Brock¹⁰⁴, G. Brooijmans³⁸, T. Brooks⁹¹, W.K. Brooks^{144b}, E. Brost¹¹⁹, J.H. Broughton²¹, P.A. Bruckman de Renstrom⁸², D. Bruncko^{28b}, A. Bruni^{23b}, G. Bruni^{23b}, L.S. Bruni¹¹⁸, S. Bruno^{71a,71b}, B.H. Brunt³¹, M. Bruschi^{23b}, N. Bruscino¹³⁵,

P. Bryant³⁶, L. Bryngemark⁴⁴, T. Buanes¹⁷, Q. Buat³⁵, P. Buchholz¹⁴⁸, A.G. Buckley⁵⁵, I.A. Budagov⁷⁷, F. Buehrer⁵⁰, M.K. Bugge¹³⁰, O. Bulekov¹¹⁰, D. Bullock⁸, T.J. Burch¹¹⁹, S. Burdin⁸⁸, C.D. Burgard¹¹⁸, A.M. Burger⁵, B. Burghgrave¹¹⁹, K. Burka⁸², S. Burke¹⁴¹, I. Burmeister⁴⁵, J.T.P. Burr¹³¹, D. Büscher⁵⁰, V. Büscher⁹⁷, E. Buschmann⁵¹, P. Bussey⁵⁵, J.M. Butler²⁵, C.M. Buttar⁵⁵, J.M. Butterworth⁹², P. Butti³⁵, W. Buttinger³⁵, A. Buzatu¹⁵⁵, A.R. Buzykaev^{120b,120a}, G. Cabras^{23b,23a}, S. Cabrera Urbán¹⁷¹, D. Caforio¹³⁸, H. Cai¹⁷⁰, V.M.M. Cairo², O. Cakir^{4a}, N. Calace⁵², P. Calafiura¹⁸, A. Calandri⁹⁹, G. Calderini¹³², P. Calfayan⁶³, G. Callea^{40b,40a}, L.P. Caloba^{78b}, S. Calvente Lopez⁹⁶, D. Calvet³⁷, S. Calvet³⁷, T.P. Calvet¹⁵², M. Calvetti^{69a,69b}, R. Camacho Toro¹³², S. Camarda³⁵, P. Camarri^{71a,71b}, D. Cameron¹³⁰, R. Caminal Armadans¹⁰⁰, C. Camincher³⁵, S. Campana³⁵, M. Campanelli⁹², A. Camplani³⁹, A. Campoverde¹⁴⁸, V. Canale^{67a,67b}, M. Cano Bret^{58c}, J. Cantero¹²⁵, T. Cao¹⁵⁸, Y. Cao¹⁷⁰, M.D.M. Capeans Garrido³⁵, I. Caprini^{27b}, M. Caprini^{27b}, M. Capua^{40b,40a}, R.M. Carbone³⁸, R. Cardarelli^{71a}, F.C. Cardillo¹⁴⁶, I. Carli¹³⁹, T. Carli³⁵, G. Carlino^{67a}, B.T. Carlson¹³⁵, L. Carminati^{66a,66b}, R.M.D. Carney^{43a,43b}, S. Caron¹¹⁷, E. Carquin^{144b}, S. Carrá^{66a,66b}, G.D. Carrillo-Montoya³⁵, D. Casadei^{32b}, M.P. Casado^{14f}, A.F. Casha¹⁶⁴, D.W. Casper¹⁶⁸, R. Castelijin¹¹⁸, F.L. Castillo¹⁷¹, V. Castillo Gimenez¹⁷¹, N.F. Castro^{136a,136e}, A. Catinaccio³⁵, J.R. Catmore¹³⁰, A. Cattai³⁵, J. Caudron²⁴, V. Cavaliere²⁹, E. Cavallaro¹⁴, D. Cavalli^{66a}, M. Cavalli-Sforza¹⁴, V. Cavasinni^{69a,69b}, E. Celebi^{12b}, F. Ceradini^{72a,72b}, L. Cerda Alberich¹⁷¹, A.S. Cerqueira^{78a}, A. Cerri¹⁵³, L. Cerrito^{71a,71b}, F. Cerutti¹⁸, A. Cervelli^{23b,23a}, S.A. Cetin^{12b}, A. Chafaq^{34a}, D. Chakraborty¹¹⁹, S.K. Chan⁵⁷, W.S. Chan¹¹⁸, Y.L. Chan^{61a}, J.D. Chapman³¹, B. Chargeishvili^{156b}, D.G. Charlton²¹, C.C. Chau³³, C.A. Chavez Barajas¹⁵³, S. Che¹²², A. Chegwiddden¹⁰⁴, S. Chekanov⁶, S.V. Chekulaev^{165a}, G.A. Chelkov^{77,ap}, M.A. Chelstowska³⁵, C. Chen^{58a}, C.H. Chen⁷⁶, H. Chen²⁹, J. Chen^{58a}, J. Chen³⁸, S. Chen¹³³, S.J. Chen^{15c}, X. Chen^{15b,ao}, Y. Chen⁸⁰, Y.-H. Chen⁴⁴, H.C. Cheng¹⁰³, H.J. Cheng^{15d}, A. Cheplakov⁷⁷, E. Cheremushkina¹⁴⁰, R. Cherkaoui El Moursli^{34e}, E. Cheu⁷, K. Cheung⁶², L. Chevalier¹⁴², V. Chiarella⁴⁹, G. Chiarelli^{69a}, G. Chiodini^{65a}, A.S. Chisholm³⁵, A. Chitan^{27b}, I. Chiu¹⁶⁰, Y.H. Chiu¹⁷³, M.V. Chizhov⁷⁷, K. Choi⁶³, A.R. Chomont¹²⁸, S. Chouridou¹⁵⁹, Y.S. Chow¹¹⁸, V. Christodoulou⁹², M.C. Chu^{61a}, J. Chudoba¹³⁷, A.J. Chuinard¹⁰¹, J.J. Chwastowski⁸², L. Chytka¹²⁶, D. Cinca⁴⁵, V. Cindro⁸⁹, I.A. Cioară²⁴, A. Ciocio¹⁸, F. Ciotto^{67a,67b}, Z.H. Citron¹⁷⁷, M. Citterio^{66a}, A. Clark⁵², M.R. Clark³⁸, P.J. Clark⁴⁸, C. Clement^{43a,43b}, Y. Coadou⁹⁹, M. Cobl^{64a,64c}, A. Coccaro^{53b,53a}, J. Cochran⁷⁶, H. Cohen¹⁵⁸, A.E.C. Coimbra¹⁷⁷, L. Colasurdo¹¹⁷, B. Cole³⁸, A.P. Colijn¹¹⁸, J. Collot⁵⁶, P. Conde Muiño^{136a,136b}, E. Coniavitis⁵⁰, S.H. Connell^{32b}, I.A. Connelly⁹⁸, S. Constantinescu^{27b}, F. Conventi^{67a,ar}, A.M. Cooper-Sarkar¹³¹, F. Cormier¹⁷², K.J.R. Cormier¹⁶⁴, M. Corradi^{70a,70b}, E.E. Corrigan⁹⁴, F. Corriveau^{101,ab}, A. Cortes-Gonzalez³⁵, M.J. Costa¹⁷¹, D. Costanzo¹⁴⁶, G. Cottin³¹, G. Cowan⁹¹, B.E. Cox⁹⁸, J. Crane⁹⁸, K. Cranmer¹²¹, S.J. Crawley⁵⁵, R.A. Creager¹³³, G. Cree³³, S. Crépe-Renaudin⁵⁶, F. Crescioli¹³², M. Cristinziani²⁴, V. Croft¹²¹, G. Crosetti^{40b,40a}, A. Cueto⁹⁶, T. Cuhadar Donszelmann¹⁴⁶, A.R. Cukierman¹⁵⁰, J. Cúth⁹⁷, S. Czekierda⁸², P. Czodrowski³⁵, M.J. Da Cunha Sargedas De Sousa^{58b,136b}, C. Da Via⁹⁸, W. Dabrowski^{81a}, T. Dado^{28a,w}, S. Dahbi^{34e}, T. Dai¹⁰³, F. Dallaire¹⁰⁷, C. Dallapiccola¹⁰⁰, M. Dam³⁹, G. D'amen^{23b,23a}, J. Damp⁹⁷, J.R. Dandoy¹³³, M.F. Daneri³⁰, N.P. Dang^{178,j}, N.D. Dann⁹⁸, M. Danninger¹⁷², V. Dao³⁵, G. Darbo^{53b}, S. Darmora⁸, O. Dartsis⁵, A. Dattagupta¹²⁷, T. Daubney⁴⁴, S. D'Auria⁵⁵, W. Davey²⁴, C. David⁴⁴, T. Davidek¹³⁹, D.R. Davis⁴⁷, E. Dawe¹⁰², I. Dawson¹⁴⁶, K. De⁸, R. De Asmundis^{67a}, A. De Benedetti¹²⁴, M. De Beurs¹¹⁸, S. De Castro^{23b,23a}, S. De Cecco^{70a,70b}, N. De Groot¹¹⁷, P. de Jong¹¹⁸, H. De la Torre¹⁰⁴, F. De Lorenzi⁷⁶, A. De Maria^{51,r}, D. De Pedis^{70a}, A. De Salvo^{70a}, U. De Sanctis^{71a,71b}, M. De Santis^{71a,71b}, A. De Santo¹⁵³, K. De Vasconcelos Corga⁹⁹, J.B. De Vivie De Regie¹²⁸, C. Debenedetti¹⁴³, D.V. Dedovich⁷⁷, N. Dehghanian³, M. Del Gaudio^{40b,40a}, J. Del Peso⁹⁶, Y. Delabat Diaz⁴⁴, D. Delgove¹²⁸, F. Deliot¹⁴², C.M. Delitzsch⁷, M. Della Pietra^{67a,67b}, D. Della Volpe⁵², A. Dell'Acqua³⁵, L. Dell'Asta²⁵, M. Delmastro⁵, C. Delporte¹²⁸, P.A. Delsart⁵⁶, D.A. DeMarco¹⁶⁴, S. Demers¹⁸⁰, M. Demichev⁷⁷, S.P. Denisov¹⁴⁰, D. Denysiuk¹¹⁸, L. D'Eramo¹³², D. Derendarz⁸², J.E. Derkaoui^{34d}, F. Derue¹³², P. Dervan⁸⁸, K. Desch²⁴, C. Deterre⁴⁴, K. Dette¹⁶⁴, M.R. Devesa³⁰, P.O. Deviveiros³⁵, A. Dewhurst¹⁴¹, S. Dhaliwal²⁶, F.A. Di Bello⁵², A. Di Ciaccio^{71a,71b}, L. Di Ciaccio⁵, W.K. Di Clemente¹³³, C. Di Donato^{67a,67b}, A. Di Girolamo³⁵, B. Di Micco^{72a,72b}, R. Di Nardo¹⁰⁰, K.F. Di Petrillo⁵⁷, R. Di Sipio¹⁶⁴, D. Di Valentino³³, C. Diaconu⁹⁹, M. Diamond¹⁶⁴, F.A. Dias³⁹, T. Dias Do Vale^{136a}, M.A. Diaz^{144a}, J. Dickinson¹⁸, E.B. Diehl¹⁰³, J. Dietrich¹⁹, S. Díez Cornell⁴⁴, A. Dimitrievska¹⁸, J. Dingfelder²⁴, F. Dittus³⁵, F. Djama⁹⁹, T. Djobava^{156b}, J.I. Djuvsland^{59a},

M.A.B. Do Vale ^{78c}, M. Dobre ^{27b}, D. Dodsworth ²⁶, C. Doglioni ⁹⁴, J. Dolejsi ¹³⁹, Z. Dolezal ¹³⁹, M. Donadelli ^{78d}, J. Donini ³⁷, A. D'Onofrio ⁹⁰, M. D'Onofrio ⁸⁸, J. Dopke ¹⁴¹, A. Doria ^{67a}, M.T. Dova ⁸⁶, A.T. Doyle ⁵⁵, E. Drechsler ⁵¹, E. Dreyer ¹⁴⁹, T. Dreyer ⁵¹, Y. Du ^{58b}, J. Duarte-Campderros ¹⁵⁸, F. Dubinin ¹⁰⁸, M. Dubovsky ^{28a}, A. Dubreuil ⁵², E. Duchovni ¹⁷⁷, G. Duckeck ¹¹², A. Ducourthial ¹³², O.A. Ducu ^{107,v}, D. Duda ¹¹³, A. Dudarev ³⁵, A.C. Dudder ⁹⁷, E.M. Duffield ¹⁸, L. Duflot ¹²⁸, M. Dührssen ³⁵, C. Dülse ¹⁷⁹, M. Dumancic ¹⁷⁷, A.E. Dumitriu ^{27b,d}, A.K. Duncan ⁵⁵, M. Dunford ^{59a}, A. Duperrin ⁹⁹, H. Duran Yildiz ^{4a}, M. Düren ⁵⁴, A. Durglishvili ^{156b}, D. Duschinger ⁴⁶, B. Dutta ⁴⁴, D. Duvnjak ¹, M. Dyndal ⁴⁴, S. Dysch ⁹⁸, B.S. Dziedzic ⁸², C. Eckardt ⁴⁴, K.M. Ecker ¹¹³, R.C. Edgar ¹⁰³, T. Eifert ³⁵, G. Eigen ¹⁷, K. Einsweiler ¹⁸, T. Ekelof ¹⁶⁹, M. El Kacimi ^{34c}, R. El Kosseifi ⁹⁹, V. Ellajosyula ⁹⁹, M. Ellert ¹⁶⁹, F. Ellinghaus ¹⁷⁹, A.A. Elliot ⁹⁰, N. Ellis ³⁵, J. Elmsheuser ²⁹, M. Elsing ³⁵, D. Emelianov ¹⁴¹, Y. Enari ¹⁶⁰, J.S. Ennis ¹⁷⁵, M.B. Epland ⁴⁷, J. Erdmann ⁴⁵, A. Ereditato ²⁰, S. Errede ¹⁷⁰, M. Escalier ¹²⁸, C. Escobar ¹⁷¹, O. Estrada Pastor ¹⁷¹, A.I. Etienne ¹⁴², E. Etzion ¹⁵⁸, H. Evans ⁶³, A. Ezhilov ¹³⁴, M. Ezzi ^{34e}, F. Fabbri ⁵⁵, L. Fabbri ^{23b,23a}, V. Fabiani ¹¹⁷, G. Facini ⁹², R.M. Faisca Rodrigues Pereira ^{136a}, R.M. Fakhrutdinov ¹⁴⁰, S. Falciano ^{70a}, P.J. Falke ⁵, S. Falke ⁵, J. Faltova ¹³⁹, Y. Fang ^{15a}, M. Fanti ^{66a,66b}, A. Farbin ⁸, A. Farilla ^{72a}, E.M. Farina ^{68a,68b}, T. Farooque ¹⁰⁴, S. Farrell ¹⁸, S.M. Farrington ¹⁷⁵, P. Farthouat ³⁵, F. Fassi ^{34e}, P. Fassnacht ³⁵, D. Fassouliotis ⁹, M. Fauci Giannelli ⁴⁸, A. Favareto ^{53b,53a}, W.J. Fawcett ³¹, L. Fayard ¹²⁸, O.L. Fedin ^{134,o}, W. Fedorko ¹⁷², M. Feickert ⁴¹, S. Feigl ¹³⁰, L. Feligioni ⁹⁹, C. Feng ^{58b}, E.J. Feng ³⁵, M. Feng ⁴⁷, M.J. Fenton ⁵⁵, A.B. Fenyuk ¹⁴⁰, L. Feremenga ⁸, J. Ferrando ⁴⁴, A. Ferrari ¹⁶⁹, P. Ferrari ¹¹⁸, R. Ferrari ^{68a}, D.E. Ferreira de Lima ^{59b}, A. Ferrer ¹⁷¹, D. Ferrere ⁵², C. Ferretti ¹⁰³, F. Fiedler ⁹⁷, A. Filipčič ⁸⁹, F. Filthaut ¹¹⁷, K.D. Finelli ²⁵, M.C.N. Fiolhais ^{136a,136c,a}, L. Fiorini ¹⁷¹, C. Fischer ¹⁴, W.C. Fisher ¹⁰⁴, N. Flaschel ⁴⁴, I. Fleck ¹⁴⁸, P. Fleischmann ¹⁰³, R.R.M. Fletcher ¹³³, T. Flick ¹⁷⁹, B.M. Flierl ¹¹², L.M. Flores ¹³³, L.R. Flores Castillo ^{61a}, F.M. Follega ^{73a,73b}, N. Fomin ¹⁷, G.T. Forcolin ⁹⁸, A. Formica ¹⁴², F.A. Förster ¹⁴, A.C. Forti ⁹⁸, A.G. Foster ²¹, D. Fournier ¹²⁸, H. Fox ⁸⁷, S. Fracchia ¹⁴⁶, P. Francavilla ^{69a,69b}, M. Franchini ^{23b,23a}, S. Franchino ^{59a}, D. Francis ³⁵, L. Franconi ¹³⁰, M. Franklin ⁵⁷, M. Frate ¹⁶⁸, M. Fraternali ^{68a,68b}, A.N. Fray ⁹⁰, D. Freeborn ⁹², S.M. Fressard-Batraneanu ³⁵, B. Freund ¹⁰⁷, W.S. Freund ^{78b}, D.C. Frizzell ¹²⁴, D. Froidevaux ³⁵, J.A. Frost ¹³¹, C. Fukunaga ¹⁶¹, E. Fullana Torregrosa ¹⁷¹, T. Fusayasu ¹¹⁴, J. Fuster ¹⁷¹, O. Gabizon ¹⁵⁷, A. Gabrielli ^{23b,23a}, A. Gabrielli ¹⁸, G.P. Gach ^{81a}, S. Gadatsch ⁵², P. Gadow ¹¹³, G. Gagliardi ^{53b,53a}, L.G. Gagnon ¹⁰⁷, C. Galea ^{27b}, B. Galhardo ^{136a,136c}, E.J. Gallas ¹³¹, B.J. Gallop ¹⁴¹, P. Gallus ¹³⁸, G. Galster ³⁹, R. Gamboa Goni ⁹⁰, K.K. Gan ¹²², S. Ganguly ¹⁷⁷, J. Gao ^{58a}, Y. Gao ⁸⁸, Y.S. Gao ^{150,i}, C. García ¹⁷¹, J.E. García Navarro ¹⁷¹, J.A. García Pascual ^{15a}, M. Garcia-Sciveres ¹⁸, R.W. Gardner ³⁶, N. Garelli ¹⁵⁰, V. Garonne ¹³⁰, K. Gasnikova ⁴⁴, A. Gaudiello ^{53b,53a}, G. Gaudio ^{68a}, I.L. Gavrilenko ¹⁰⁸, A. Gavrilyuk ¹⁰⁹, C. Gay ¹⁷², G. Gaycken ²⁴, E.N. Gazis ¹⁰, C.N.P. Gee ¹⁴¹, J. Geisen ⁵¹, M. Geisen ⁹⁷, M.P. Geisler ^{59a}, K. Gellerstedt ^{43a,43b}, C. Gemme ^{53b}, M.H. Genest ⁵⁶, C. Geng ¹⁰³, S. Gentile ^{70a,70b}, S. George ⁹¹, D. Gerbaudo ¹⁴, G. Gessner ⁴⁵, S. Ghasemi ¹⁴⁸, M. Ghasemi Bostanabad ¹⁷³, M. Ghneimat ²⁴, B. Giacobbe ^{23b}, S. Giagu ^{70a,70b}, N. Giangiacomi ^{23b,23a}, P. Giannetti ^{69a}, A. Giannini ^{67a,67b}, S.M. Gibson ⁹¹, M. Gignac ¹⁴³, D. Gillberg ³³, G. Gilles ¹⁷⁹, D.M. Gingrich ^{3,aq}, M.P. Giordani ^{64a,64c}, F.M. Giorgi ^{23b}, P.F. Giraud ¹⁴², P. Giromini ⁵⁷, G. Giugliarelli ^{64a,64c}, D. Giugni ^{66a}, F. Giuli ¹³¹, M. Giulini ^{59b}, S. Gkaitatzis ¹⁵⁹, I. Gkialas ^{9,i}, E.L. Gkougkousis ¹⁴, P. Gkoutoumis ¹⁰, L.K. Gladilin ¹¹¹, C. Glasman ⁹⁶, J. Glatzer ¹⁴, P.C.F. Glaysher ⁴⁴, A. Glazov ⁴⁴, M. Goblirsch-Kolb ²⁶, J. Godlewski ⁸², S. Goldfarb ¹⁰², T. Golling ⁵², D. Golubkov ¹⁴⁰, A. Gomes ^{136a,136b,136d}, R. Goncalves Gama ^{78a}, R. Gonçalves ^{136a}, G. Gonella ⁵⁰, L. Gonella ²¹, A. Gongadze ⁷⁷, F. Gonnella ²¹, J.L. Gonski ⁵⁷, S. González de la Hoz ¹⁷¹, S. Gonzalez-Sevilla ⁵², L. Goossens ³⁵, P.A. Gorbounov ¹⁰⁹, H.A. Gordon ²⁹, B. Gorini ³⁵, E. Gorini ^{65a,65b}, A. Gorišek ⁸⁹, A.T. Goshaw ⁴⁷, C. Gössling ⁴⁵, M.I. Gostkin ⁷⁷, C.A. Gottardo ²⁴, C.R. Goudet ¹²⁸, D. Goujdami ^{34c}, A.G. Goussiou ¹⁴⁵, N. Govender ^{32b,b}, C. Goy ⁵, E. Gozani ¹⁵⁷, I. Grabowska-Bold ^{81a}, P.O.J. Gradin ¹⁶⁹, E.C. Graham ⁸⁸, J. Gramling ¹⁶⁸, E. Gramstad ¹³⁰, S. Grancagnolo ¹⁹, V. Gratchev ¹³⁴, P.M. Gravila ^{27f}, F.G. Gravili ^{65a,65b}, C. Gray ⁵⁵, H.M. Gray ¹⁸, Z.D. Greenwood ^{93,ah}, C. Grefe ²⁴, K. Gregersen ⁹⁴, I.M. Gregor ⁴⁴, P. Grenier ¹⁵⁰, K. Grevtsov ⁴⁴, N.A. Grieser ¹²⁴, J. Griffiths ⁸, A.A. Grillo ¹⁴³, K. Grimm ¹⁵⁰, S. Grinstein ^{14,x}, Ph. Gris ³⁷, J.-F. Grivaz ¹²⁸, S. Groh ⁹⁷, E. Gross ¹⁷⁷, J. Grosse-Knetter ⁵¹, G.C. Grossi ⁹³, Z.J. Grout ⁹², C. Grud ¹⁰³, A. Grummer ¹¹⁶, L. Guan ¹⁰³, W. Guan ¹⁷⁸, J. Guenther ³⁵, A. Guerguichon ¹²⁸, F. Guescini ^{165a}, D. Guest ¹⁶⁸, R. Gugel ⁵⁰, B. Gui ¹²², T. Guillemin ⁵, S. Guindon ³⁵, U. Gul ⁵⁵, C. Gumpert ³⁵, J. Guo ^{58c}, W. Guo ¹⁰³, Y. Guo ^{58a,q}, Z. Guo ⁹⁹, R. Gupta ⁴¹, S. Gurbuz ^{12c}, G. Gustavino ¹²⁴, B.J. Gutelman ¹⁵⁷, P. Gutierrez ¹²⁴, C. Gutsche ⁹²,

C. Guyot¹⁴², M.P. Guzik^{81a}, C. Gwenlan¹³¹, C.B. Gwilliam⁸⁸, A. Haas¹²¹, C. Haber¹⁸, H.K. Hadavand⁸, N. Haddad^{34e}, A. Hadeef^{58a}, S. Hageböck²⁴, M. Hagihara¹⁶⁶, H. Hakobyan^{181,*}, M. Haleem¹⁷⁴, J. Haley¹²⁵, G. Halladjian¹⁰⁴, G.D. Hallewell⁹⁹, K. Hamacher¹⁷⁹, P. Hamal¹²⁶, K. Hamano¹⁷³, A. Hamilton^{32a}, G.N. Hamity¹⁴⁶, K. Han^{58a,ag}, L. Han^{58a}, S. Han^{15d}, K. Hanagaki^{79,t}, M. Hance¹⁴³, D.M. Handl¹¹², B. Haney¹³³, R. Hankache¹³², P. Hanke^{59a}, E. Hansen⁹⁴, J.B. Hansen³⁹, J.D. Hansen³⁹, M.C. Hansen²⁴, P.H. Hansen³⁹, K. Hara¹⁶⁶, A.S. Hard¹⁷⁸, T. Harenberg¹⁷⁹, S. Harkusha¹⁰⁵, P.F. Harrison¹⁷⁵, N.M. Hartmann¹¹², Y. Hasegawa¹⁴⁷, A. Hasib⁴⁸, S. Hassani¹⁴², S. Haug²⁰, R. Hauser¹⁰⁴, L. Hauswald⁴⁶, L.B. Havener³⁸, M. Havranek¹³⁸, C.M. Hawkes²¹, R.J. Hawkins³⁵, D. Hayden¹⁰⁴, C. Hayes¹⁵², C.P. Hays¹³¹, J.M. Hays⁹⁰, H.S. Hayward⁸⁸, S.J. Haywood¹⁴¹, M.P. Heath⁴⁸, V. Hedberg⁹⁴, L. Heelan⁸, S. Heer²⁴, K.K. Heidegger⁵⁰, J. Heilman³³, S. Heim⁴⁴, T. Heim¹⁸, B. Heinemann^{44,al}, J.J. Heinrich¹¹², L. Heinrich¹²¹, C. Heinz⁵⁴, J. Hejbal¹³⁷, L. Helary³⁵, A. Held¹⁷², S. Hellesund¹³⁰, S. Hellman^{43a,43b}, C. Helsens³⁵, R.C.W. Henderson⁸⁷, Y. Heng¹⁷⁸, S. Henkelmann¹⁷², A.M. Henriques Correia³⁵, G.H. Herbert¹⁹, H. Herde²⁶, V. Herget¹⁷⁴, Y. Hernández Jiménez^{32c}, H. Herr⁹⁷, M.G. Herrmann¹¹², G. Herten⁵⁰, R. Hertenberger¹¹², L. Hervas³⁵, T.C. Herwig¹³³, G.G. Hesketh⁹², N.P. Hessey^{165a}, J.W. Hetherly⁴¹, S. Higashino⁷⁹, E. Higón-Rodríguez¹⁷¹, K. Hildebrand³⁶, E. Hill¹⁷³, J.C. Hill³¹, K.K. Hill²⁹, K.H. Hiller⁴⁴, S.J. Hillier²¹, M. Hils⁴⁶, I. Hinchliffe¹⁸, M. Hirose¹²⁹, D. Hirschbuehl¹⁷⁹, B. Hiti⁸⁹, O. Hladik¹³⁷, D.R. Hlaluku^{32c}, X. Hoad⁴⁸, J. Hobbs¹⁵², N. Hod^{165a}, M.C. Hodgkinson¹⁴⁶, A. Hoecker³⁵, M.R. Hoferkamp¹¹⁶, F. Hoenig¹¹², D. Hohn²⁴, D. Hohov¹²⁸, T.R. Holmes³⁶, M. Holzbock¹¹², M. Homann⁴⁵, S. Honda¹⁶⁶, T. Honda⁷⁹, T.M. Hong¹³⁵, A. Hönle¹¹³, B.H. Hooberman¹⁷⁰, W.H. Hopkins¹²⁷, Y. Horii¹¹⁵, P. Horn⁴⁶, A.J. Horton¹⁴⁹, L.A. Horyn³⁶, J.-Y. Hostachy⁵⁶, A. Hostiuc¹⁴⁵, S. Hou¹⁵⁵, A. Hoummada^{34a}, J. Howarth⁹⁸, J. Hoya⁸⁶, M. Hrabovsky¹²⁶, J. Hrdinka³⁵, I. Hristova¹⁹, J. Hrivnac¹²⁸, A. Hrynevich¹⁰⁶, T. Hryn'ova⁵, P.J. Hsu⁶², S.-C. Hsu¹⁴⁵, Q. Hu²⁹, S. Hu^{58c}, Y. Huang^{15a}, Z. Hubacek¹³⁸, F. Hubaut⁹⁹, M. Huebner²⁴, F. Huegging²⁴, T.B. Huffman¹³¹, E.W. Hughes³⁸, M. Huhtinen³⁵, R.F.H. Hunter³³, P. Huo¹⁵², A.M. Hupe³³, N. Huseynov^{77,ad}, J. Huston¹⁰⁴, J. Huth⁵⁷, R. Hyneman¹⁰³, G. Iacobucci⁵², G. Iakovidis²⁹, I. Ibragimov¹⁴⁸, L. Iconomidou-Fayard¹²⁸, Z. Idrissi^{34e}, P. Iengo³⁵, R. Ignazzi³⁹, O. Igonkina^{118,z}, R. Iguchi¹⁶⁰, T. Iizawa⁵², Y. Ikegami⁷⁹, M. Ikeno⁷⁹, D. Iliadis¹⁵⁹, N. Ilic¹⁵⁰, F. Iltzsche⁴⁶, G. Introzzi^{68a,68b}, M. Iodice^{72a}, K. Iordanidou³⁸, V. Ippolito^{70a,70b}, M.F. Isacson¹⁶⁹, N. Ishijima¹²⁹, M. Ishino¹⁶⁰, M. Ishitsuka¹⁶², W. Islam¹²⁵, C. Issever¹³¹, S. Istin¹⁵⁷, F. Ito¹⁶⁶, J.M. Iturbe Ponce^{61a}, R. Iuppa^{73a,73b}, A. Ivina¹⁷⁷, H. Iwasaki⁷⁹, J.M. Izen⁴², V. Izzo^{67a}, P. Jacka¹³⁷, P. Jackson¹, R.M. Jacobs²⁴, V. Jain², G. Jäkel¹⁷⁹, K.B. Jakobi⁹⁷, K. Jakobs⁵⁰, S. Jakobsen⁷⁴, T. Jakoubek¹³⁷, D.O. Jamin¹²⁵, D.K. Jana⁹³, R. Jansky⁵², J. Janssen²⁴, M. Janus⁵¹, P.A. Janus^{81a}, G. Jarlskog⁹⁴, N. Javadov^{77,ad}, T. Javůrek³⁵, M. Javurkova⁵⁰, F. Jeanneau¹⁴², L. Jeanty¹⁸, J. Jejelava^{156a,ae}, A. Jelinskas¹⁷⁵, P. Jenni^{50,c}, J. Jeong⁴⁴, S. Jézéquel⁵, H. Ji¹⁷⁸, J. Jia¹⁵², H. Jiang⁷⁶, Y. Jiang^{58a}, Z. Jiang¹⁵⁰, S. Jiggins⁵⁰, F.A. Jimenez Morales³⁷, J. Jimenez Pena¹⁷¹, S. Jin^{15c}, A. Jinaru^{27b}, O. Jinnouchi¹⁶², H. Jivan^{32c}, P. Johansson¹⁴⁶, K.A. Johns⁷, C.A. Johnson⁶³, W.J. Johnson¹⁴⁵, K. Jon-And^{43a,43b}, R.W.L. Jones⁸⁷, S.D. Jones¹⁵³, S. Jones⁷, T.J. Jones⁸⁸, J. Jongmanns^{59a}, P.M. Jorge^{136a,136b}, J. Jovicevic^{165a}, X. Ju¹⁸, J.J. Junggeburth¹¹³, A. Juste Rozas^{14,x}, A. Kaczmarska⁸², M. Kado¹²⁸, H. Kagan¹²², M. Kagan¹⁵⁰, T. Kaji¹⁷⁶, E. Kajomovitz¹⁵⁷, C.W. Kalderon⁹⁴, A. Kaluza⁹⁷, S. Kama⁴¹, A. Kamenshchikov¹⁴⁰, L. Kanjir⁸⁹, Y. Kano¹⁶⁰, V.A. Kantserov¹¹⁰, J. Kanzaki⁷⁹, B. Kaplan¹²¹, L.S. Kaplan¹⁷⁸, D. Kar^{32c}, M.J. Kareem^{165b}, E. Karentzos¹⁰, S.N. Karpov⁷⁷, Z.M. Karpova⁷⁷, V. Kartvelishvili⁸⁷, A.N. Karyukhin¹⁴⁰, L. Kashif¹⁷⁸, R.D. Kass¹²², A. Kastanas¹⁵¹, Y. Kataoka¹⁶⁰, C. Kato^{58d,58c}, J. Katzy⁴⁴, K. Kawade⁸⁰, K. Kawagoe⁸⁵, T. Kawamoto¹⁶⁰, G. Kawamura⁵¹, E.F. Kay⁸⁸, V.F. Kazanin^{120b,120a}, R. Keeler¹⁷³, R. Kehoe⁴¹, J.S. Keller³³, E. Kellermann⁹⁴, J.J. Kempster²¹, J. Kendrick²¹, O. Kepka¹³⁷, S. Kersten¹⁷⁹, B.P. Kerševan⁸⁹, R.A. Keyes¹⁰¹, M. Khader¹⁷⁰, F. Khalil-Zada¹³, A. Khanov¹²⁵, A.G. Kharlamov^{120b,120a}, T. Kharlamova^{120b,120a}, E.E. Khoda¹⁷², A. Khodinov¹⁶³, T.J. Khoo⁵², E. Khramov⁷⁷, J. Khubua^{156b}, S. Kido⁸⁰, M. Kiehn⁵², C.R. Kilby⁹¹, Y.K. Kim³⁶, N. Kimura^{64a,64c}, O.M. Kind¹⁹, B.T. King⁸⁸, D. Kirchmeier⁴⁶, J. Kirk¹⁴¹, A.E. Kiryunin¹¹³, T. Kishimoto¹⁶⁰, D. Kisielewska^{81a}, V. Kitali⁴⁴, O. Kivernyk⁵, E. Kladiva^{28b}, T. Klapdor-Kleingrothaus⁵⁰, M.H. Klein¹⁰³, M. Klein⁸⁸, U. Klein⁸⁸, K. Kleinknecht⁹⁷, P. Klimek¹¹⁹, A. Klimentov²⁹, R. Klingenberg^{45,*}, T. Klingl²⁴, T. Klioutchnikova³⁵, F.F. Klitzner¹¹², P. Kluit¹¹⁸, S. Kluth¹¹³, E. Kneringer⁷⁴, E.B.F.G. Knoops⁹⁹, A. Knue⁵⁰, A. Kobayashi¹⁶⁰, D. Kobayashi⁸⁵, T. Kobayashi¹⁶⁰, M. Kobel⁴⁶, M. Kocian¹⁵⁰, P. Kodys¹³⁹, P.T. Koenig²⁴, T. Koffas³³, E. Koffeman¹¹⁸, N.M. Köhler¹¹³, T. Koi¹⁵⁰, M. Kolb^{59b}, I. Koletsou⁵,

T. Kondo⁷⁹, N. Kondrashova^{58c}, K. Köneke⁵⁰, A.C. König¹¹⁷, T. Kono⁷⁹, R. Konoplich^{121,ai}, V. Konstantinides⁹², N. Konstantinidis⁹², B. Konya⁹⁴, R. Kopeliansky⁶³, S. Koperny^{81a}, K. Korcyl⁸², K. Kordas¹⁵⁹, G. Koren¹⁵⁸, A. Korn⁹², I. Korolkov¹⁴, E.V. Korolkova¹⁴⁶, N. Korotkova¹¹¹, O. Kortner¹¹³, S. Kortner¹¹³, T. Kosek¹³⁹, V.V. Kostyukhin²⁴, A. Kotwal⁴⁷, A. Koulouris¹⁰, A. Kourkoumeli-Charalampidi^{68a,68b}, C. Kourkoumelis⁹, E. Kourlitis¹⁴⁶, V. Kouskoura²⁹, A.B. Kowalewska⁸², R. Kowalewski¹⁷³, T.Z. Kowalski^{81a}, C. Kozakai¹⁶⁰, W. Kozanecki¹⁴², A.S. Kozhin¹⁴⁰, V.A. Kramarenko¹¹¹, G. Kramberger⁸⁹, D. Krasnopevtsev^{58a}, M.W. Krasny¹³², A. Krasznahorkay³⁵, D. Krauss¹¹³, J.A. Kremer^{81a}, J. Kretzschmar⁸⁸, P. Krieger¹⁶⁴, K. Krizka¹⁸, K. Kroeninger⁴⁵, H. Kroha¹¹³, J. Kroll¹³⁷, J. Kroll¹³³, J. Krstic¹⁶, U. Kruchonak⁷⁷, H. Krüger²⁴, N. Krumnack⁷⁶, M.C. Kruse⁴⁷, T. Kubota¹⁰², S. Kудay^{4b}, J.T. Kuechler¹⁷⁹, S. Kuehn³⁵, A. Kugel^{59a}, F. Kuger¹⁷⁴, T. Kuhl⁴⁴, V. Kukhtin⁷⁷, R. Kukla⁹⁹, Y. Kulchitsky¹⁰⁵, S. Kuleshov^{144b}, Y.P. Kulinich¹⁷⁰, M. Kuna⁵⁶, T. Kunigo⁸³, A. Kupco¹³⁷, T. Kupfer⁴⁵, O. Kuprash¹⁵⁸, H. Kurashige⁸⁰, L.L. Kurchaninov^{165a}, Y.A. Kurochkin¹⁰⁵, M.G. Kurth^{15d}, E.S. Kuwertz³⁵, M. Kuze¹⁶², J. Kvita¹²⁶, T. Kwan¹⁰¹, A. La Rosa¹¹³, J.L. La Rosa Navarro^{78d}, L. La Rotonda^{40b,40a}, F. La Ruffa^{40b,40a}, C. Lacasta¹⁷¹, F. Lacava^{70a,70b}, J. Lacey⁴⁴, D.P.J. Lack⁹⁸, H. Lacker¹⁹, D. Lacour¹³², E. Ladygin⁷⁷, R. Lafaye⁵, B. Laforge¹³², T. Lagouri^{32c}, S. Lai⁵¹, S. Lammers⁶³, W. Lampl⁷, E. Lançon²⁹, U. Landgraf⁵⁰, M.P.J. Landon⁹⁰, M.C. Lanfermann⁵², V.S. Lang⁴⁴, J.C. Lange¹⁴, R.J. Langenberg³⁵, A.J. Lankford¹⁶⁸, F. Lanni²⁹, K. Lantzsch²⁴, A. Lanza^{68a}, A. Lapertosa^{53b,53a}, S. Laplace¹³², J.F. Laporte¹⁴², T. Lari^{66a}, F. Lasagni Manghi^{23b,23a}, M. Lassnig³⁵, T.S. Lau^{61a}, A. Laudrain¹²⁸, M. Lavorgna^{67a,67b}, A.T. Law¹⁴³, P. Laycock⁸⁸, M. Lazzaroni^{66a,66b}, B. Le¹⁰², O. Le Dortz¹³², E. Le Guirriec⁹⁹, E.P. Le Quilleuc¹⁴², M. LeBlanc⁷, T. LeCompte⁶, F. Ledroit-Guillon⁵⁶, C.A. Lee²⁹, G.R. Lee^{144a}, L. Lee⁵⁷, S.C. Lee¹⁵⁵, B. Lefebvre¹⁰¹, M. Lefebvre¹⁷³, F. Legger¹¹², C. Leggett¹⁸, K. Lehmann¹⁴⁹, N. Lehmann¹⁷⁹, G. Lehmann Miotto³⁵, W.A. Leight⁴⁴, A. Leisos^{159,u}, M.A.L. Leite^{78d}, R. Leitner¹³⁹, D. Lellouch¹⁷⁷, B. Lemmer⁵¹, K.J.C. Leney⁹², T. Lenz²⁴, B. Lenzi³⁵, R. Leone⁷, S. Leone^{69a}, C. Leonidopoulos⁴⁸, G. Lerner¹⁵³, C. Leroy¹⁰⁷, R. Les¹⁶⁴, A.A.J. Lesage¹⁴², C.G. Lester³¹, M. Levchenko¹³⁴, J. Levêque⁵, D. Levin¹⁰³, L.J. Levinson¹⁷⁷, D. Lewis⁹⁰, B. Li¹⁰³, C.-Q. Li^{58a}, H. Li^{58b}, L. Li^{58c}, Q. Li^{15d}, Q.Y. Li^{58a}, S. Li^{58d,58c}, X. Li^{58c}, Y. Li¹⁴⁸, Z. Liang^{15a}, B. Liberti^{71a}, A. Liblong¹⁶⁴, K. Lie^{61c}, S. Liem¹¹⁸, A. Limosani¹⁵⁴, C.Y. Lin³¹, K. Lin¹⁰⁴, T.H. Lin⁹⁷, R.A. Linck⁶³, J.H. Lindon²¹, B.E. Lindquist¹⁵², A.L. Lioni⁵², E. Lipeles¹³³, A. Lipniacka¹⁷, M. Lisovyi^{59b}, T.M. Liss^{170,an}, A. Lister¹⁷², A.M. Litke¹⁴³, J.D. Little⁸, B. Liu⁷⁶, B.L. Liu⁶, H.B. Liu²⁹, H. Liu¹⁰³, J.B. Liu^{58a}, J.K.K. Liu¹³¹, K. Liu¹³², M. Liu^{58a}, P. Liu¹⁸, Y. Liu^{15a}, Y.L. Liu^{58a}, Y.W. Liu^{58a}, M. Livan^{68a,68b}, A. Lleres⁵⁶, J. Llorente Merino^{15a}, S.L. Lloyd⁹⁰, C.Y. Lo^{61b}, F. Lo Sterzo⁴¹, E.M. Lobodzinska⁴⁴, P. Loch⁷, A. Loesle⁵⁰, T. Lohse¹⁹, K. Lohwasser¹⁴⁶, M. Lokajicek¹³⁷, B.A. Long²⁵, J.D. Long¹⁷⁰, R.E. Long⁸⁷, L. Longo^{65a,65b}, K.A. Looper¹²², J.A. Lopez^{144b}, I. Lopez Paz¹⁴, A. Lopez Solis¹⁴⁶, J. Lorenz¹¹², N. Lorenzo Martinez⁵, M. Losada²², P.J. Lösel¹¹², X. Lou⁴⁴, X. Lou^{15a}, A. Lounis¹²⁸, J. Love⁶, P.A. Love⁸⁷, J.J. Lozano Bahilo¹⁷¹, H. Lu^{61a}, M. Lu^{58a}, N. Lu¹⁰³, Y.J. Lu⁶², H.J. Lubatti¹⁴⁵, C. Luci^{70a,70b}, A. Lucotte⁵⁶, C. Luedtke⁵⁰, F. Luehring⁶³, I. Luise¹³², L. Luminari^{70a}, B. Lund-Jensen¹⁵¹, M.S. Lutz¹⁰⁰, P.M. Luzzi¹³², D. Lynn²⁹, R. Lysak¹³⁷, E. Lytken⁹⁴, F. Lyu^{15a}, V. Lyubushkin⁷⁷, H. Ma²⁹, L.L. Ma^{58b}, Y. Ma^{58b}, G. Maccarrone⁴⁹, A. Macchiolo¹¹³, C.M. Macdonald¹⁴⁶, J. Machado Miguens^{133,136b}, D. Madaffari¹⁷¹, R. Madar³⁷, W.F. Mader⁴⁶, A. Madsen⁴⁴, N. Madysa⁴⁶, J. Maeda⁸⁰, K. Maekawa¹⁶⁰, S. Maeland¹⁷, T. Maeno²⁹, A.S. Maevskiy¹¹¹, V. Magerl⁵⁰, C. Maidantchik^{78b}, T. Maier¹¹², A. Maio^{136a,136b,136d}, O. Majersky^{28a}, S. Majewski¹²⁷, Y. Makida⁷⁹, N. Makovec¹²⁸, B. Malaescu¹³², Pa. Malecki⁸², V.P. Maleev¹³⁴, F. Malek⁵⁶, U. Mallik⁷⁵, D. Malon⁶, C. Malone³¹, S. Maltezos¹⁰, S. Malyukov³⁵, J. Mamuzic¹⁷¹, G. Mancini⁴⁹, I. Mandić⁸⁹, J. Maneira^{136a}, L. Manhaes de Andrade Filho^{78a}, J. Manjarres Ramos⁴⁶, K.H. Mankinen⁹⁴, A. Mann¹¹², A. Manousos⁷⁴, B. Mansoulie¹⁴², J.D. Mansour^{15a}, M. Mantoani⁵¹, S. Manzoni^{66a,66b}, G. Marceca³⁰, L. March⁵², L. Marchese¹³¹, G. Marchiori¹³², M. Marcisovsky¹³⁷, C.A. Marin Tobon³⁵, M. Marjanovic³⁷, D.E. Marley¹⁰³, F. Marroquim^{78b}, Z. Marshall¹⁸, M.U.F. Martensson¹⁶⁹, S. Marti-Garcia¹⁷¹, C.B. Martin¹²², T.A. Martin¹⁷⁵, V.J. Martin⁴⁸, B. Martin dit Latour¹⁷, M. Martinez^{14,x}, V.I. Martinez Outschoorn¹⁰⁰, S. Martin-Haugh¹⁴¹, V.S. Martoiu^{27b}, A.C. Martyniuk⁹², A. Marzin³⁵, L. Masetti⁹⁷, T. Mashimo¹⁶⁰, R. Mashinistov¹⁰⁸, J. Masik⁹⁸, A.L. Maslennikov^{120b,120a}, L.H. Mason¹⁰², L. Massa^{71a,71b}, P. Massarotti^{67a,67b}, P. Mastrandrea⁵, A. Mastroberardino^{40b,40a}, T. Masubuchi¹⁶⁰, P. Mättig¹⁷⁹, J. Maurer^{27b}, B. Maček⁸⁹, S.J. Maxfield⁸⁸, D.A. Maximov^{120b,120a}, R. Mazini¹⁵⁵, I. Maznas¹⁵⁹, S.M. Mazza¹⁴³, N.C. Mc Fadden¹¹⁶, G. Mc Goldrick¹⁶⁴, S.P. Mc Kee¹⁰³, A. McCarn¹⁰³,

T.G. McCarthy¹¹³, L.I. McClymont⁹², E.F. McDonald¹⁰², J.A. McFayden³⁵, G. Mchedlidze⁵¹, M.A. McKay⁴¹, K.D. McLean¹⁷³, S.J. McMahon¹⁴¹, P.C. McNamara¹⁰², C.J. McNicol¹⁷⁵, R.A. McPherson^{173,ab}, J.E. Mdhluli^{32c}, Z.A. Meadows¹⁰⁰, S. Meehan¹⁴⁵, T. Megy⁵⁰, S. Mehlhase¹¹², A. Mehta⁸⁸, T. Meideck⁵⁶, B. Meirose⁴², D. Melini^{171,g}, B.R. Mellado Garcia^{32c}, J.D. Mellenthin⁵¹, M. Melo^{28a}, F. Meloni⁴⁴, A. Melzer²⁴, S.B. Menary⁹⁸, E.D. Mendes Gouveia^{136a}, L. Meng⁸⁸, X.T. Meng¹⁰³, A. Mengarelli^{23b,23a}, S. Menke¹¹³, E. Meoni^{40b,40a}, S. Mergelmeyer¹⁹, C. Merlassino²⁰, P. Mermod⁵², L. Merola^{67a,67b}, C. Meroni^{66a}, F.S. Merritt³⁶, A. Messina^{70a,70b}, J. Metcalfe⁶, A.S. Mete¹⁶⁸, C. Meyer¹³³, J. Meyer¹⁵⁷, J.-P. Meyer¹⁴², H. Meyer Zu Theenhausen^{59a}, F. Miano¹⁵³, R.P. Middleton¹⁴¹, L. Mijović⁴⁸, G. Mikenberg¹⁷⁷, M. Mikestikova¹³⁷, M. Mikuž⁸⁹, M. Milesi¹⁰², A. Milic¹⁶⁴, D.A. Millar⁹⁰, D.W. Miller³⁶, A. Milov¹⁷⁷, D.A. Milstead^{43a,43b}, A.A. Minaenko¹⁴⁰, M. Miñano Moya¹⁷¹, I.A. Minashvili^{156b}, A.I. Mincer¹²¹, B. Mindur^{81a}, M. Mineev⁷⁷, Y. Minegishi¹⁶⁰, Y. Ming¹⁷⁸, L.M. Mir¹⁴, A. Mirto^{65a,65b}, K.P. Mistry¹³³, T. Mitani¹⁷⁶, J. Mitrevski¹¹², V.A. Mitsou¹⁷¹, A. Miucci²⁰, P.S. Miyagawa¹⁴⁶, A. Mizukami⁷⁹, J.U. Mjörnmark⁹⁴, T. Mkrtchyan¹⁸¹, M. Mlynarikova¹³⁹, T. Moa^{43a,43b}, K. Mochizuki¹⁰⁷, P. Mogg⁵⁰, S. Mohapatra³⁸, S. Molander^{43a,43b}, R. Moles-Valls²⁴, M.C. Mondragon¹⁰⁴, K. Mönig⁴⁴, J. Monk³⁹, E. Monnier⁹⁹, A. Montalbano¹⁴⁹, J. Montejo Berlingen³⁵, F. Monticelli⁸⁶, S. Monzani^{66a}, N. Morange¹²⁸, D. Moreno²², M. Moreno Llácer³⁵, P. Morettini^{53b}, M. Morgenstern¹¹⁸, S. Morgenstern⁴⁶, D. Mori¹⁴⁹, M. Morii⁵⁷, M. Morinaga¹⁷⁶, V. Morisbak¹³⁰, A.K. Morley³⁵, G. Mornacchi³⁵, A.P. Morris⁹², J.D. Morris⁹⁰, L. Morvaj¹⁵², P. Moschovakos¹⁰, M. Mosidze^{156b}, H.J. Moss¹⁴⁶, J. Moss^{150,m}, K. Motohashi¹⁶², R. Mount¹⁵⁰, E. Mountricha³⁵, E.J.W. Moyse¹⁰⁰, S. Muanza⁹⁹, F. Mueller¹¹³, J. Mueller¹³⁵, R.S.P. Mueller¹¹², D. Muenstermann⁸⁷, G.A. Mullier²⁰, F.J. Munoz Sanchez⁹⁸, P. Murin^{28b}, W.J. Murray^{175,141}, A. Murrone^{66a,66b}, M. Muškinja⁸⁹, C. Mwewa^{32a}, A.G. Myagkov^{140,aj}, J. Myers¹²⁷, M. Myska¹³⁸, B.P. Nachman¹⁸, O. Nackenhorst⁴⁵, K. Nagai¹³¹, K. Nagano⁷⁹, Y. Nagasaka⁶⁰, M. Nagel⁵⁰, E. Nagy⁹⁹, A.M. Nairz³⁵, Y. Nakahama¹¹⁵, K. Nakamura⁷⁹, T. Nakamura¹⁶⁰, I. Nakano¹²³, H. Nanjo¹²⁹, F. Napolitano^{59a}, R.F. Naranjo Garcia⁴⁴, R. Narayan¹¹, D.I. Narrias Villar^{59a}, I. Naryshkin¹³⁴, T. Naumann⁴⁴, G. Navarro²², R. Nayyar⁷, H.A. Neal¹⁰³, P.Y. Nechaeva¹⁰⁸, T.J. Neep¹⁴², A. Negri^{68a,68b}, M. Negrini^{23b}, S. Nektarijevic¹¹⁷, C. Nellist⁵¹, M.E. Nelson¹³¹, S. Nemecek¹³⁷, P. Nemethy¹²¹, M. Nessi^{35,e}, M.S. Neubauer¹⁷⁰, M. Neumann¹⁷⁹, P.R. Newman²¹, T.Y. Ng^{61c}, Y.S. Ng¹⁹, H.D.N. Nguyen⁹⁹, T. Nguyen Manh¹⁰⁷, E. Nibigira³⁷, R.B. Nickerson¹³¹, R. Nicolaïdou¹⁴², J. Nielsen¹⁴³, N. Nikiforou¹¹, V. Nikolaenko^{140,aj}, I. Nikolic-Audit¹³², K. Nikolopoulos²¹, P. Nilsson²⁹, Y. Ninomiya⁷⁹, A. Nisati^{70a}, N. Nishu^{58c}, R. Nisius¹¹³, I. Nitsche⁴⁵, T. Nitta¹⁷⁶, T. Nobe¹⁶⁰, Y. Noguchi⁸³, M. Nomachi¹²⁹, I. Nomidis¹³², M.A. Nomura²⁹, T. Nooney⁹⁰, M. Nordberg³⁵, N. Norjoharuddeen¹³¹, T. Novak⁸⁹, O. Novgorodova⁴⁶, R. Novotny¹³⁸, L. Nozka¹²⁶, K. Ntekas¹⁶⁸, E. Nurse⁹², F. Nuti¹⁰², F.G. Oakham^{33,aq}, H. Oberlack¹¹³, T. Obermann²⁴, J. Ocariz¹³², A. Ochi⁸⁰, I. Ochoa³⁸, J.P. Ochoa-Ricoux^{144a}, K. O'Connor²⁶, S. Oda⁸⁵, S. Odaka⁷⁹, S. Oerdek⁵¹, A. Oh⁹⁸, S.H. Oh⁴⁷, C.C. Ohm¹⁵¹, H. Oide^{53b,53a}, M.L. Ojeda¹⁶⁴, H. Okawa¹⁶⁶, Y. Okazaki⁸³, Y. Okumura¹⁶⁰, T. Okuyama⁷⁹, A. Olariu^{27b}, L.F. Oleiro Seabra^{136a}, S.A. Olivares Pino^{144a}, D. Oliveira Damazio²⁹, J.L. Oliver¹, M.J.R. Olsson³⁶, A. Olszewski⁸², J. Olszowska⁸², D.C. O'Neil¹⁴⁹, A. Onofre^{136a,136e}, K. Onogi¹¹⁵, P.U.E. Onyisi¹¹, H. Oppen¹³⁰, M.J. Oreglia³⁶, Y. Oren¹⁵⁸, D. Orestano^{72a,72b}, E.C. Orgill⁹⁸, N. Orlando^{61b}, A.A. O'Rourke⁴⁴, R.S. Orr¹⁶⁴, B. Osculati^{53b,53a,*}, V. O'Shea⁵⁵, R. Ospanov^{58a}, G. Otero y Garzon³⁰, H. Otono⁸⁵, M. Ouchrif^{34d}, F. Ould-Saada¹³⁰, A. Ouraou¹⁴², Q. Ouyang^{15a}, M. Owen⁵⁵, R.E. Owen²¹, V.E. Ozcan^{12c}, N. Ozturk⁸, J. Pacalt¹²⁶, H.A. Pacey³¹, K. Pachal¹⁴⁹, A. Pacheco Pages¹⁴, L. Pacheco Rodriguez¹⁴², C. Padilla Aranda¹⁴, S. Pagan Griso¹⁸, M. Paganini¹⁸⁰, G. Palacino⁶³, S. Palazzo^{40b,40a}, S. Palestini³⁵, M. Palka^{81b}, D. Pallin³⁷, I. Panagoulas¹⁰, C.E. Pandini³⁵, J.G. Panduro Vazquez⁹¹, P. Pani³⁵, G. Panizzo^{64a,64c}, L. Paolozzi⁵², T.D. Papadopoulou¹⁰, K. Papageorgiou^{9,i}, A. Paramonov⁶, D. Paredes Hernandez^{61b}, S.R. Paredes Saenz¹³¹, B. Parida^{58c}, A.J. Parker⁸⁷, K.A. Parker⁴⁴, M.A. Parker³¹, F. Parodi^{53b,53a}, J.A. Parsons³⁸, U. Parzefall⁵⁰, V.R. Pascuzzi¹⁶⁴, J.M.P. Pasner¹⁴³, E. Pasqualucci^{70a}, S. Passaggio^{53b}, F. Pastore⁹¹, P. Pasuwan^{43a,43b}, S. Patariaia⁹⁷, J.R. Pater⁹⁸, A. Pathak^{178,j}, T. Pauly³⁵, B. Pearson¹¹³, M. Pedersen¹³⁰, L. Pedraza Diaz¹¹⁷, R. Pedro^{136a,136b}, S.V. Peleganchuk^{120b,120a}, O. Penc¹³⁷, C. Peng^{15d}, H. Peng^{58a}, B.S. Peralva^{78a}, M.M. Perego¹⁴², A.P. Pereira Peixoto^{136a}, D.V. Perepelitsa²⁹, F. Peri¹⁹, L. Perini^{66a,66b}, H. Pernegger³⁵, S. Perrella^{67a,67b}, V.D. Peshekhonov^{77,*}, K. Peters⁴⁴, R.F.Y. Peters⁹⁸, B.A. Petersen³⁵, T.C. Petersen³⁹, E. Petit⁵⁶, A. Petridis¹, C. Petridou¹⁵⁹, P. Petroff¹²⁸, M. Petrov¹³¹,

F. Petrucci ^{72a,72b}, M. Pettee ¹⁸⁰, N.E. Pettersson ¹⁰⁰, A. Peyaud ¹⁴², R. Pezoa ^{144b}, T. Pham ¹⁰², F.H. Phillips ¹⁰⁴, P.W. Phillips ¹⁴¹, G. Piacquadio ¹⁵², E. Pianori ¹⁸, A. Picazio ¹⁰⁰, M.A. Pickering ¹³¹, R.H. Pickles ⁹⁸, R. Piegaia ³⁰, J.E. Pilcher ³⁶, A.D. Pilkington ⁹⁸, M. Pinamonti ^{71a,71b}, J.L. Pinfold ³, M. Pitt ¹⁷⁷, M.-A. Pleier ²⁹, V. Pleskot ¹³⁹, E. Plotnikova ⁷⁷, D. Pluth ⁷⁶, P. Podberezko ^{120b,120a}, R. Poettgen ⁹⁴, R. Poggi ⁵², L. Poggioli ¹²⁸, I. Pogrebnyak ¹⁰⁴, D. Pohl ²⁴, I. Pokharel ⁵¹, G. Polesello ^{68a}, A. Poley ¹⁸, A. Policicchio ^{70a,70b}, R. Polifka ³⁵, A. Polini ^{23b}, C.S. Pollard ⁴⁴, V. Polychronakos ²⁹, D. Ponomarenko ¹¹⁰, L. Pontecorvo ^{70a}, G.A. Popeneciu ^{27d}, D.M. Portillo Quintero ¹³², S. Pospisil ¹³⁸, K. Potamianos ⁴⁴, I.N. Potrap ⁷⁷, C.J. Potter ³¹, H. Potti ¹¹, T. Poulsen ⁹⁴, J. Poveda ³⁵, T.D. Powell ¹⁴⁶, M.E. Pozo Astigarraga ³⁵, P. Pralavorio ⁹⁹, S. Prell ⁷⁶, D. Price ⁹⁸, M. Primavera ^{65a}, S. Prince ¹⁰¹, N. Proklova ¹¹⁰, K. Prokofiev ^{61c}, F. Prokoshin ^{144b}, S. Protopopescu ²⁹, J. Proudfoot ⁶, M. Przybycien ^{81a}, A. Puri ¹⁷⁰, P. Puzo ¹²⁸, J. Qian ¹⁰³, Y. Qin ⁹⁸, A. Quadt ⁵¹, M. Queitsch-Maitland ⁴⁴, A. Qureshi ¹, P. Rados ¹⁰², F. Ragusa ^{66a,66b}, G. Rahal ⁹⁵, J.A. Raine ⁵², S. Rajagopalan ²⁹, A. Ramirez Morales ⁹⁰, T. Rashid ¹²⁸, S. Raspopov ⁵, M.G. Ratti ^{66a,66b}, D.M. Rauch ⁴⁴, F. Rauscher ¹¹², S. Rave ⁹⁷, B. Ravina ¹⁴⁶, I. Ravinovich ¹⁷⁷, J.H. Rawling ⁹⁸, M. Raymond ³⁵, A.L. Read ¹³⁰, N.P. Readoff ⁵⁶, M. Reale ^{65a,65b}, D.M. Rebuzzi ^{68a,68b}, A. Redelbach ¹⁷⁴, G. Redlinger ²⁹, R. Reece ¹⁴³, R.G. Reed ^{32c}, K. Reeves ⁴², L. Rehnisch ¹⁹, J. Reichert ¹³³, A. Reiss ⁹⁷, C. Rembser ³⁵, H. Ren ^{15d}, M. Rescigno ^{70a}, S. Resconi ^{66a}, E.D. Resseguie ¹³³, S. Rettie ¹⁷², E. Reynolds ²¹, O.L. Rezanova ^{120b,120a}, P. Reznicek ¹³⁹, E. Ricci ^{73a,73b}, R. Richter ¹¹³, S. Richter ⁹², E. Richter-Was ^{81b}, O. Ricken ²⁴, M. Ridel ¹³², P. Rieck ¹¹³, C.J. Riegel ¹⁷⁹, O. Rifki ⁴⁴, M. Rijssenbeek ¹⁵², A. Rimoldi ^{68a,68b}, M. Rimoldi ²⁰, L. Rinaldi ^{23b}, G. Ripellino ¹⁵¹, B. Ristić ⁸⁷, E. Ritsch ³⁵, I. Riu ¹⁴, J.C. Rivera Vergara ^{144a}, F. Rizatdinova ¹²⁵, E. Rizvi ⁹⁰, C. Rizzi ¹⁴, R.T. Roberts ⁹⁸, S.H. Robertson ^{101,ab}, D. Robinson ³¹, J.E.M. Robinson ⁴⁴, A. Robson ⁵⁵, E. Rocco ⁹⁷, C. Roda ^{69a,69b}, Y. Rodina ⁹⁹, S. Rodriguez Bosca ¹⁷¹, A. Rodriguez Perez ¹⁴, D. Rodriguez Rodriguez ¹⁷¹, A.M. Rodríguez Vera ^{165b}, S. Roe ³⁵, C.S. Rogan ⁵⁷, O. Røhne ¹³⁰, R. Röhrig ¹¹³, C.P.A. Roland ⁶³, J. Roloff ⁵⁷, A. Romaniouk ¹¹⁰, M. Romano ^{23b,23a}, N. Rompotis ⁸⁸, M. Ronzani ¹²¹, L. Roos ¹³², S. Rosati ^{70a}, K. Rosbach ⁵⁰, P. Rose ¹⁴³, N.-A. Rosien ⁵¹, E. Rossi ⁴⁴, E. Rossi ^{67a,67b}, L.P. Rossi ^{53b}, L. Rossini ^{66a,66b}, J.H.N. Rosten ³¹, R. Rosten ¹⁴, M. Rotaru ^{27b}, J. Rothberg ¹⁴⁵, D. Rousseau ¹²⁸, D. Roy ^{32c}, A. Rozanov ⁹⁹, Y. Rozen ¹⁵⁷, X. Ruan ^{32c}, F. Rubbo ¹⁵⁰, F. Rühr ⁵⁰, A. Ruiz-Martinez ¹⁷¹, Z. Rurikova ⁵⁰, N.A. Rusakovich ⁷⁷, H.L. Russell ¹⁰¹, J.P. Rutherford ⁷, E.M. Rüttinger ^{44,k}, Y.F. Ryabov ¹³⁴, M. Rybar ¹⁷⁰, G. Rybkin ¹²⁸, S. Ryu ⁶, A. Ryzhov ¹⁴⁰, G.F. Rzehorz ⁵¹, P. Sabatini ⁵¹, G. Sabato ¹¹⁸, S. Sacerdoti ¹²⁸, H.F.-W. Sadrozinski ¹⁴³, R. Sadykov ⁷⁷, F. Safai Tehrani ^{70a}, P. Saha ¹¹⁹, M. Sahinsoy ^{59a}, A. Sahu ¹⁷⁹, M. Saimpert ⁴⁴, M. Saito ¹⁶⁰, T. Saito ¹⁶⁰, H. Sakamoto ¹⁶⁰, A. Sakharov ^{121,ai}, D. Salamani ⁵², G. Salamanna ^{72a,72b}, J.E. Salazar Loyola ^{144b}, D. Salek ¹¹⁸, P.H. Sales De Bruin ¹⁶⁹, D. Salihagic ¹¹³, A. Salnikov ¹⁵⁰, J. Salt ¹⁷¹, D. Salvatore ^{40b,40a}, F. Salvatore ¹⁵³, A. Salvucci ^{61a,61b,61c}, A. Salzburger ³⁵, J. Samarati ³⁵, D. Sammel ⁵⁰, D. Sampsonidis ¹⁵⁹, D. Sampsonidou ¹⁵⁹, J. Sánchez ¹⁷¹, A. Sanchez Pineda ^{64a,64c}, H. Sandaker ¹³⁰, C.O. Sander ⁴⁴, M. Sandhoff ¹⁷⁹, C. Sandoval ²², D.P.C. Sankey ¹⁴¹, M. Sannino ^{53b,53a}, Y. Sano ¹¹⁵, A. Sansoni ⁴⁹, C. Santoni ³⁷, H. Santos ^{136a}, I. Santoyo Castillo ¹⁵³, A. Santra ¹⁷¹, A. Saponov ⁷⁷, J.G. Saraiva ^{136a,136d}, O. Sasaki ⁷⁹, K. Sato ¹⁶⁶, E. Sauvan ⁵, P. Savard ^{164,aq}, N. Savic ¹¹³, R. Sawada ¹⁶⁰, C. Sawyer ¹⁴¹, L. Sawyer ^{93,ah}, C. Sbarra ^{23b}, A. Sbrizzi ^{23b,23a}, T. Scanlon ⁹², J. Schaarschmidt ¹⁴⁵, P. Schacht ¹¹³, B.M. Schachtner ¹¹², D. Schaefer ³⁶, L. Schaefer ¹³³, J. Schaeffer ⁹⁷, S. Schaepe ³⁵, U. Schäfer ⁹⁷, A.C. Schaffer ¹²⁸, D. Schaile ¹¹², R.D. Schamberger ¹⁵², N. Scharmberg ⁹⁸, V.A. Schegelsky ¹³⁴, D. Scheirich ¹³⁹, F. Schenck ¹⁹, M. Schernau ¹⁶⁸, C. Schiavi ^{53b,53a}, S. Schier ¹⁴³, L.K. Schildgen ²⁴, Z.M. Schillaci ²⁶, E.J. Schioppa ³⁵, M. Schioppa ^{40b,40a}, K.E. Schleicher ⁵⁰, S. Schlenker ³⁵, K.R. Schmidt-Sommerfeld ¹¹³, K. Schmieden ³⁵, C. Schmitt ⁹⁷, S. Schmitt ⁴⁴, S. Schmitz ⁹⁷, J.C. Schmoeckel ⁴⁴, U. Schnoor ⁵⁰, L. Schoeffel ¹⁴², A. Schoening ^{59b}, E. Schopf ²⁴, M. Schott ⁹⁷, J.F.P. Schouwenaar ¹¹⁷, J. Schovancova ³⁵, S. Schramm ⁵², A. Schulte ⁹⁷, H.-C. Schultz-Coulon ^{59a}, M. Schumacher ⁵⁰, B.A. Schumm ¹⁴³, Ph. Schune ¹⁴², A. Schwartzman ¹⁵⁰, T.A. Schwarz ¹⁰³, H. Schweiger ⁹⁸, Ph. Schwemling ¹⁴², R. Schwienhorst ¹⁰⁴, A. Sciandra ²⁴, G. Sciolla ²⁶, M. Scornajenghi ^{40b,40a}, F. Scuri ^{69a}, F. Scutti ¹⁰², L.M. Scyboz ¹¹³, J. Searcy ¹⁰³, C.D. Sebastiani ^{70a,70b}, P. Seema ²⁴, S.C. Seidel ¹¹⁶, A. Seiden ¹⁴³, T. Seiss ³⁶, J.M. Seixas ^{78b}, G. Sekhniaidze ^{67a}, K. Sekhon ¹⁰³, S.J. Sekula ⁴¹, N. Semprini-Cesari ^{23b,23a}, S. Sen ⁴⁷, S. Senkin ³⁷, C. Serfon ¹³⁰, L. Serin ¹²⁸, L. Serkin ^{64a,64b}, M. Sessa ^{72a,72b}, H. Severini ¹²⁴, F. Sforza ¹⁶⁷, A. Sfyrila ⁵², E. Shabalina ⁵¹, J.D. Shahinian ¹⁴³, N.W. Shaikh ^{43a,43b}, L.Y. Shan ^{15a}, R. Shang ¹⁷⁰, J.T. Shank ²⁵, M. Shapiro ¹⁸, A.S. Sharma ¹, A. Sharma ¹³¹,

P.B. Shatalov¹⁰⁹, K. Shaw¹⁵³, S.M. Shaw⁹⁸, A. Shcherbakova¹³⁴, Y. Shen¹²⁴, N. Sherafati³³, A.D. Sherman²⁵, P. Sherwood⁹², L. Shi^{155,am}, S. Shimizu⁷⁹, C.O. Shimmin¹⁸⁰, M. Shimojima¹¹⁴, I.P.J. Shipsey¹³¹, S. Shirabe⁸⁵, M. Shiyakova⁷⁷, J. Shlomi¹⁷⁷, A. Shmeleva¹⁰⁸, D. Shoaleh Saadi¹⁰⁷, M.J. Shochet³⁶, S. Shojaii¹⁰², D.R. Shope¹²⁴, S. Shrestha¹²², E. Shulga¹¹⁰, P. Sicho¹³⁷, A.M. Sickles¹⁷⁰, P.E. Sidebo¹⁵¹, E. Sideras Haddad^{32c}, O. Sidiropoulou³⁵, A. Sidoti^{23b,23a}, F. Siegert⁴⁶, Dj. Sijacki¹⁶, J. Silva^{136a}, M. Silva Jr.¹⁷⁸, M.V. Silva Oliveira^{78a}, S.B. Silverstein^{43a}, L. Simic⁷⁷, S. Simion¹²⁸, E. Simioni⁹⁷, M. Simon⁹⁷, R. Simoniello⁹⁷, P. Sinervo¹⁶⁴, N.B. Sinev¹²⁷, M. Sioli^{23b,23a}, G. Siragusa¹⁷⁴, I. Siral¹⁰³, S.Yu. Sivoklokov¹¹¹, J. Sjölin^{43a,43b}, P. Skubic¹²⁴, M. Slater²¹, T. Slavicek¹³⁸, M. Slawinska⁸², K. Sliwa¹⁶⁷, R. Slovak¹³⁹, V. Smakhtin¹⁷⁷, B.H. Smart⁵, J. Smiesko^{28a}, N. Smirnov¹¹⁰, S.Yu. Smirnov¹¹⁰, Y. Smirnov¹¹⁰, L.N. Smirnova¹¹¹, O. Smirnova⁹⁴, J.W. Smith⁵¹, M.N.K. Smith³⁸, M. Smizanska⁸⁷, K. Smolek¹³⁸, A. Smykiewicz⁸², A.A. Snesarev¹⁰⁸, I.M. Snyder¹²⁷, S. Snyder²⁹, R. Sobie^{173,ab}, A.M. Soffa¹⁶⁸, A. Soffer¹⁵⁸, A. Søgaard⁴⁸, D.A. Soh¹⁵⁵, G. Sokhrannyi⁸⁹, C.A. Solans Sanchez³⁵, M. Solar¹³⁸, E.Yu. Soldatov¹¹⁰, U. Soldevila¹⁷¹, A.A. Solodkov¹⁴⁰, A. Soloshenko⁷⁷, O.V. Solovyanov¹⁴⁰, V. Solovyev¹³⁴, P. Sommer¹⁴⁶, H. Son¹⁶⁷, W. Song¹⁴¹, W.Y. Song^{165b}, A. Sopczak¹³⁸, F. Sopkova^{28b}, D. Sosa^{59b}, C.L. Sotiropoulou^{69a,69b}, S. Sottocornola^{68a,68b}, R. Soualah^{64a,64c,h}, A.M. Soukharev^{120b,120a}, D. South⁴⁴, B.C. Sowden⁹¹, S. Spagnolo^{65a,65b}, M. Spalla¹¹³, M. Spangenberg¹⁷⁵, F. Spanò⁹¹, D. Sperlich¹⁹, F. Spettel¹¹³, T.M. Spieker^{59a}, R. Spighi^{23b}, G. Spigo³⁵, L.A. Spiller¹⁰², D.P. Spiteri⁵⁵, M. Spousta¹³⁹, A. Stabile^{66a,66b}, R. Stamen^{59a}, S. Stamm¹⁹, E. Stanecka⁸², R.W. Stanek⁶, C. Stancescu^{72a}, B. Stanislaus¹³¹, M.M. Stanitzki⁴⁴, B. Stapf¹¹⁸, S. Stapnes¹³⁰, E.A. Starchenko¹⁴⁰, G.H. Stark³⁶, J. Stark⁵⁶, S.H. Stark³⁹, P. Staroba¹³⁷, P. Starovoitov^{59a}, S. Stärz³⁵, R. Staszewski⁸², M. Stegler⁴⁴, P. Steinberg²⁹, B. Stelzer¹⁴⁹, H.J. Stelzer³⁵, O. Stelzer-Chilton^{165a}, H. Stenzel⁵⁴, T.J. Stevenson⁹⁰, G.A. Stewart⁵⁵, M.C. Stockton¹²⁷, G. Stoica^{27b}, P. Stolte⁵¹, S. Stonjek¹¹³, A. Straessner⁴⁶, J. Strandberg¹⁵¹, S. Strandberg^{43a,43b}, M. Strauss¹²⁴, P. Strizenec^{28b}, R. Ströhmer¹⁷⁴, D.M. Strom¹²⁷, R. Stroynowski⁴¹, A. Strubig⁴⁸, S.A. Stucci²⁹, B. Stugu¹⁷, J. Stupak¹²⁴, N.A. Styles⁴⁴, D. Su¹⁵⁰, J. Su¹³⁵, S. Suchek^{59a}, Y. Sugaya¹²⁹, M. Suk¹³⁸, V.V. Sulin¹⁰⁸, D.M.S. Sultan⁵², S. Sultansoy^{4c}, T. Sumida⁸³, S. Sun¹⁰³, X. Sun³, K. Suruliz¹⁵³, C.J.E. Suster¹⁵⁴, M.R. Sutton¹⁵³, S. Suzuki⁷⁹, M. Svatos¹³⁷, M. Swiatlowski³⁶, S.P. Swift², A. Sydorenko⁹⁷, I. Sykora^{28a}, T. Sykora¹³⁹, D. Ta⁹⁷, K. Tackmann^{44,y}, J. Taenzer¹⁵⁸, A. Taffard¹⁶⁸, R. Tafirout^{165a}, E. Tahirovic⁹⁰, N. Taiblum¹⁵⁸, H. Takai²⁹, R. Takashima⁸⁴, E.H. Takasugi¹¹³, K. Takeda⁸⁰, T. Takeshita¹⁴⁷, Y. Takubo⁷⁹, M. Talby⁹⁹, A.A. Talyshev^{120b,120a}, J. Tanaka¹⁶⁰, M. Tanaka¹⁶², R. Tanaka¹²⁸, B.B. Tannenwald¹²², S. Tapia Araya^{144b}, S. Tapprogge⁹⁷, A. Tarek Abouelfadl Mohamed¹³², S. Tarem¹⁵⁷, G. Tarna^{27b,d}, G.F. Tartarelli^{66a}, P. Tas¹³⁹, M. Tasevsky¹³⁷, T. Tashiro⁸³, E. Tassi^{40b,40a}, A. Tavares Delgado^{136a,136b}, Y. Tayalati^{34e}, A.C. Taylor¹¹⁶, A.J. Taylor⁴⁸, G.N. Taylor¹⁰², P.T.E. Taylor¹⁰², W. Taylor^{165b}, A.S. Tee⁸⁷, P. Teixeira-Dias⁹¹, H. Ten Kate³⁵, P.K. Teng¹⁵⁵, J.J. Teoh¹¹⁸, F. Tepel¹⁷⁹, S. Terada⁷⁹, K. Terashi¹⁶⁰, J. Terron⁹⁶, S. Terzo¹⁴, M. Testa⁴⁹, R.J. Teuscher^{164,ab}, S.J. Thais¹⁸⁰, T. Theveneaux-Pelzer⁴⁴, F. Thiele³⁹, D.W. Thomas⁹¹, J.P. Thomas²¹, A.S. Thompson⁵⁵, P.D. Thompson²¹, L.A. Thomsen¹⁸⁰, E. Thomson¹³³, Y. Tian³⁸, R.E. Ticse Torres⁵¹, V.O. Tikhomirov^{108,ak}, Yu.A. Tikhonov^{120b,120a}, S. Timoshenko¹¹⁰, P. Tipton¹⁸⁰, S. Tisserant⁹⁹, K. Todome¹⁶², S. Todorova-Nova⁵, S. Todt⁴⁶, J. Tojo⁸⁵, S. Tokár^{28a}, K. Tokushuku⁷⁹, E. Tolley¹²², K.G. Tomiwa^{32c}, M. Tomoto¹¹⁵, L. Tompkins¹⁵⁰, K. Toms¹¹⁶, B. Tong⁵⁷, P. Tornambe⁵⁰, E. Torrence¹²⁷, H. Torres⁴⁶, E. Torró Pastor¹⁴⁵, C. Toscirì¹³¹, J. Toth^{99,aa}, F. Touchard⁹⁹, D.R. Tovey¹⁴⁶, C.J. Treado¹²¹, T. Trefzger¹⁷⁴, F. Tresoldi¹⁵³, A. Tricoli²⁹, I.M. Trigger^{165a}, S. Trincaz-Duvold¹³², M.F. Tripiana¹⁴, W. Trischuk¹⁶⁴, B. Trocmé⁵⁶, A. Trofymov¹²⁸, C. Troncon^{66a}, M. Trovatelli¹⁷³, F. Trovato¹⁵³, L. Truong^{32b}, M. Trzebinski⁸², A. Trzupek⁸², F. Tsai⁴⁴, J.C.-L. Tseng¹³¹, P.V. Tsiarshka¹⁰⁵, A. Tsirigotis¹⁵⁹, N. Tsirintanis⁹, V. Tsiskaridze¹⁵², E.G. Tskhadadze^{156a}, I.I. Tsukerman¹⁰⁹, V. Tsulaia¹⁸, S. Tsuno⁷⁹, D. Tsybychev^{152,163}, Y. Tu^{61b}, A. Tudorache^{27b}, V. Tudorache^{27b}, T.T. Tulbure^{27a}, A.N. Tuna⁵⁷, S. Turchikhin⁷⁷, D. Turgeman¹⁷⁷, I. Turk Cakir^{4b,s}, R. Turra^{66a}, P.M. Tuts³⁸, E. Tzovara⁹⁷, G. Uccielli^{23b,23a}, I. Ueda⁷⁹, M. Ughetto^{43a,43b}, F. Ukegawa¹⁶⁶, G. Unal³⁵, A. Undrus²⁹, G. Unel¹⁶⁸, F.C. Ungaro¹⁰², Y. Unno⁷⁹, K. Uno¹⁶⁰, J. Urban^{28b}, P. Urquijo¹⁰², P. Urrejola⁹⁷, G. Usai⁸, J. Usui⁷⁹, L. Vacavant⁹⁹, V. Vacek¹³⁸, B. Vachon¹⁰¹, K.O.H. Vadla¹³⁰, A. Vaidya⁹², C. Valderanis¹¹², E. Valdes Santurio^{43a,43b}, M. Valente⁵², S. Valentini^{23b,23a}, A. Valero¹⁷¹, L. Valéry⁴⁴, R.A. Vallance²¹, A. Vallier⁵, J.A. Valls Ferrer¹⁷¹, T.R. Van Daalen¹⁴, H. Van der Graaf¹¹⁸, P. Van Gemmeren⁶, J. Van Nieuwkoop¹⁴⁹, I. Van Vulpén¹¹⁸, M. Vanadia^{71a,71b}, W. Vandelli³⁵, A. Vaniachine¹⁶³,

P. Vankov¹¹⁸, R. Vari^{70a}, E.W. Varnes⁷, C. Varni^{53b,53a}, T. Varol⁴¹, D. Varouchas¹²⁸, K.E. Varvell¹⁵⁴, G.A. Vasquez^{144b}, J.G. Vasquez¹⁸⁰, F. Vazeille³⁷, D. Vazquez Furelos¹⁴, T. Vazquez Schroeder¹⁰¹, J. Veatch⁵¹, V. Vecchio^{72a,72b}, L.M. Veloce¹⁶⁴, F. Veloso^{136a,136c}, S. Veneziano^{70a}, A. Ventura^{65a,65b}, M. Venturi¹⁷³, N. Venturi³⁵, V. Vercesi^{68a}, M. Verducci^{72a,72b}, C.M. Vergel Infante⁷⁶, C. Vergis²⁴, W. Verkerke¹¹⁸, A.T. Vermeulen¹¹⁸, J.C. Vermeulen¹¹⁸, M.C. Vetterli^{149,aq}, N. Viaux Maira^{144b}, M. Vicente Barreto Pinto⁵², I. Vichou^{170,*}, T. Vickey¹⁴⁶, O.E. Vickey Boeriu¹⁴⁶, G.H.A. Viehhauser¹³¹, S. Viel¹⁸, L. Vigani¹³¹, M. Villa^{23b,23a}, M. Villaplana Perez^{66a,66b}, E. Vilucchi⁴⁹, M.G. Vinciter³³, V.B. Vinogradov⁷⁷, A. Vishwakarma⁴⁴, C. Vittori^{23b,23a}, I. Vivarelli¹⁵³, S. Vlachos¹⁰, M. Vogel¹⁷⁹, P. Vokac¹³⁸, G. Volpi¹⁴, S.E. Von Buddenbrock^{32c}, E. Von Toerne²⁴, V. Vorobel¹³⁹, K. Vorobev¹¹⁰, M. Vos¹⁷¹, J.H. Vosseveld⁸⁸, N. Vranjes¹⁶, M. Vranjes Milosavljevic¹⁶, V. Vrba¹³⁸, M. Vreeswijk¹¹⁸, T. Šfiligoj⁸⁹, R. Vuillermet³⁵, I. Vukotic³⁶, T. Ženiš^{28a}, L. Živković¹⁶, P. Wagner²⁴, W. Wagner¹⁷⁹, J. Wagner-Kuhr¹¹², H. Wahlberg⁸⁶, S. Wahrhund⁴⁶, K. Wakamiya⁸⁰, V.M. Walbrecht¹¹³, J. Walder⁸⁷, R. Walker¹¹², S.D. Walker⁹¹, W. Walkowiak¹⁴⁸, V. Wallangen^{43a,43b}, A.M. Wang⁵⁷, C. Wang^{58b,d}, F. Wang¹⁷⁸, H. Wang¹⁸, H. Wang³, J. Wang¹⁵⁴, J. Wang^{59b}, P. Wang⁴¹, Q. Wang¹²⁴, R.-J. Wang¹³², R. Wang^{58a}, R. Wang⁶, S.M. Wang¹⁵⁵, W.T. Wang^{58a}, W. Wang^{15c,ac}, W.X. Wang^{58a,ac}, Y. Wang^{58a}, Z. Wang^{58c}, C. Wanotayaroj⁴⁴, A. Warburton¹⁰¹, C.P. Ward³¹, D.R. Wardrope⁹², A. Washbrook⁴⁸, P.M. Watkins²¹, A.T. Watson²¹, M.F. Watson²¹, G. Watts¹⁴⁵, S. Watts⁹⁸, B.M. Waugh⁹², A.F. Webb¹¹, S. Webb⁹⁷, C. Weber¹⁸⁰, M.S. Weber²⁰, S.A. Weber³³, S.M. Weber^{59a}, A.R. Weidberg¹³¹, B. Weinert⁶³, J. Weingarten⁵¹, M. Weirich⁹⁷, C. Weiser⁵⁰, P.S. Wells³⁵, T. Wenaus²⁹, T. Wengler³⁵, S. Wenig³⁵, N. Wermes²⁴, M.D. Werner⁷⁶, P. Werner³⁵, M. Wessels^{59a}, T.D. Weston²⁰, K. Whalen¹²⁷, N.L. Whallon¹⁴⁵, A.M. Wharton⁸⁷, A.S. White¹⁰³, A. White⁸, M.J. White¹, R. White^{144b}, D. Whiteson¹⁶⁸, B.W. Whitmore⁸⁷, F.J. Wickens¹⁴¹, W. Wiedenmann¹⁷⁸, M. Wielers¹⁴¹, C. Wigglesworth³⁹, L.A.M. Wiik-Fuchs⁵⁰, A. Wildauer¹¹³, F. Wilk⁹⁸, H.G. Wilkens³⁵, L.J. Wilkins⁹¹, H.H. Williams¹³³, S. Williams³¹, C. Willis¹⁰⁴, S. Willocq¹⁰⁰, J.A. Wilson²¹, I. Wingerter-Seez⁵, E. Winkels¹⁵³, F. Winklmeier¹²⁷, O.J. Winston¹⁵³, B.T. Winter²⁴, M. Wittgen¹⁵⁰, M. Wobisch⁹³, A. Wolf⁹⁷, T.M.H. Wolf¹¹⁸, R. Wolff⁹⁹, M.W. Wolter⁸², H. Wolters^{136a,136c}, V.W.S. Wong¹⁷², N.L. Woods¹⁴³, S.D. Worm²¹, B.K. Wosiek⁸², K.W. Woźniak⁸², K. Wraight⁵⁵, M. Wu³⁶, S.L. Wu¹⁷⁸, X. Wu⁵², Y. Wu^{58a}, T.R. Wyatt⁹⁸, B.M. Wynne⁴⁸, S. Xella³⁹, Z. Xi¹⁰³, L. Xia¹⁷⁵, D. Xu^{15a}, H. Xu^{58a}, L. Xu²⁹, T. Xu¹⁴², W. Xu¹⁰³, B. Yabsley¹⁵⁴, S. Yacoob^{32a}, K. Yajima¹²⁹, D.P. Yallup⁹², D. Yamaguchi¹⁶², Y. Yamaguchi¹⁶², A. Yamamoto⁷⁹, T. Yamanaka¹⁶⁰, F. Yamane⁸⁰, M. Yamatani¹⁶⁰, T. Yamazaki¹⁶⁰, Y. Yamazaki⁸⁰, Z. Yan²⁵, H.J. Yang^{58c,58d}, H.T. Yang¹⁸, S. Yang⁷⁵, Y. Yang¹⁶⁰, Z. Yang¹⁷, W.-M. Yao¹⁸, Y.C. Yap⁴⁴, Y. Yasu⁷⁹, E. Yatsenko^{58c,58d}, J. Ye⁴¹, S. Ye²⁹, I. Yeletsikh⁷⁷, E. Yigitbasi²⁵, E. Yildirim⁹⁷, K. Yorita¹⁷⁶, K. Yoshihara¹³³, C.J.S. Young³⁵, C. Young¹⁵⁰, J. Yu⁸, J. Yu⁷⁶, X. Yue^{59a}, S.P.Y. Yuen²⁴, B. Zabinski⁸², G. Zacharis¹⁰, E. Zaffaroni⁵², R. Zaidan¹⁴, A.M. Zaitsev^{140,aq}, T. Zakareishvili^{156b}, N. Zakharchuk⁴⁴, J. Zalieckas¹⁷, S. Zambito⁵⁷, D. Zanzi³⁵, D.R. Zaripovas⁵⁵, S.V. Zeiβner⁴⁵, C. Zeitnitz¹⁷⁹, G. Zemaityte¹³¹, J.C. Zeng¹⁷⁰, Q. Zeng¹⁵⁰, O. Zenin¹⁴⁰, D. Zerwas¹²⁸, M. Zgubič¹³¹, D.F. Zhang^{58b}, D. Zhang¹⁰³, F. Zhang¹⁷⁸, G. Zhang^{58a}, H. Zhang^{15c}, J. Zhang⁶, L. Zhang^{15c}, L. Zhang^{58a}, M. Zhang¹⁷⁰, P. Zhang^{15c}, R. Zhang^{58a}, R. Zhang²⁴, X. Zhang^{58b}, Y. Zhang^{15d}, Z. Zhang¹²⁸, X. Zhao⁴¹, Y. Zhao^{58b,128,ag}, Z. Zhao^{58a}, A. Zhemchugov⁷⁷, B. Zhou¹⁰³, C. Zhou¹⁷⁸, L. Zhou⁴¹, M.S. Zhou^{15d}, M. Zhou¹⁵², N. Zhou^{58c}, Y. Zhou⁷, C.G. Zhu^{58b}, H.L. Zhu^{58a}, H. Zhu^{15a}, J. Zhu¹⁰³, Y. Zhu^{58a}, X. Zhuang^{15a}, K. Zhukov¹⁰⁸, V. Zhulanov^{120b,120a}, A. Zibell¹⁷⁴, D. Zieminska⁶³, N.I. Zimine⁷⁷, S. Zimmermann⁵⁰, Z. Zinonos¹¹³, M. Zinser⁹⁷, M. Ziolkowski¹⁴⁸, G. Zobernig¹⁷⁸, A. Zoccoli^{23b,23a}, K. Zoch⁵¹, T.G. Zorbas¹⁴⁶, R. Zou³⁶, M. Zur Nedden¹⁹, L. Zwalinski³⁵

¹ Department of Physics, University of Adelaide, Adelaide, Australia

² Physics Department, SUNY Albany, Albany, NY, United States of America

³ Department of Physics, University of Alberta, Edmonton, AB, Canada

⁴ (a) Department of Physics, Ankara University, Ankara; (b) Istanbul Aydin University, Istanbul; (c) Division of Physics, TOBB University of Economics and Technology, Ankara, Turkey

⁵ LAPP, Université Grenoble Alpes, Université Savoie Mont Blanc, CNRS/IN2P3, Annecy, France

⁶ High Energy Physics Division, Argonne National Laboratory, Argonne, IL, United States of America

⁷ Department of Physics, University of Arizona, Tucson, AZ, United States of America

⁸ Department of Physics, University of Texas at Arlington, Arlington, TX, United States of America

⁹ Physics Department, National and Kapodistrian University of Athens, Athens, Greece

¹⁰ Physics Department, National Technical University of Athens, Zografou, Greece

¹¹ Department of Physics, University of Texas at Austin, Austin, TX, United States of America

¹² (a) Bahcesehir University, Faculty of Engineering and Natural Sciences, Istanbul; (b) Istanbul Bilgi University, Faculty of Engineering and Natural Sciences, Istanbul; (c) Department of Physics, Bogazici University, Istanbul; (d) Department of Physics Engineering, Gaziantep University, Gaziantep, Turkey

- ¹³ Institute of Physics, Azerbaijan Academy of Sciences, Baku, Azerbaijan
- ¹⁴ Institut de Física d'Altes Energies (IFAE), Barcelona Institute of Science and Technology, Barcelona, Spain
- ¹⁵ ^(a) Institute of High Energy Physics, Chinese Academy of Sciences, Beijing; ^(b) Physics Department, Tsinghua University, Beijing; ^(c) Department of Physics, Nanjing University, Nanjing;
- ^(d) University of Chinese Academy of Science (UCAS), Beijing, China
- ¹⁶ Institute of Physics, University of Belgrade, Belgrade, Serbia
- ¹⁷ Department for Physics and Technology, University of Bergen, Bergen, Norway
- ¹⁸ Physics Division, Lawrence Berkeley National Laboratory and University of California, Berkeley, CA, United States of America
- ¹⁹ Institut für Physik, Humboldt Universität zu Berlin, Berlin, Germany
- ²⁰ Albert Einstein Center for Fundamental Physics and Laboratory for High Energy Physics, University of Bern, Bern, Switzerland
- ²¹ School of Physics and Astronomy, University of Birmingham, Birmingham, United Kingdom
- ²² Centro de Investigaciones, Universidad Antonio Nariño, Bogotá, Colombia
- ²³ ^(a) Dipartimento di Fisica e Astronomia, Università di Bologna, Bologna; ^(b) INFN Sezione di Bologna, Italy
- ²⁴ Physikalisches Institut, Universität Bonn, Bonn, Germany
- ²⁵ Department of Physics, Boston University, Boston, MA, United States of America
- ²⁶ Department of Physics, Brandeis University, Waltham, MA, United States of America
- ²⁷ ^(a) Transilvania University of Brasov, Brasov; ^(b) Horia Hulubei National Institute of Physics and Nuclear Engineering, Bucharest; ^(c) Department of Physics, Alexandru Ioan Cuza University of Iasi, Iasi; ^(d) National Institute for Research and Development of Isotopic and Molecular Technologies, Physics Department, Cluj-Napoca; ^(e) University Politehnica Bucharest, Bucharest; ^(f) West University in Timisoara, Timisoara, Romania
- ²⁸ ^(a) Faculty of Mathematics, Physics and Informatics, Comenius University, Bratislava; ^(b) Department of Subnuclear Physics, Institute of Experimental Physics of the Slovak Academy of Sciences, Kosice, Slovak Republic
- ²⁹ Physics Department, Brookhaven National Laboratory, Upton, NY, United States of America
- ³⁰ Departamento de Física, Universidad de Buenos Aires, Buenos Aires, Argentina
- ³¹ Cavendish Laboratory, University of Cambridge, Cambridge, United Kingdom
- ³² ^(a) Department of Physics, University of Cape Town, Cape Town; ^(b) Department of Mechanical Engineering Science, University of Johannesburg, Johannesburg; ^(c) School of Physics, University of the Witwatersrand, Johannesburg, South Africa
- ³³ Department of Physics, Carleton University, Ottawa, ON, Canada
- ³⁴ ^(a) Faculté des Sciences Ain Chock, Réseau Universitaire de Physique des Hautes Energies – Université Hassan II, Casablanca; ^(b) Centre National de l'Energie des Sciences Techniques Nucleaires (CNSTEN), Rabat; ^(c) Faculté des Sciences Semlalia, Université Cadi Ayyad, LPHEA, Marrakech; ^(d) Faculté des Sciences, Université Mohamed Premier and LPTPM, Oujda; ^(e) Faculté des sciences, Université Mohammed V, Rabat, Morocco
- ³⁵ CERN, Geneva, Switzerland
- ³⁶ Enrico Fermi Institute, University of Chicago, Chicago, IL, United States of America
- ³⁷ LPC, Université Clermont Auvergne, CNRS/IN2P3, Clermont-Ferrand, France
- ³⁸ Nevis Laboratory, Columbia University, Irvington, NY, United States of America
- ³⁹ Niels Bohr Institute, University of Copenhagen, Copenhagen, Denmark
- ⁴⁰ ^(a) Dipartimento di Fisica, Università della Calabria, Rende; ^(b) INFN Gruppo Collegato di Cosenza, Laboratori Nazionali di Frascati, Italy
- ⁴¹ Physics Department, Southern Methodist University, Dallas, TX, United States of America
- ⁴² Physics Department, University of Texas at Dallas, Richardson, TX, United States of America
- ⁴³ ^(a) Department of Physics, Stockholm University; ^(b) Oskar Klein Centre, Stockholm, Sweden
- ⁴⁴ Deutsches Elektronen-Synchrotron DESY, Hamburg and Zeuthen, Germany
- ⁴⁵ Lehrstuhl für Experimentelle Physik IV, Technische Universität Dortmund, Dortmund, Germany
- ⁴⁶ Institut für Kern- und Teilchenphysik, Technische Universität Dresden, Dresden, Germany
- ⁴⁷ Department of Physics, Duke University, Durham, NC, United States of America
- ⁴⁸ SUPA – School of Physics and Astronomy, University of Edinburgh, Edinburgh, United Kingdom
- ⁴⁹ INFN e Laboratori Nazionali di Frascati, Frascati, Italy
- ⁵⁰ Physikalisches Institut, Albert-Ludwigs-Universität Freiburg, Freiburg, Germany
- ⁵¹ II. Physikalisches Institut, Georg-August-Universität Göttingen, Göttingen, Germany
- ⁵² Département de Physique Nucléaire et Corpusculaire, Université de Genève, Genève, Switzerland
- ⁵³ ^(a) Dipartimento di Fisica, Università di Genova, Genova; ^(b) INFN Sezione di Genova, Italy
- ⁵⁴ II. Physikalisches Institut, Justus-Liebig-Universität Giessen, Giessen, Germany
- ⁵⁵ SUPA – School of Physics and Astronomy, University of Glasgow, Glasgow, United Kingdom
- ⁵⁶ LPSC, Université Grenoble Alpes, CNRS/IN2P3, Grenoble INP, Grenoble, France
- ⁵⁷ Laboratory for Particle Physics and Cosmology, Harvard University, Cambridge, MA, United States of America
- ⁵⁸ ^(a) Department of Modern Physics and State Key Laboratory of Particle Detection and Electronics, University of Science and Technology of China, Hefei; ^(b) Institute of Frontier and Interdisciplinary Science and Key Laboratory of Particle Physics and Particle Irradiation (MOE), Shandong University, Qingdao; ^(c) School of Physics and Astronomy, Shanghai Jiao Tong University, KLPPAC-MoE, SKLPPC, Shanghai; ^(d) Tsung-Dao Lee Institute, Shanghai, China
- ⁵⁹ ^(a) Kirchhoff-Institut für Physik, Ruprecht-Karls-Universität Heidelberg, Heidelberg; ^(b) Physikalisches Institut, Ruprecht-Karls-Universität Heidelberg, Heidelberg, Germany
- ⁶⁰ Faculty of Applied Information Science, Hiroshima Institute of Technology, Hiroshima, Japan
- ⁶¹ ^(a) Department of Physics, Chinese University of Hong Kong, Shatin, N.T., Hong Kong; ^(b) Department of Physics, University of Hong Kong, Hong Kong; ^(c) Department of Physics and Institute for Advanced Study, Hong Kong University of Science and Technology, Clear Water Bay, Kowloon, Hong Kong, China
- ⁶² Department of Physics, National Tsing Hua University, Hsinchu, Taiwan
- ⁶³ Department of Physics, Indiana University, Bloomington, IN, United States of America
- ⁶⁴ ^(a) INFN Gruppo Collegato di Udine, Sezione di Trieste, Udine; ^(b) ICTP, Trieste; ^(c) Dipartimento di Chimica, Fisica e Ambiente, Università di Udine, Udine, Italy
- ⁶⁵ ^(a) INFN Sezione di Lecce; ^(b) Dipartimento di Matematica e Fisica, Università del Salento, Lecce, Italy
- ⁶⁶ ^(a) INFN Sezione di Milano; ^(b) Dipartimento di Fisica, Università di Milano, Milano, Italy
- ⁶⁷ ^(a) INFN Sezione di Napoli; ^(b) Dipartimento di Fisica, Università di Napoli, Napoli, Italy
- ⁶⁸ ^(a) INFN Sezione di Pavia; ^(b) Dipartimento di Fisica, Università di Pavia, Pavia, Italy
- ⁶⁹ ^(a) INFN Sezione di Pisa; ^(b) Dipartimento di Fisica E. Fermi, Università di Pisa, Pisa, Italy
- ⁷⁰ ^(a) INFN Sezione di Roma; ^(b) Dipartimento di Fisica, Sapienza Università di Roma, Roma, Italy
- ⁷¹ ^(a) INFN Sezione di Roma Tor Vergata; ^(b) Dipartimento di Fisica, Università di Roma Tor Vergata, Roma, Italy
- ⁷² ^(a) INFN Sezione di Roma Tre; ^(b) Dipartimento di Matematica e Fisica, Università Roma Tre, Roma, Italy
- ⁷³ ^(a) INFN-TIFPA; ^(b) Università degli Studi di Trento, Trento, Italy
- ⁷⁴ Institut für Astro- und Teilchenphysik, Leopold-Franzens-Universität, Innsbruck, Austria
- ⁷⁵ University of Iowa, Iowa City, IA, United States of America
- ⁷⁶ Department of Physics and Astronomy, Iowa State University, Ames, IA, United States of America
- ⁷⁷ Joint Institute for Nuclear Research, Dubna, Russia
- ⁷⁸ ^(a) Departamento de Engenharia Elétrica, Universidade Federal de Juiz de Fora (UFJF), Juiz de Fora; ^(b) Universidade Federal do Rio De Janeiro COPPE/EE/IF, Rio de Janeiro;
- ^(c) Universidade Federal de São João del Rei (UFSJ), São João del Rei; ^(d) Instituto de Física, Universidade de São Paulo, São Paulo, Brazil
- ⁷⁹ KEK, High Energy Accelerator Research Organization, Tsukuba, Japan
- ⁸⁰ Graduate School of Science, Kobe University, Kobe, Japan

- 81 ^(a) AGH University of Science and Technology, Faculty of Physics and Applied Computer Science, Krakow; ^(b) Marian Smoluchowski Institute of Physics, Jagiellonian University, Krakow, Poland
- 82 Institute of Nuclear Physics Polish Academy of Sciences, Krakow, Poland
- 83 Faculty of Science, Kyoto University, Kyoto, Japan
- 84 Kyoto University of Education, Kyoto, Japan
- 85 Research Center for Advanced Particle Physics and Department of Physics, Kyushu University, Fukuoka, Japan
- 86 Instituto de Física La Plata, Universidad Nacional de La Plata and CONICET, La Plata, Argentina
- 87 Physics Department, Lancaster University, Lancaster, United Kingdom
- 88 Oliver Lodge Laboratory, University of Liverpool, Liverpool, United Kingdom
- 89 Department of Experimental Particle Physics, Jožef Stefan Institute and Department of Physics, University of Ljubljana, Ljubljana, Slovenia
- 90 School of Physics and Astronomy, Queen Mary University of London, London, United Kingdom
- 91 Department of Physics, Royal Holloway University of London, Egham, United Kingdom
- 92 Department of Physics and Astronomy, University College London, London, United Kingdom
- 93 Louisiana Tech University, Ruston, LA, United States of America
- 94 Fysiska institutionen, Lunds universitet, Lund, Sweden
- 95 Centre de Calcul de l'Institut National de Physique Nucléaire et de Physique des Particules (IN2P3), Villeurbanne, France
- 96 Departamento de Física Teórica C-15 and CIAFF, Universidad Autónoma de Madrid, Madrid, Spain
- 97 Institut für Physik, Universität Mainz, Mainz, Germany
- 98 School of Physics and Astronomy, University of Manchester, Manchester, United Kingdom
- 99 CPPM, Aix-Marseille Université, CNRS/IN2P3, Marseille, France
- 100 Department of Physics, University of Massachusetts, Amherst, MA, United States of America
- 101 Department of Physics, McGill University, Montreal, QC, Canada
- 102 School of Physics, University of Melbourne, Victoria, Australia
- 103 Department of Physics, University of Michigan, Ann Arbor, MI, United States of America
- 104 Department of Physics and Astronomy, Michigan State University, East Lansing, MI, United States of America
- 105 B.I. Stepanov Institute of Physics, National Academy of Sciences of Belarus, Minsk, Belarus
- 106 Research Institute for Nuclear Problems of Byelorussian State University, Minsk, Belarus
- 107 Group of Particle Physics, University of Montreal, Montreal, QC, Canada
- 108 P.N. Lebedev Physical Institute of the Russian Academy of Sciences, Moscow, Russia
- 109 Institute for Theoretical and Experimental Physics (ITEP), Moscow, Russia
- 110 National Research Nuclear University MEPhI, Moscow, Russia
- 111 D.V. Skobel'syn Institute of Nuclear Physics, M.V. Lomonosov Moscow State University, Moscow, Russia
- 112 Fakultät für Physik, Ludwig-Maximilians-Universität München, München, Germany
- 113 Max-Planck-Institut für Physik (Werner-Heisenberg-Institut), München, Germany
- 114 Nagasaki Institute of Applied Science, Nagasaki, Japan
- 115 Graduate School of Science and Kobayashi-Maskawa Institute, Nagoya University, Nagoya, Japan
- 116 Department of Physics and Astronomy, University of New Mexico, Albuquerque, NM, United States of America
- 117 Institute for Mathematics, Astrophysics and Particle Physics, Radboud University Nijmegen/Nikhef, Nijmegen, Netherlands
- 118 Nikhef National Institute for Subatomic Physics and University of Amsterdam, Amsterdam, Netherlands
- 119 Department of Physics, Northern Illinois University, DeKalb, IL, United States of America
- 120 ^(a) Budker Institute of Nuclear Physics, SB RAS, Novosibirsk; ^(b) Novosibirsk State University Novosibirsk, Russia
- 121 Department of Physics, New York University, New York, NY, United States of America
- 122 Ohio State University, Columbus, OH, United States of America
- 123 Faculty of Science, Okayama University, Okayama, Japan
- 124 Homer L. Dodge Department of Physics and Astronomy, University of Oklahoma, Norman, OK, United States of America
- 125 Department of Physics, Oklahoma State University, Stillwater, OK, United States of America
- 126 Palacký University, RPTM, Joint Laboratory of Optics, Olomouc, Czech Republic
- 127 Center for High Energy Physics, University of Oregon, Eugene, OR, United States of America
- 128 LAL, Université Paris-Sud, CNRS/IN2P3, Université Paris-Saclay, Orsay, France
- 129 Graduate School of Science, Osaka University, Osaka, Japan
- 130 Department of Physics, University of Oslo, Oslo, Norway
- 131 Department of Physics, Oxford University, Oxford, United Kingdom
- 132 LPNHE, Sorbonne Université, Paris Diderot Sorbonne Paris Cité, CNRS/IN2P3, Paris, France
- 133 Department of Physics, University of Pennsylvania, Philadelphia, PA, United States of America
- 134 Konstantinov Nuclear Physics Institute of National Research Centre "Kurchatov Institute", PNPI, St. Petersburg, Russia
- 135 Department of Physics and Astronomy, University of Pittsburgh, Pittsburgh, PA, United States of America
- 136 ^(a) Laboratório de Instrumentação e Física Experimental de Partículas – LIP; ^(b) Departamento de Física, Faculdade de Ciências, Universidade de Lisboa, Lisboa; ^(c) Departamento de Física, Universidade de Coimbra, Coimbra; ^(d) Centro de Física Nuclear da Universidade de Lisboa, Lisboa; ^(e) Departamento de Física, Universidade do Minho, Braga; ^(f) Departamento de Física Teórica y del Cosmos, Universidad de Granada, Granada (Spain); ^(g) Dep Física and CEFITEC of Faculdade de Ciências e Tecnologia, Universidade Nova de Lisboa, Caparica, Portugal
- 137 Institute of Physics, Academy of Sciences of the Czech Republic, Prague, Czech Republic
- 138 Czech Technical University in Prague, Prague, Czech Republic
- 139 Charles University, Faculty of Mathematics and Physics, Prague, Czech Republic
- 140 State Research Center Institute for High Energy Physics, NRC KI, Protvino, Russia
- 141 Particle Physics Department, Rutherford Appleton Laboratory, Didcot, United Kingdom
- 142 IRFU, CEA, Université Paris-Saclay, Gif-sur-Yvette, France
- 143 Santa Cruz Institute for Particle Physics, University of California Santa Cruz, Santa Cruz, CA, United States of America
- 144 ^(a) Departamento de Física, Pontificia Universidad Católica de Chile, Santiago; ^(b) Departamento de Física, Universidad Técnica Federico Santa María, Valparaíso, Chile
- 145 Department of Physics, University of Washington, Seattle, WA, United States of America
- 146 Department of Physics and Astronomy, University of Sheffield, Sheffield, United Kingdom
- 147 Department of Physics, Shinshu University, Nagano, Japan
- 148 Department Physik, Universität Siegen, Siegen, Germany
- 149 Department of Physics, Simon Fraser University, Burnaby, BC, Canada
- 150 SLAC National Accelerator Laboratory, Stanford, CA, United States of America
- 151 Physics Department, Royal Institute of Technology, Stockholm, Sweden
- 152 Departments of Physics and Astronomy, Stony Brook University, Stony Brook, NY, United States of America
- 153 Department of Physics and Astronomy, University of Sussex, Brighton, United Kingdom
- 154 School of Physics, University of Sydney, Sydney, Australia
- 155 Institute of Physics, Academia Sinica, Taipei, Taiwan
- 156 ^(a) E. Andronikashvili Institute of Physics, Iv. Javakishvili Tbilisi State University, Tbilisi; ^(b) High Energy Physics Institute, Tbilisi State University, Tbilisi, Georgia

- ¹⁵⁷ Department of Physics, Technion, Israel Institute of Technology, Haifa, Israel
¹⁵⁸ Raymond and Beverly Sackler School of Physics and Astronomy, Tel Aviv University, Tel Aviv, Israel
¹⁵⁹ Department of Physics, Aristotle University of Thessaloniki, Thessaloniki, Greece
¹⁶⁰ International Center for Elementary Particle Physics and Department of Physics, University of Tokyo, Tokyo, Japan
¹⁶¹ Graduate School of Science and Technology, Tokyo Metropolitan University, Tokyo, Japan
¹⁶² Department of Physics, Tokyo Institute of Technology, Tokyo, Japan
¹⁶³ Tomsk State University, Tomsk, Russia
¹⁶⁴ Department of Physics, University of Toronto, Toronto, ON, Canada
¹⁶⁵ ^(a) TRIUMF, Vancouver, BC; ^(b) Department of Physics and Astronomy, York University, Toronto, ON, Canada
¹⁶⁶ Division of Physics and Tomonaga Center for the History of the Universe, Faculty of Pure and Applied Sciences, University of Tsukuba, Tsukuba, Japan
¹⁶⁷ Department of Physics and Astronomy, Tufts University, Medford, MA, United States of America
¹⁶⁸ Department of Physics and Astronomy, University of California Irvine, Irvine, CA, United States of America
¹⁶⁹ Department of Physics and Astronomy, University of Uppsala, Uppsala, Sweden
¹⁷⁰ Department of Physics, University of Illinois, Urbana, IL, United States of America
¹⁷¹ Instituto de Física Corpuscular (IFIC), Centro Mixto Universidad de Valencia – CSIC, Valencia, Spain
¹⁷² Department of Physics, University of British Columbia, Vancouver, BC, Canada
¹⁷³ Department of Physics and Astronomy, University of Victoria, Victoria, BC, Canada
¹⁷⁴ Fakultät für Physik und Astronomie, Julius-Maximilians-Universität Würzburg, Würzburg, Germany
¹⁷⁵ Department of Physics, University of Warwick, Coventry, United Kingdom
¹⁷⁶ Waseda University, Tokyo, Japan
¹⁷⁷ Department of Particle Physics, Weizmann Institute of Science, Rehovot, Israel
¹⁷⁸ Department of Physics, University of Wisconsin, Madison, WI, United States of America
¹⁷⁹ Fakultät für Mathematik und Naturwissenschaften, Fachgruppe Physik, Bergische Universität Wuppertal, Wuppertal, Germany
¹⁸⁰ Department of Physics, Yale University, New Haven, CT, United States of America
¹⁸¹ Yerevan Physics Institute, Yerevan, Armenia

- ^a Also at Borough of Manhattan Community College, City University of New York, NY; United States of America.
^b Also at Centre for High Performance Computing, CSIR Campus, Rosebank, Cape Town; South Africa.
^c Also at CERN, Geneva; Switzerland.
^d Also at CPPM, Aix-Marseille Université, CNRS/IN2P3, Marseille; France.
^e Also at Département de Physique Nucléaire et Corpusculaire, Université de Genève, Genève; Switzerland.
^f Also at Departament de Física de la Universitat Autònoma de Barcelona, Barcelona; Spain.
^g Also at Departamento de Física Teórica y del Cosmos, Universidad de Granada, Granada (Spain); Spain.
^h Also at Department of Applied Physics and Astronomy, University of Sharjah, Sharjah; United Arab Emirates.
ⁱ Also at Department of Financial and Management Engineering, University of the Aegean, Chios; Greece.
^j Also at Department of Physics and Astronomy, University of Louisville, Louisville, KY; United States of America.
^k Also at Department of Physics and Astronomy, University of Sheffield, Sheffield; United Kingdom.
^l Also at Department of Physics, California State University, Fresno CA; United States of America.
^m Also at Department of Physics, California State University, Sacramento CA; United States of America.
ⁿ Also at Department of Physics, King's College London, London; United Kingdom.
^o Also at Department of Physics, St. Petersburg State Polytechnical University, St. Petersburg; Russia.
^p Also at Department of Physics, University of Fribourg, Fribourg; Switzerland.
^q Also at Department of Physics, University of Michigan, Ann Arbor MI; United States of America.
^r Also at Dipartimento di Fisica E. Fermi, Università di Pisa, Pisa; Italy.
^s Also at Giresun University, Faculty of Engineering, Giresun; Turkey.
^t Also at Graduate School of Science, Osaka University, Osaka; Japan.
^u Also at Hellenic Open University, Patras; Greece.
^v Also at Horia Hulubei National Institute of Physics and Nuclear Engineering, Bucharest; Romania.
^w Also at II. Physikalisches Institut, Georg-August-Universität Göttingen, Göttingen; Germany.
^x Also at Institutio Catalana de Recerca i Estudis Avancats, ICREA, Barcelona; Spain.
^y Also at Institut für Experimentalphysik, Universität Hamburg, Hamburg; Germany.
^z Also at Institute for Mathematics, Astrophysics and Particle Physics, Radboud University Nijmegen/Nikhef, Nijmegen; Netherlands.
^{aa} Also at Institute for Particle and Nuclear Physics, Wigner Research Centre for Physics, Budapest; Hungary.
^{ab} Also at Institute of Particle Physics (IPP); Canada.
^{ac} Also at Institute of Physics, Academia Sinica, Taipei; Taiwan.
^{ad} Also at Institute of Physics, Azerbaijan Academy of Sciences, Baku; Azerbaijan.
^{ae} Also at Institute of Theoretical Physics, Ilia State University, Tbilisi; Georgia.
^{af} Also at Istanbul University, Dept. of Physics, Istanbul; Turkey.
^{ag} Also at LAL, Université Paris-Sud, CNRS/IN2P3, Université Paris-Saclay, Orsay; France.
^{ah} Also at Louisiana Tech University, Ruston LA; United States of America.
^{ai} Also at Manhattan College, New York NY; United States of America.
^{aj} Also at Moscow Institute of Physics and Technology State University, Dolgoprudny; Russia.
^{ak} Also at National Research Nuclear University MEPhI, Moscow; Russia.
^{al} Also at Physikalisches Institut, Albert-Ludwigs-Universität Freiburg, Freiburg; Germany.
^{am} Also at School of Physics, Sun Yat-sen University, Guangzhou; China.
^{an} Also at The City College of New York, New York NY; United States of America.
^{ao} Also at The Collaborative Innovation Center of Quantum Matter (CICQM), Beijing; China.
^{ap} Also at Tomsk State University, Tomsk, and Moscow Institute of Physics and Technology State University, Dolgoprudny; Russia.
^{aq} Also at TRIUMF, Vancouver BC; Canada.
^{ar} Also at Università di Napoli Parthenope, Napoli; Italy.
^{*} Deceased.